Repurposing Natural Gas Infrastructure for Hydrogen Transmission

Development of a network optimisation model for finding minimum cost networks that utilise existing infrastructure

Author
Dennis Geutjes
5153344

Supervisors
Dr.ir. P.W. Heijnen
Dr. A.F. Correljé

TU Delft

REPURPOSING NATURAL GAS INFRASTRUCTURE FOR HYDROGEN TRANSMISSION: DEVELOPMENT OF A NETWORK OPTIMISATION MODEL FOR FINDING MINIMUM COST NETWORKS THAT UTILISE EXISTING INFRASTRUCTURE

A master thesis submitted to Delft University of Technology in partial fulfilment of the requirements for the degree of

Master of Science in Complex Systems Engineering and Management
with an annotation in Technology in Sustainable Development

by

Dennis Geutjes

December 2021

Dennis Geutjes: *Repurposing Natural Gas Infrastructure for Hydrogen Transmission: Development of a network optimisation model for finding minimum cost networks that utilise existing infrastructure* (2021)

The work in this thesis was made at the:

Faculty of Technology, Policy and Management
Delft University of Technology

Supervisors: Dr.ir. P.W. Heijnen
Dr. A.F. Correljé

EXECUTIVE SUMMARY

Societal concern is growing regarding the effect fossil energy use has on our planet and societies. Many promising sustainable energy solutions, like hydrogen, carbon capture and storage, and district heating, require long-distance distribution and transmission through networked infrastructure. Often, existing infrastructure can be repurposed to reduce overall network costs. Examples are the repurposing of natural gas infrastructure for hydrogen transport or the repurposing of oil pipelines for transport of CO_2. This repurposing of existing infrastructure is expected to have a major influence on future network layouts, which uncovers an interesting research question. *What is a suitable network optimisation approach that aids in the design of cost-effective future network layouts, taking into account repurposing of existing infrastructure?*.

Reviewing the available literature on network optimisation modelling in relation to repurposing of existing infrastructure, we find that Geometric Graph Theoretical methods are the most promising approach to the problem at hand. Mixed Integer (Non-)linear programming approaches are computationally heavy, and do not provide the flexibility necessary to gain quick insights into design implications. Agent Based models provide more than enough flexibility, but no suitable methodology for integrating repurposing was found. A network optimisation model by Heijnen et al. (2020) is selected for adaption because of its already integrated existing pipeline functionality.

Limitations of the existing model are that it does not take into account costs related to the repurposing of existing infrastructure, and that it can not work with cycles in the network. These cycles, defined by a multitude of paths between two points, are necessary because existing infrastructure often contains cycles, and the optimal addition of new infrastructure can include cycles that contain existing infrastructure. To address these limitations, first, repurposing costs were integrated into the objective function of the model. A novel variable called the repurposing cost coefficient is used to allow model users to input the cost of repurposing relative to the building of new pipelines. Three novel heuristics are also introduced. The *network_simplex_repurposing heuristic* creates optimal network layouts for a single moment in time and allows for cycles in the network to be created if this is the most optimal layout. When investigating supply and demand patterns that differentiate over time, the heuristic is supplemented by the *timesteps_merged heuristic* that combines the networks created for each separate moment in time into one network. Finally, the *joined_edges heuristic* removes redundancies from the network to create a cost optimised network layout. The model was unit tested by applying it to small experiments, and the basic functionalities of the model were verified.

The model is applied to the case of repurposing existing natural gas pipeline infrastructure for hydrogen transport in the Netherlands. The case is scoped to include production of gaseous hydrogen in five industrial clusters by means of renewable assisted electrolysis and fossil fuels in combination with carbon sequestration. Hydrogen is transmitted from these production sources via pipelines to a centralised storage location in Groningen, or to end uses in the transport, power or industrial sectors. Hydrogen demand in the transport sector is expected to be located in industrial clusters, as it will be transported through pipelines to industrial clusters and subsequently shipped to fuelling stations by means of trucks. Future scenarios for the years 2030, 2040 and 2050 are created, and each scenario is defined in terms of model inputs. National demand and supply data for the scenarios from the Energy Transition Model is regionalised by creating allocation keys. International shipping via pipeline interconnection or shipping routes is also included in those allocation keys. Available existing capacities for every scenario are sourced

from open access information by Gasunie, Gasunie Transport Services and the HyWay27 project. By 2050, we assume that the entire high-calorific natural gas network of the Netherlands is available for repurposing. It is expected that repurposing of existing infrastructure in this case will cost between 10 and 35% of the cost of building new pipelines.

Applying the novel model to the case, we find that the natural gas infrastructure made available for repurposing to hydrogen pipelines by Gasunie by 2030 is sufficient to meet all transmission capacity demands, except for a few short stretches of new pipelines that connect industrial clusters to the main network. Adapting the natural gas pipeline network to hydrogen will cost between 192 and 358 million EUR. Between 2030 and 2040, Gasunie will have to make significant amounts of natural gas pipeline infrastructure available for repurposing in order to keep hydrogen network costs low. Cost savings of up to 900 million EUR are possible if enough capacity is made available by 2040. In 2050, repurposing the entire high-calorific natural gas network for hydrogen transmission is no longer sufficient to meet all capacity demands in three out of four 2050 scenarios. Additional capacity is needed that stretches from storage locations in Groningen, to industrial clusters in the west of the country. Investing in an overcapacity on these stretches by 2040 can result in cost overall cost reductions by 2050.

When comparing the novel model's performance to the original model by Heijnen et al. (2020), we find that the novel model is better suited for investigating network layouts when existing capacity can be repurposed. The novel model produces network layouts that are 0 to 786% less expensive than the network layouts created by the original model for the same scenarios. When repurposing of existing capacity is not possible, however, the original model outperforms the novel model by 0 to 14%. This indicates that the original model is better suited at finding cost-minimised network layouts when repurposing of existing infrastructure is impossible.

Because of its flexibility and relative ease of use, the novel model can be applied to many cases, ranging from repurposing of pipeline infrastructure for CO_2 transport to the repurposing of road infrastructure. We have demonstrated that the model can provide valuable insights into design implications of networked systems and opened interesting directions for further research on the topics of networked infrastructure repurposing and optimisation.

CONTENTS

LIST OF FIGURES

LIST OF TABLES

List of Algorithms

LIST OF ACRONYMS

"It ought to be remembered that there is nothing more difficult to take in hand, more perilous to conduct, or more uncertain in its success, than to take the lead in the introduction of a new order of things. Because the innovator has for enemies all those who have done well under the old conditions, and lukewarm defenders in those who may do well under the new. This coolness arises partly from fear of the opponents, who have the laws on their side, and partly from the incredulity of men, who do not readily believe in new things until they have had a long experience of them."

Niccolò Machiavelli, The Prince

1 INTRODUCTION

1.1 A NEED FOR NEW TRANSMISSION NETWORKS

Currently, societal concern is growing regarding the effect traditional (fossil) energy use has on our planet and societies. Fossil fuel supplies are finite, and their use as energy sources has proven to be harmful in many ways. As a result, a global transition towards sustainable energy is taking place, with many countries around the world planning and making significant structural changes to their energy systems (Arabzadeh et al., 2020). Limitations to electrification and the benefits of diversity in the energy mix are becoming clearer, paving the way for promising alternatives. Many of these alternatives require transmission through networked infrastructure over longer distances.

A prominent example is the use of hydrogen in the energy transition. Recent years have seen a re-sparked academic and commercial interest in hydrogen as an energy carrier (Weisz, 2004). It has many possible applications ranging from spacecraft to residential housing and can serve as an answer to limitations to electrification like high heat processes in industry and long-distance transport (Ogden, 2002). Its widespread possibilities for application, natural abundance and high sustainability potential make hydrogen a strong potential energy carrier in a sustainable future. Currently, 180 PJ of hydrogen is being produced annually in the Netherlands, with almost all of it being locally used in the industrial clusters in which it is produced (Weeda and Segers, 2020). It is expected, however, that increases in demand and variability of supply will cause a local mismatch between supply and demand, subsequently resulting in the need for hydrogen transmission over longer distances (Afman and Rooijers, 2017, Detz et al., 2019). A consortium of European gas transmission system operators expect that a European hydrogen transmission network will be emerging in the coming decade (Enagás et al., 2020).

According to the International Energy Agency (2021), another high-potential technology in the energy transition is Carbon Capture, Utilisation and Storage (CCUS). CCUS involves the capture of CO_2 from emission sources like industrial facilities and power generation and storing it at centralised locations like in salt caverns or empty gas fields, subsequently reducing net carbon emissions (Regufe et al., 2021). CCUS has been identified as one of the main priorities of the energy transition, and research into the field has seen much recent attention (Marocco Stuardi et al., 2019, Regufe et al., 2021). Onshore and offshore pipeline infrastructure will serve a critical role in future transmission of CO_2 from emission sources to storage locations, and is expected to be the main mode of transport (Bandilla, 2020, Svensson et al., 2004).

Another major challenge in the energy transition is to provide sustainable heating to households. The Netherlands, for example, currently uses Natural Gas (NG) to provide heat to households. One of the most promising ways to reduce CO_2 emissions in this sector is district heating, which is expected to play a major role in scaling down NG consumption in the Netherlands (Accenture, 2020), and has many possibilities for application worldwide (Werner, 2017). District heating involves the movement of heat from centralised sources like power plants and industrial facilities to end uses in, for example, public housing (Werner, 2013). Transport of heat is performed by heating up a medium, often water, at a heat source and transporting

it through pipelines to end uses (Werner, 2017). In order to meet heating demands with district heating, investments in pipeline infrastructure have to be made.

Other examples of energy transition solutions that require transmission through new networked infrastructure include methanol (IRENA and Methanol Institute, 2021), liquid ammonia (Nicholas Salmon and René Bañares-Alcántara, 2021) and dimethyl ether, a promising replacement for liquefied petroleum gas and conventional diesel (Yoon and Han, 2009) (Al-Breiki and Bicer, 2021).

1.2 THE BENEFITS OF REPURPOSING EXISTING INFRASTRUCTURE

We have established that the energy transition creates a demand for transmission capacity to transport new energy carriers, subsequently increasing the need for networked infrastructure, often in the form of pipelines. As new energy infrastructure is being introduced, old infrastructure is being decommissioned, and sustainable use of old infrastructure can provide a strong boost to the energy transition (Invernizzi et al., 2020). In the Netherlands, for example, Dutch Transmission System Operator (TSO) Gasunie and TenneT (2019), expect that existing NG pipelines will be repurposed for hydrogen transport. The expected cost for repurposing this infrastructure is between 10 and 35% of the cost of building new infrastructure (Tezel and Hensgens, 2021). The Dutch NG network is not only expected to be used for future transport of hydrogen. Gasunie and TenneT (2019) expect certain pipelines to be used for transport of other gases like methanol and CO_2. Similar benefits of repurposing existing infrastructure can be found in other cases. ACT Acorn (2019), a project initiated by the European Commission, expect the cost of repurposing an existing oil or gas pipeline for CO_2 transport to range between 1 and 10% of the cost of installing new pipeline infrastructure. Beals (2003) found that using unused gas pipelines for laying fibre-optic cables could reduce costs by 50 to 70%, with Sun et al. (2014) proposing reducing expenditures by installing fibre-optic cables parallel to pipelines that are still in use and taking advantage of land ownership rights. Other examples of infrastructure repurposing include the redesign of mobility infrastructure to support different mobility modes (Givoni and Perl, 2017).

Repurposing existing infrastructure is expected to have a significant effect on future network layouts (Enagás et al., 2020, Gasunie and TenneT, 2019). This uncovers an interesting question. How can the repurposing of existing infrastructure be included into the search for optimal future network layouts, and how can the implications of this repurposing, like necessary expansions, be studied? The repurposing of existing infrastructure is subject to many variables and uncertainties (Enagás et al., 2020, Gasunie and TenneT, 2019). According to Zachary (1986), decision-making under these circumstances is difficult without decision support technologies because humans lack the computational skills to take into account all parameters and are possibly subject to bias. Zachary's claims are supported by more recent literature indicating that complex engineering challenges, with multiple stakeholders involved, require clear, efficient, visualised and flexible technological support (Frey et al., 2009, 2010, Garber et al., 2017, Simpson et al., 2017). It is therefore valuable to provide decision makers with a decision support tool that can efficiently provide them with quick, clear, visualised and flexible insights regarding the impact that the repurposing of existing infrastructure has on optimal network design.

1.3 CORE CONCEPTS REGARDING NETWORKED INFRASTRUCTURE DESIGN

Networked infrastructure comes in many forms, and they share a number of characteristics, including high capital investment costs and long lifetimes resulting in irreversibility of design decisions (Herder et al., 2011). Minimising the initial investment in networked infrastructure drastically decreases overall cost and is therefore of paramount importance in the design of new infrastructure. The irreversible nature of networked infrastructure projects requires proper exploration of possible system configurations and future scenarios so that cost inefficient investment decisions can be avoided. When repurposing existing infrastructure, it is also important to include the repurposing into the design process so that the right decisions can be made. These three concepts thus form the focus of this research, and will be discussed in more detail below.

1.3.1 Minimising investment costs

Dagdougui (2012) found that mathematical optimisation is the best way to find optimal future network layouts. Network optimisation is done by either minimising or maximising one or multiple performance indicator(s). Physical networked infrastructure investments are notoriously expensive. Reddi et al. (2016) found that natural gas transmission pipelines often exceed costs of 2 million EUR per kilometre of pipeline, with costs mainly consisting of material, right of way and labour costs. The envisioned European hydrogen transmission backbone is expected to require an investment of 42 to 81 billion EUR before 2040 (Enagás et al., 2020). Optimising the network layout so that investments costs are reduced and simultaneously taking into account future network capacity demands to optimise expenditures over time is therefore of paramount importance by both decreasing the investment threshold and allowing for more money to be invested in other sustainable solutions. This research therefore focuses on cost-minimisation of network layouts.

1.3.2 Exploration of system configurations

Networked infrastructure is expensive, but when maintained correctly, it can pass the test of time. Most oil and gas infrastructure in the United States, for example, is over 50 years old (Wirfs-Brock, 2014). Some pipelines in use today have been installed over a century ago (Wirfs-Brock, 2014). It is evident that design choices can have major impact over the years, and the cheapest design option between now and 2030 might not be the cheapest design option between now and 2050. The problem is, however, that the further we try to look into the future, the more opaque it becomes. Dealing with this level of uncertainty, it is important to be able to explore different system configurations and scenarios when designing and reassigning networks. Complex, networked utility systems often have multiple locations of demand (sinks) and supply (sources). For example, production of hydrogen in the Netherlands is not situated in one location, and neither is demand. For exploration of different system design choices, it is important that network optimisation can deal with multiple producers and consumers at the same time. These producers and consumers can also change from being a producer or consumer over time.

1.3.3 Repurposing existing infrastructure

We have established that repurposing of existing infrastructure has many benefits, including a significant reduction of investment costs resulting from the fact that repurposing infrastructure is often cheaper than building new infrastructure.

When computing a minimal cost network, it is important to include infrastructure reassignment into the optimisation mathematically when the case allows for it. This has several implications, among which is the cost for repurposing that has to be included into the cost-function of the optimisation. Another implication for repurposing is that the optimisation should allow for more than one path between two locations in the network. Because of its evolutionary characteristic, many networked utility systems already have multiple paths to get from one location to the other. In Figure 1.1 we see a schematic map of the Dutch NG network, with examples of alternative paths highlighted in more detail. Both the schematic and more detailed representations are sourced from Gasunie Transport Services (2012).

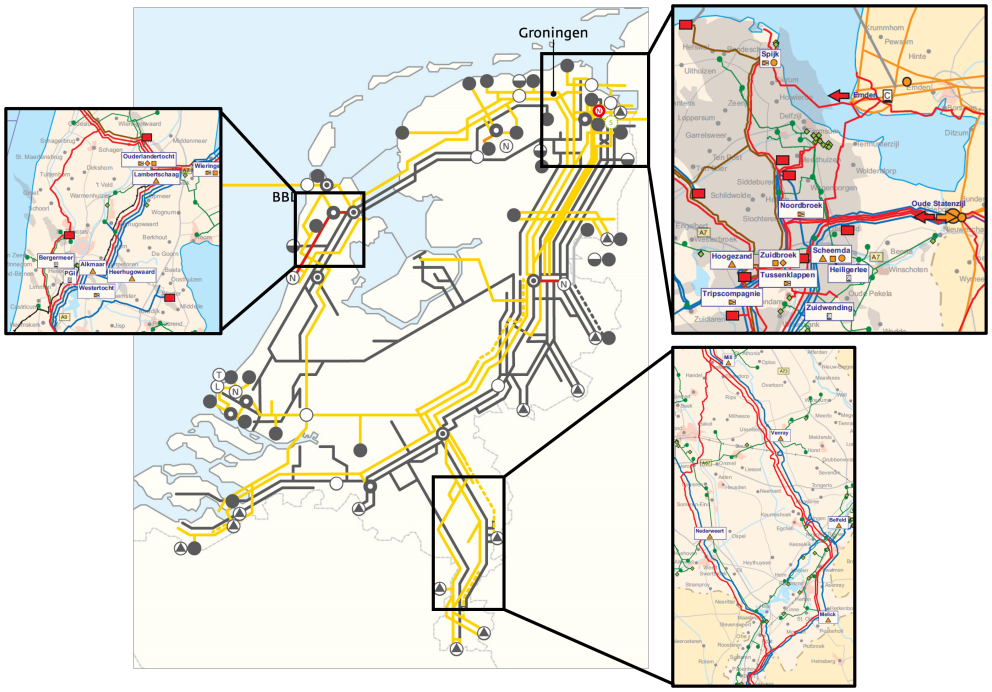

Figure 1.1: The Dutch natural gas network

Situations like these often result from the capacity expansion of existing infrastructure, resulting in new pipelines being added that create new paths between nodes in the network (Lenz and Schwarz, 2016). We will now provide a simple example of this process. Imagine an existing situation where a town, with an electricity demand of 5 MW, is directly connected to a wind-farm that produces a supply of 5 MW (see Figure 1.2). The cable connecting the wind-farm and the town has the capacity to transport 10 MW.

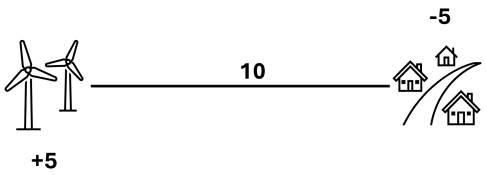

Figure 1.2: Example of emerging double path (1/3)

Now imagine a new town emerges south of the original town which also has an electricity demand of 5 MW and the wind-farm production capacity being doubled to 10 MW to accommodate increased demand. Assuming a linear relation between pipeline costs, length and capacity, the cheapest solution to deliver all demand would be to add a new pipeline between the two towns that can deliver 5 MW to the new town, as the distance between the two towns is less than the distance

between the wind-farm and the new town, and there is still a remaining capacity to be utilised (see Figure 1.3).

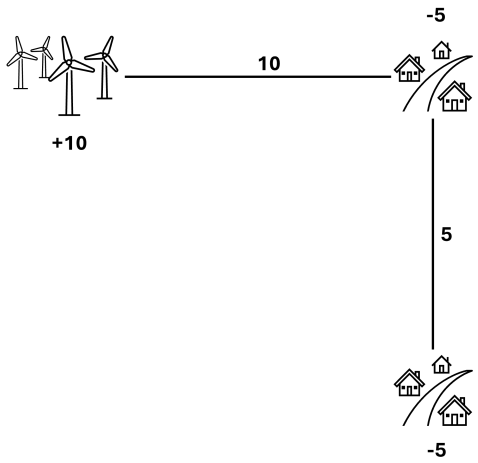

Figure 1.3: Example of emerging double path (2/3)

The new town subsequently doubles in size. Its increase in demand is met by another expansion of the wind-farm. Existing transmission capacity is no longer sufficient to connect all electricity supplies to demands, and there is no remaining capacity to be utilised. The cheapest option to increase electricity supply to the newly grown town is to now build a connection directly between the town and the wind-farm, subsequently creating a new path in the network between the wind farm and the biggest town (see Figure 1.4). Iterative capacity expansions have now caused the forming of a situation where there are two paths between any two locations in the network.

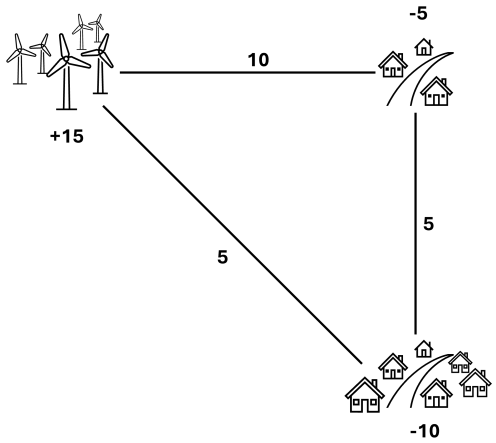

Figure 1.4: Example of emerging double path (3/3

1.4 GAPS IN NETWORK OPTIMISATION LITERATURE

There is an impressive body of research on network optimisation modelling (Li et al., 2019). Older models mainly use step-wise optimisation, first optimising the network layout for minimal total network length, and then optimising the capacity of all pipelines in the created layout (Gim et al., 2012, Johnson and Ogden, 2012, Murthy Konda et al., 2012). André et al. (2013) combined these separate steps for optimising the length and capacity of a hydrogen network into one heuristic.

This allowed them to compute a model optimised for both pipeline length and capacity more efficiently. In a continuation of their research, they used the model to investigate the incremental development of France's future hydrogen grid (André et al., 2014). The model, however, only supports cases with 1 source and multiple sinks. Similar models were applied to cases in the Netherlands (Murthy Konda et al., 2012). These models do not meet the design criterion we have earlier identified of being able to work with multiple sinks and multiple sources.

Johnson and Ogden (2012) developed a model that was capable of connecting multiple production facilities to multiple demand locations. However, their model lacks the dynamic component necessary to investigate temporal variations in supply and demand. Similar limitations were found in other models (Baufumé et al., 2013, Gim et al., 2012, Murthy Konda et al., 2012). Middleton et al. (2012) created a mixed integer programming model for CO_2 pipeline network optimisation that could also be used for different applications. Similarly to the models described before, however, their model lacks the dynamic component to quickly gain insight into design implications and is computationally heavy.

Moreno-Benito et al. (2017) used Mixed Integer Linear Programming (MILP) to create an optimal framework for hydrogen infrastructure development in the UK. Their model takes into account imports and various means of production. The model however is not able to take into account existing infrastructure and is computationally heavy. Similar limitations are found in other recent hydrogen network optimisation research using MILP (Hwangbo et al., 2017, Kim and Kim, 2016, Seo et al., 2020). Also in different research areas like CCUS network optimisation these computationally heavy and inflexible models appear to be the status quo with d'Amore et al. (2021) using MILP to optimise a Europe-wide supply chain of pipelines for CCUS and Elahi et al. (2017) integrating MILP into a stochastic framework to deal with uncertainty in finding the optimal CCUS pipeline network layout for the UK. Zhu et al. (2018) created a model based on economic potential theory and Geometric Graph Theory (GGT) to analyse the expansion of an already existing NG network in China. Their focus was on the addition of new pipelines to an existing network, but the optimisation did not include those existing pipelines.

In our review of relevant modelling literature, several important research gaps were identified. There appears to be a lack of an integrated systems based approach to optimising networked infrastructure design, with research focusing mainly on specific applications of certain infrastructure like fuel cell vehicles in hydrogen economies. Additionally, many recent models fail to take into consideration complex temporal dynamic components regarding demand and supply profiles. Others are too complicated to quickly provide insights regarding network design implications under different future scenarios. Whilst a large body of literature indicates future possibilities for repurposing existing infrastructure (Abdin et al., 2020, Ogden et al., 2018, Schiebahn et al., 2015), no literature was found on including the repurposing of existing infrastructure into the modelling of future network layouts, other than building new hydrogen pipelines along pathways of NG infrastructure to reduce right-of-way costs (Baufumé et al., 2013).

1.5 RESEARCH OBJECTIVE

The objective of this research is *to find or develop a network optimisation approach that can be used to find a cost-effective network design, taking into account the repurposing of existing infrastructure, temporal and spatial variations in supply and demand and different system configurations. The created tool should allow users to quickly gain insights regarding network design choices regarding the repurposing of existing infrastructure*. This research objective leads to the following main research question:

> What is a suitable network optimisation approach that aids in the design of cost-effective future network layouts, taking into account repurposing of existing infrastructure?

When identifying the knowledge gap, we found that most recent literature on network optimisation mentioning repurposing of existing infrastructure is done on hydrogen network optimisation. In order to test the applicability of our approach, we will therefore apply the model to the case of NG repurposing for hydrogen transport in the Netherlands.

1.5.1 Sub-questions

Dissecting the main research question results in the following sub-questions.

1. How can networked infrastructure be modelled, minimising investment costs?

2. How can the repurposing of existing infrastructure and the exploration of different system configurations be taken into account in the modelling approach?

3. How can the model be applied to the case of repurposing NG pipelines for hydrogen transport?

4. What insights are created by the model when applied to the case of repurposing NG pipelines for hydrogen transport?

5. What can be learned about the general applicability of the model?

1.6 OVERVIEW OF RESEARCH APPROACH

In Chapter 2 we will identify suitable methods to model networked infrastructure, taking into account the previously introduced core concepts of minimisation of investment costs, the repurposing of existing infrastructure and exploration of different system configurations. The chapter will be concluded with the selection of an approach that will be used to build our model. Chapter 3 will start with a general introduction of the selected approach, followed by the description of an existing model we will be adapting. We will then describe adaptions to the model that are necessary to answer our research questions. The model is verified and calibrated in Chapter 4. The case will be introduced and scoped in Chapter 5 and subsequently expressed in terms of model inputs in Chapter 6. In Chapter 7, the model is applied to the case of repurposing natural gas infrastructure for hydrogen transport in the Netherlands and results are shared and discussed. This research is concluded with conclusions, recommendations and a reflection on the research in Chapter 8. Appendices are found at the end of this research.

2 LITERATURE REVIEW

The goal of this chapter is to review the existing literature addressing our main research question, and using this literature to select a research methodology.

2.1 NETWORKED SYSTEM OPTIMISATION

There are several tried and tested approaches to modelling network optimisation that have been applied to a range of different problems in different fields. Heijnen et al. (2020) identify three main approaches to solving networked system design problems, MILP/Mixed Integer Non-linear Programming (MINLP), Agent Based Modelling (ABM) and the use of GGT. We will now perform a review of the literature on these approaches in relation to the core concepts defined in the previous chapter: cost minimisation of network layouts, exploration of different system layouts and integration of the repurposing of existing infrastructure.

2.1.1 Mixed Integer (Non-)linear Programming

MILP and MINLP are effective mathematical modelling approaches that can handle complex optimisation problems, identify important trade-offs and subsequently solve them (Guo and Shah, 2015, Weimann et al., 2019). Their structured and clear approach to optimisation has proven to be beneficial in application to a wide range of network optimisation problems, ranging from neural networks and energy systems to fresh water networks and medical waste disposal (Shi, 2009). They are usually applied to multi-objective optimisation problems that often include cost minimisation in the objective function. Kalitventzeff (1991) proposed a methodology for applying MINLP to the management of utility networks, minimising network costs, and maximising utility. André et al. (2014) included cost minimisation of hydrogen transport in the cost function of their network optimisation model for a hydrogen supply chain in France. By integrating cost minimisation into their objective function, Seo et al. (2020) found that a hydrogen network layout in Korea with centralised storage is cheaper than one with decentralised storage.

Several attempts at integration of the repurposing of existing infrastructure into MILP and MINLP approaches can be found in the literature. Jagannath et al. (2018) used MILP to model the retrofitting of hydrogen infrastructure to minimise total network costs. The model is focused on retrofitting of production, consumption and purifying installations and does not take into account distribution or transmission infrastructure, but indicates that it is possible to include repurposing of existing infrastructure into MILP models. In their research into optimal hydrogen pipeline layout in Germany, Baufumé et al. (2013) explored the possibility of building new pipelines besides existing pathways of waterways, railways, main roads and existing NG or high voltage transmission networks. They used a combination of GIS and MILP to minimise the total cost of the pipeline network layout. Their model did not take into account the building of new pipeline infrastructure not installed besides existing pathways. Cost differentiation was included by, for example, making instalment besides NG pipelines cheaper than the other options. Papanikolaou et al. (2018) created a MILP model that cost minimizes the incremental planning of optical network layouts, utilising existing infrastructure present and assigning costs to said

infrastructure. They assigned costs to the reconfiguration of existing infrastructure, and minimised a cost function so that the total cost of new infrastructure plus the total cost of existing infrastructure reconfiguration is kept at a minimum. This allowed them to mathematically assess whether the reuse of existing infrastructure is cost-effective, or if it was more efficient to build new pathways. Their model is, however, focused on fixed pathways where creation of infrastructure is possible and lacks the temporal resolution to assess complex network layouts. Wickham et al. (2022) included the option to repurpose gas distribution networks for hydrogen transport into their linear programming model that builds optimal hydrogen supply chains for the transport sector, optimising for multiple objectives. They included the option of repurposing existing NG distribution networks to 100% hydrogen pipelines into their objective function. Costs for repurposing were significantly cheaper than building new pipelines, which resulted in repurposing of the distribution net being cheaper than building new infrastructure. The model by Wickham et al. (2022) can only decide to repurpose all existing infrastructure and is not able to repurpose parts of the existing infrastructure, and build additional new distribution pipelines depending on supply and demand profiles.

The main benefits of MILP are that it can efficiently balance multiple objectives simultaneously, including cost minimisation, and guarantee to find a global optimum (Guo and Shah, 2015). Geographical elements can be included into the optimisation by making the approach spatially explicit as showcased by Johnson and Ogden (2012), Moreno-Benito et al. (2017) and Seo et al. (2020). This makes MILP especially suitable for optimisation of multi-objective network problems where the main goal is to find a singular optimal solution (Urbanucci, 2018, Yamchi et al., 2021). However, we are not looking for a singular optimal solution, but want to create a tool that can provide insights into cost-effective network layouts with the possibility for exploration of different scenarios. Other limitations of the approach include having to consider all time steps at once, limiting the investigation of cases with a dynamic temporal component (Urbanucci, 2018). Furthermore, its structured and rigid mathematical approach requires much preliminary work on the set-up of the model, making MILP less flexible and thus less suitable for on-the-spot exploration of numerous possible scenarios and outcomes. Repurposing of existing infrastructure was found to be possible to include into this optimisation approach, however, no method of doing so was found to be easily applicable to our research question.

2.1.2 Agent Based Modelling

An alternative approach to networked system optimisation, more suitable for scenario exploration, is ABM. According to Heijnen et al. (2020), there are two main approaches of doing so, Particle Swarm Optimisation (PSO) and Ant Colony Optimisation (ACO). Both of these approaches use the behaviour of living organisms to find an optimal solution for an optimisation problem. PSO is based on the flocking or schooling behaviour of birds or fish (Sivanandam and Deepa, 2008). After being firstly proposed by Kennedy and Eberhart (1995), PSO has been successfully applied to hundreds of optimisation problems covering an incredible range of areas (Poli, 2007). ACO, as the name may suggest, is a form of ABM that utilises the behaviour of ants to optimise network layouts (Chandra Mohan and Baskaran, 2012). Ants are programmed as agents that drop pheromones to alert other ants to the shortest paths to food sources. After its first introduction by Dorigo (1992), the approach has proven to be suitable to use in many engineering challenges (Chandra Mohan and Baskaran, 2012).

ABM can be applied to minimise the cost of networked infrastructures. Mtolera et al. (2014) applied PSO to the cost-minimisation of a pipeline irrigation network. The model was successful in reducing the pipeline investment costs of irrigation projects. Liu et al. (2017) used an ACO approach to route optimisation of power pipeline network layouts. The model created was able to find cost-effective network

layouts given a predetermined grid where pipelines could be built. The model optimises for both cost and capacity flow of pipelines. In search of minimum-cost and reliable water distribution networks, Torkomany et al. (2020) created a PSO model that optimises an objective function that contains network resilience and total network costs. The model was successfully applied to the water distribution network of Yemen.

Little research has been performed on repurposing networked infrastructure using ABM techniques. Silva et al. (2009) used PSO to model the repurposing of parts of heat exchanger networks when retrofitting such systems. They successfully minimised the total cost of retrofitting whilst taking into account the possibility for reuse of existing infrastructure. The model is, however, mainly focused on thermodynamic workings of system elements like heat exchangers and does not provide an analysis of network topology. Luo et al. (2011) combined ACO and PSO to minimise the power loss of the reconfiguration of a distribution network. They used existing infrastructure and altered its characteristics like flow and voltage in such a manner that power loss was minimised. The possibility for building new infrastructure additional to the existing infrastructure was not within the scope of this research. This is in line with findings by Yang and Karamanoglu (2020), who state that ABM are especially suitable for discrete optimisation, like in the case of routing problems where potential paths are already encoded.

2.1.3 Geometric Graph Theory

The final approach we will be discussing, is the use of GGT in modelling. Similar to ABM, this approach uses heuristics and algorithms in a manner that produces local optimisations. In the case of GGT, heuristics are not based on animal behaviour but on a combination of geometric and graph theories. A graph being a combination of nodes represented by points and edges that are represented by straight lines connecting two nodes (Ackerman et al., 2009). This top-down approach is a more rigid and structural methodology than the bottom-up approach applied in ACO as described by Heijnen et al. (2014) in their direct comparison of ACO and GGT approaches. This suggests that GGT is better suited to handle network design problems where a more structural approach is required, but where MILP does not offer enough flexibility, like in the case of the problem we are investigating in this thesis. This is supported by Zarghami et al. (2019) and Heijnen et al. (2020), who claim that an approach based on GGT is best suited for supporting actors and system engineers in infrastructure design.

Numerous examples of the application of GGT to network cost minimisation can be found, often using shortest path algorithms like the one created by Dijkstra (1959) (Zhou et al., 2021). Other approaches were also encountered. De Villiers et al. (2018) successfully combined GGT with ACO to create a model that minimises the total network cost of a sewer pipeline layout. Chen and Zhu (2019) combined several graph theoretical approaches, including Prim's algorithm (Prim, 1957) and the dynamic spanning tree, to optimise regional energy network planning in China. They successfully applied it to create an optimal network layout for a Shanghai neighbourhood, taking into account routing and capacity constraints. Similarly, Zhou et al. (2021) combined a genetic algorithm with graph theoretical foundations to minimise the total annual cost of a regional distributed energy system.

Little research has been performed on integrating the repurposing of existing infrastructure into graph theoretical approaches to network optimisation modelling. Zhu et al. (2018) created a model based on economic potential theory and GGT to analyse the expansion of an already existing NG network in China. Their focus was on the addition of new pipelines to an existing network, but the existing pipelines were not included into the objective function, thus leaving them out of the optimisation. Heijnen et al. (2020) created a novel approach to network optimisation using GGT that finds minimum-cost solutions for network layouts by minimising an

objective function that takes multiple cost elements into account. The model is also able to include the repurposing of existing infrastructure into the optimisation, but does not have the ability to assign costs to repurposing in the objective function. This was the only model found that includes the repurposing of existing pipeline infrastructure in a manner that can be applied to our main research question. Furthermore, the model works with simple, flexible inputs and is computationally light. It is created with easy and quick operation by decision makers in mind, in a manner that differentiates it from the other modelling approaches reviewed. Spatial and temporal flexibility is worked into the inputs of the model, and multiple sinks and sources can be accounted for. For these reasons, the model appears to be the right candidate for further investigation into repurposing existing infrastructure. In Chapter 3 we will describe the model in detail, discuss its limitations and explain adaptions made to the model in order to create a new model that can be directly applied to a case to answer our main research question.

3 METHODS AND MODEL CREATION

Before diving into the explanation of our research approach, it is important to adopt names for the original model created by Heijnen et al. (2020) and the model that will result from the adaption covered in this thesis. This will make it easier to differentiate between the models in the coming chapters. From this point on, the original model will be referred to as the Network Optimisation Model (NOM). The model that will be created by adapting the NOM, will be referred to as the Network Repurposing Optimisation Model (NROM).

We will start this chapter by introducing GGT and highlight elements important to our research. The introduction will be followed by a description of the relevant modelling steps of the NOMl, and a discussion on why and where adaptions have to be made. We will then give a step by step account of adaptions made to the model. Novel heuristics of the NROM will also be described.

3.1 AN INTRODUCTION TO GEOMETRIC GRAPH THEORY

In this section, we will provide a general introduction to GGT and discuss elements important to our methodology. We will then define the core concepts introduced in Chapter 1 in terms of GGT. Information in this section is based on Thulasiraman and Arumugam (2016).

3.1.1 Graphs, nodes and edges

A graph is a mathematical representation of a network (Koutrouli et al., 2020). A graph G is described by $G = (N, E)$ where N is a set of nodes n and E is a set of edges e. Nodes are represented by points in a two-dimensional plane, and their locations are described by coordinates (x, y) in said plane. Nodes can be connected by edges (i, j) that have two end-points each located at a node, in this case nodes i and j. The most basic type of graph is an *undirected graph* in which all edges are the same in that they do not have a forced direction of flow. Figure 3.1 shows a basic undirected graph with four nodes and four edges.

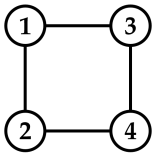

Figure 3.1: Example of an undirected graph

Directed graphs are graphs in which all edges have a directional flow. An example of a directed graph is shown in Figure 3.2. A directional flow means that the flow through an edge can only flow one way, say from node 4 to node 2 in the example. If a flow needs to get from node 2 to node 4 it can not flow directly through edge (2,4) but it will have to pass nodes 1 and 3. In the case of utility infrastructure, which is the focus of this research, we will be dealing with both directed and undirected graphs. Usually, for a certain point in time, edges are directional. Gas can only flow one way through a pipeline in one point of time, and can not

simultaneously flow in the opposite direction. Direction of flow can, however, be changed over time when node demands and/or supplies change, possibly resulting in undirected graphs when working with a dynamic temporal resolution.

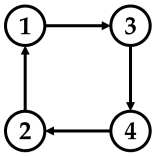

Figure 3.2: Example of a directed graph

Both graphs shown above are *connected*, meaning that there is a path of edges between each pair of nodes in the graph. When not every node in the graph can be reached from every other node in the network, the graph is *disconnected*. An example of a disconnected graph is shown in Figure 3.3

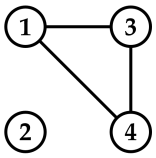

Figure 3.3: Example of a disconnected graph

In a *complete graph* every node is directly connected to every other node in the graph, with the longest path between any two nodes not exceeding the length of one edge. An example of a complete graph is given in Figure 3.4.

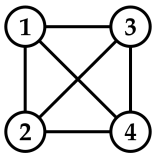

Figure 3.4: Example of a complete graph

When all pairs of nodes in a connected and undirected graph are connected by exactly one path, the graph is of a *tree topology*. Topology meaning nothing more than the layout of a graph. In other words, a tree topology graph does not contain any *cycles*, cycles being sub-graphs of a larger graph that have more than one path between pairs of nodes. Figure 3.5 shows an example of a tree topology graph.

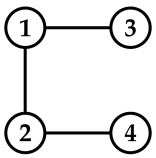

Figure 3.5: Example of a tree topology graph

A *weighted graph* is a graph that has numbers assigned to each edge. These numbers can represent anything, but are often used to defined edge length, capacity and/or cost. An example of a weighted graph is given in Figure 3.6.

3.1.2 Network optimisation

One of the simplest and oldest network optimisation problems is the *minimum spanning tree*, which is a tree topology network that connects all nodes in a graph whilst

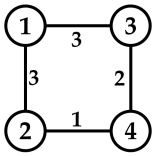

Figure 3.6: Example of a weighted graph

minimizing the sum of the weight of edges (Pettie and Ramachandran, 2002, Thulasiraman, 2016). Prim (1957) and Kruskal (1956) provide two algorithms that provide efficient solutions to the *minimum spanning tree* problem, and their approaches have been widely adopted. Other major optimisation problems include the *shortest path problem* where the objective is to find the shortest path between two nodes, a problem efficiently dealt with in an algorithm by Dijkstra (1959).

The problems above describe optimisations of either edge length or weight. When studying complex networked infrastructure systems, however, problems often involve the flow of goods through a network, like gas through a pipeline or cars on a road. The Minimum Cost Flow (MCF) problem describes the minimization of total network costs whilst sufficing all flows of goods needed to be transported through the network (Vaidyanathan et al., 2016). In the MCF problem, nodes act as either suppliers of goods (sources), demanders of goods (sinks) or have no supply or demand at all (transshipment nodes). Nodes should be connected with edges of a certain capacity so that the network is connected, meaning that there is a path between every pair of nodes in the network, and goods originating from all sources can reach all sinks. The objective function (see Equation 3.1) for the problem given a directed graph $G = (N, E)$ with costs c_{ij} and flows f_{ij} for all edges $(i, j) \in E$ is as follows:

$$\textit{Minimise} \sum_{(i,j)\in E} c_{ij} f_{ij} \tag{3.1}$$

$$\textit{Subject to} \sum_{j:(i,j)\in E} f_{ij} - \sum_{j:(j,i)\in E} f_{ji} = b(i), \ \textit{for all } i \in N \tag{3.2}$$

$$0 \leq f_{ij} \leq u_{ij}, \ \textit{for all } (i,j) \in E \tag{3.3}$$

$$\sum_{i\in N} b(i) = 0 \tag{3.4}$$

where Equation 3.2 describes that subtracting all flows x_{ji} that leave a node i from all flows x_{ij} that enter the node should equal the supply $b(i)$ of the node, meaning that all node supplies are satisfied. Equation 3.3 describes that the flow through an edge (i, j) should lie between the lower bound 0 and upper bound u_{ij}. Furthermore, the sum of all node supplies should equal zero (Equation 3.4).

As we explained earlier, utility networks are often undirected when viewed in a dynamic temporal resolution, but directed when viewed in a single point in time. The MCF problem requires all edges in a network to be directional. Undirected edges can be replaced by two directed edges flowing in opposite directions in order to deal with that constraint (see Figure 3.7).

The most efficient approach to the MCF problem according to Vaidyanathan et al. (2016) is the *network simplex method*. The network simplex approach to solving the MCF problem involves the division of all edges $(i, j) \in E$ into subsets so that $E = B \cup L \cup U$ where B is the set of *basic edges* that form a spanning tree of the underlying graph, L is the set of *non-basic edges* at their lower capacity bounds $f_{ij} = 0$

(a) Undirected **(b)** Directed

Figure 3.7: Transforming an undirected graph into a directed graph

and U is the set of *non-basic edges* at their upper capacity bounds $f_{ij} = u_{ij}$. The optimal solution is then iterated towards by exchanging *basic* with $non - basic$ edges and until the optimality conditions are reached. For a detailed description of the network simplex method's approach to the MCF problem, please refer to Kelly and O'neill (1991). In *Python*, the network simplex approach to the MCF problem is applied using the *NetworkX* module (NetworkX Developers, 2004a). In the module, the problem is first described as a linear programming problem, which is subsequently made subject to the algorithm described above.

3.2 THE MODEL TO BE ADAPTED

The NOM is written in the *Python* programming language and consists of six modelling steps: (1) input data is read, (2) supply-demand profiles are analysed, (3) a representative set of k demand - supply profiles is determined, (4) the minimal spanning tree is determined, (5) the minimum-cost-spanning tree is determined and finally (6) the minimum-cost-Steiner tree is determined (Heijnen, 2020). The creation of a Steiner tree involves the addition of transshipment nodes that have a supply of zero to the network in order to reduce overall network cost. In this research we will be focusing on determination of a minimum cost network by only using supply and demand nodes, and the final step in which the Steiner tree is determined is therefore outside the scope of this research. The first five steps of the NOM will now be described, followed by a discussion on its limitations in relation to repurposing existing infrastructure. The scenario used in the visualisations is the example experiment provided by Heijnen et al. (2020) with the NOM download file.

3.2.1 Step 1 - Read input data

The input data for the NOM consists of several input files and a number of input variables. The first input file is a set of coordinates for nodes in the network, either sinks or sources. These input nodes are defined as coordinates in a two-dimensional plane. The second input file contains a number of supply-demand profiles that each contain a list of all node demands and supplies for that given time step. If there is only one time step, this input file will contain one supply-demand profile, if there are two time steps, the input file will contain two supply-demand profiles and so forth. Node demands are input as negative supplies. The sum of all supplies in a time step should equal zero. The third input file lists all existing connections in the network. These existing connections are each defined by two coordinates defining the endpoints of the connection and a capacity. An endpoint of an existing connection can be a node from the first input file, but this is not required. The NOM has two other input files that are outside the scope of this research; routing restrictions that limit the edges that the model can choose from in its optimisation and obstacles that prohibit new edges from crossing certain areas.

There are two input variables that have to be assigned a value before the model can be run. β is the capacity-cost exponent, which represents a scaling benefit of the relationship between edge cost and capacity. $\beta = 1$ means that doubling the

capacity of a pipeline also doubles its cost, where $\beta < 1$ indicates that the relative cost of a pipeline becomes cheaper when capacity is increased. The cost for extending existing pipelines is defined by capacity coefficient cpc. In this research, we will assume that capacity expansion of existing connections is done by installing new, parallel pipelines. Thus taking cpc out of the scope of our research by assigning it a fixed value of 1.

The cost-function that the model minimises in order to find the minimal-cost network layout is defined by

$$C(G) = \sum_{e \in E_n(G)} l_e q_e^{\beta} + \sum_{e \in E_0(G)} l_e (q_e - r q_e)^{\beta}, \tag{3.5}$$

where $E_n(G)$ is the set of all new edges in the network G, l_e is the absolute length of the edge e, defined by the Euclidean distance between its end points, q_e is the capacity of edge e. Costs are also included for extension of current capacity rq_e of existing edges $E_0(G)$.

3.2.2 Step 2 - Analyse the supply-demand profiles

In this step, the supply-demand profiles over all time steps are analysed and visualised to give the user a better sense of the case being studied. This modelling step can also be used to reduce the model's running time by finding a representative subset of demand-supply profiles that provide a close enough approximation of the optimal network layout. This is done by means of a k-means clustering technique.

3.2.3 Step 3 - Determine representative set of k supply-demand profiles

In this step, you have the option to manually set the value for k, which is the number of representative supply-demand profiles that the model will use in its heuristics. This value can be based off the k-means clustering analysis in step 3 in order to reduce model running time whilst maintaining an acceptable level of accuracy.

3.2.4 Step 4 - Determine minimal spanning tree

The first graph that the model generates is the minimum spanning tree, the network that connects all sinks and sources whilst minimizing the sum of edge lengths. Figure 3.8 shows the minimal spanning tree for the example experiment. The capacity added to each edge in the tree is the maximum capacity that flows through it over all time steps.

3.2.5 Step 5 - Determine minimum-cost-spanning tree

In order to improve on the minimal spanning tree, in this step costs are included into the optimisation. Connections in the minimal spanning tree are iteratively restructured by swapping two edges in order to find a better solution. This heuristic is based on the *"edge-swap"* method, as described by Heijnen et al. (2020). Iterations towards the minimum cost spanning tree and the final result of this step for the example experiment can be seen in Figure 3.8.

3.2.6 Limitations of this approach

The modelling approach of the NOM is very proficient in finding minimum-cost networks (Heijnen et al., 2020). When investigating the implications of repurposing existing infrastructure, however, it has two shortcomings. Not taking into account

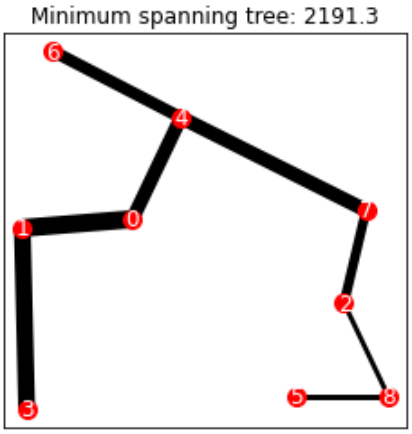

Figure 3.8: Minimal spanning tree created by the NOM

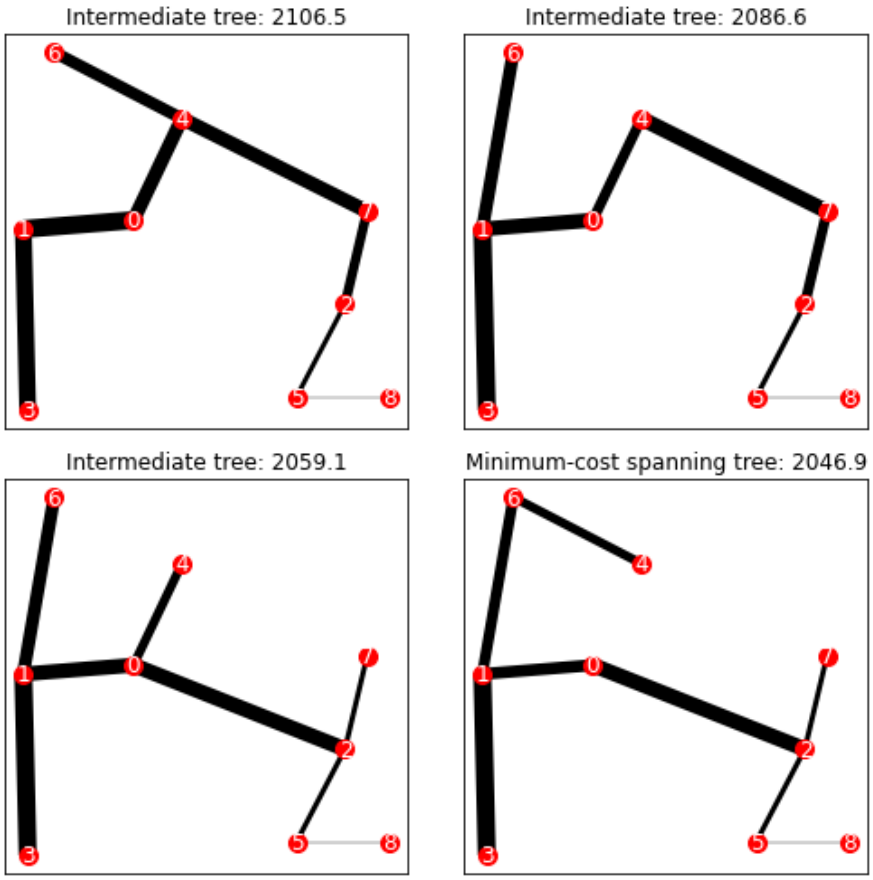

Figure 3.9: Intermediate iterations towards the minimum-cost spanning tree by the NOM

repurposing costs for existing connections, and not being able to process or create cycles in the network layout.

The costs related to the use of existing connections is given by the formula

$$\sum_{e \in E_0(G)} l_e(q_e - rq_e)^\beta \tag{3.6}$$

taken from Equation 3.5. The cost of existing connections is thus only defined by its capacity expansion $q_e - rq_e$, and no costs are related to using the remaining capacity rq_e that is already present. In Chapter 1 we have established that repur-

posing existing networked infrastructure is often paired with case-specific costs. A modelling approach fit for investigating implications for repurposing of this infrastructure should therefore include a cost function related to using existing connections.

3.3 MODEL ADAPTION

In this paragraph, we will describe adaptions made to the NOM in order to create the NROM. First, an adaption to the cost function will be described, after which the novel heuristics will be described that replace steps 4 and 5 of the NOM.

3.3.1 Cost function adaption

The cost function from the NOM is described by Equation 3.5. This cost function is used as a basis for the cost function of the NROM. A cost function that describes the cost of using existing edges is added to the original cost function. The novel cost function for using existing edges is defined as follows:

$$C_r(G) = rpc \sum_{e \in E_0(G)} l_e r q_e^\beta \tag{3.7}$$

where rpc is the relative cost of repurposing existing edges as opposed to building a new one. If $rpc = 1$, the cost of repurposing is equal to building a new pipeline. If $0 < rpc < 1$, repurposing existing infrastructure is cheaper than creating new pipelines and if $rpc = 0$, repurposing existing infrastructure is free. The cost related to repurposing an existing connection is always calculated over the full existing capacity rq_e present, as we assume that the full capacity of the existing connection has to be repurposed for it to be able to be used in the new network.

Combining the existing cost function from the NOM with the new cost function for using existing infrastructure leaves us with the following cost function used in the NROM:

$$C(G) = \sum_{e \in E_n(G)} l_e q_e^\beta + \sum_{e \in E_0(G)} l_e (q_e - r q_e)^\beta + rpc \sum_{e \in E_0(G)} l_e r q_e^\beta \tag{3.8}$$

When assigning existing connections with their capacity rq_e, capacities have to be given for the new commodity after repurposing. So when, for example, a NG pipeline is repurposed for hydrogen transport, both the capacity q_e of new pipelines and the capacity rq_e of existing pipelines should be in terms of hydrogen transport capacity.

3.3.2 Modelling steps in adapted model

In this section, we provide a detailed description of the steps in the NROM. In the actual code, these steps are sometimes intertwined and more complicated than described here. The explanation given here is a simplification that provides a general understanding of the modelling steps and the novel heuristics applied. The scenario used in the visualisations is the example experiment provided by Heijnen et al. (2020) with the NOM download file.

Step 1 - Read input data

The reading of the input data in the NROM is, for the most part, identical to the procedure in the NOM. Node locations, existing connections and supply-demand

sets are read from the input files. Values for input variables β and novel variable rpc are read.

Step 2 - Analyse the supply-demand profiles

This step is completely copied from the NOM.

Step 3 - Determine representative set of k supply-demand profiles

This step is also completely copied from the NOM.

Step 4 - Creating a complete graph

In this step, the NROM starts to substantively deviate from the approach in the NOM. In order to prepare the graph for the coming optimisation steps, a *complete graph* is created from the input data. The model creates a graph that places all the nodes at the right coordinates and connects each node to every other node in the network directly. This step does not deal with capacities and does not distinguish existing pipelines from new pipelines, it is simply a preparation step that serves as a starting point for optimisation. An example of a graph resulting from this step can be seen in Figure 3.10. Existing edges (9,10) and (10,11) are highlighted in blue, this is however merely a visual artefact of the algorithm that draws plots of the created network.

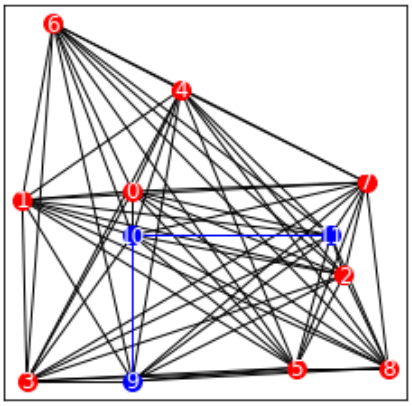

Figure 3.10: Complete graph

Step 5 - Creating the base network

The goal of this step is to create a *base network* that serves as a starting point for further optimisation. The *base network* is a connected graph in which all nodes are connected by edges that are assigned a capacity so that all node supplies and demands are satisfied, whilst minimising total network cost. This step revolves around the network simplex approach to the MCF problem (see Equation 3.1) and utilises the *min-cost-flow algorithm* from the *Python NetworkX package* (NetworkX Developers, 2004b). Because of limitations to the *network simplex algorithm*, edge cost is defined by $c_e = q_e l_e$ for new edges and by $c_e = rpc \cdot rq_e l_e$ for existing edges. This will result in a cost-minimised network, that does not take into account scaling benefits and existing capacity expansion, but serves as a good starting point for further optimisation. The scaling benefits of β and the expansion of existing connections are addressed in modelling step 6. As addressed previously, we assume that when an edge is repurposed, the complete capacity of that edge has to be repurposed. This is addressed by including rq_e in the cost function for existing edges.

The novel *network_simplex_repurposing heuristic* uses the *complete graph* created in step 4 as input to create the *base network* as output. The *base network* is the first

intermediate optimisation result that provides a network layout that connects all node supplies to demands with edges of sufficient capacity. Refer to Algorithm 3.1 for pseudocode of this algorithm. The pseudocode is shown in two colours, as there are two different pathways depending on the number of time steps given in the input files. These two pathways will now be explained.

The first, and most straightforward, pathway is used when there is only one time step involved. This pathway is indicated by the black lines in Algorithm 3.1 and consists of preparing the *complete graph* for optimisation by the *min_cost_flow algorithm* and subsequently running that algorithm. The heuristic starts with assigning all the nodes present in the *complete graph* with demands and supplies from the one time step given in the input files. The upper capacity limit u_e of all edges e in the *complete graph* is subsequently set to ∞, telling the *min_cost_flow algorithm* that there is no limit to the maximum capacity that can be assigned to these edges. An exception is made for existing edges, whose upper capacity bounds are limited to the existing capacity rq_e. This means that in this modelling step, as mentioned earlier, the capacity of existing edges can not be expanded. The cost of edges e is defined by $c_e = l_e q_e$ for new edges and by $c_e = rpc \cdot l_e rq_e$ for existing edges. The reason for limiting existing edges to their existing capacity is due to limitations in the *min_cost_flow algorithm*. This limitation occurs when repurposing an existing edge but simultaneously expanding its capacity. The costs of the edge e are then defined by both repurposing costs and expansion costs following $c_e = \cdot l_e(q_e - rq_e) + rpc \cdot l_e rq_e$. The relationship between capacity extension costs and repurposing costs are dependent on the extra capacity assigned by the *min_cost_flow algorithm*, and their influence on final edge cost can therefore not be determined before the application of the algorithm because it can not include both the repurposing and expansion of an existing pipeline in its cost calculation. When limiting the capacity of existing edges to rq_e, and not taking into account capacity expansion in this step, costs of existing edges are defined only by their repurposing costs. When $rpc < 1$, the cost of an edge e can then be defined by $c_e = rpc \cdot l_e rq_e$, which can be accounted for when applying the *min_cost_flow algorithm*.

After all maximum edge capacities and cost formulas are assigned to the edges in the *complete graph*, the graph is prepared for application of the *min_cost_flow algorithm* from the *Python NetworkX package*. First, TSG, a copy of the *complete graph*, is created to save edge capacities. All undirected edges in the *complete graph* are then replaced by two directed edges, as the *min_cost_flow algorithm* only works with directed graphs. The algorithm is subsequently applied to the *complete graph* and maximum flows through each edge are saved to the TSG. Finally, the TSG is returned as the *base graph*.

To summarise, when there is only one time step present in the input files, the *network_simplex_repurposing heuristic* performs the following steps;

1. Assign all nodes in the complete graph resulting from modelling step 4 with demands and supplies given in the input files.
2. Assign each edge in the complete graph with an upper capacity limit, depending on it being a new or existing edge.
3. Assign each edge in the complete graph with a cost function, depending on it being a new or existing edge.
4. Apply the *min_cost_flow algorithm* from the *networkX package*.
5. Save the *base graph*.

When the model is faced with multiple time steps in the form of multiple supply-demand sets, another pathway has to be used, as the *network simplex algorithm* does not support working with multiple time steps. It is now that the teal lines in Algorithm 3.1 come into play. The same optimisation described above is performed, but

Algorithm 3.1: network_simplex_repurposing heuristic

Input: Complete graph CG, repurposing cost coefficient rpc and input data from step 1
Output: Base graph BG

let XG be a copy of graph CG in which edge attributes can be saved
let *timesteps* be the file in the input data that contains supply and demand profiles, each on a separate line
for *every edge e in graph XG* **do**
    set *occurrence* of e to 0
    set *average capacity* of e to 0
for *every timestep in timesteps* **do**
    assign nodes in CG with supplies and demands from timestep
    for *every edge e in graph CG* **do**
        if *e is an existing edge* **then**
            set *upper capacity limit* of e to *existingcapacity rq* of e
            let *cost* of e be defined by $c_e = rpc \cdot l_e q_e$
        else
            set *upper capacity limit* of e to ∞
            let *cost* of e be defined by $c_e = l_e q_e$
let TSG be a copy of graph CG
let $flows$ be a dictionary of flows over edges $\#flows = min\_cost\_flow(CG)$
for *every edge* (i,j) *in* TSG **do**
    if $flow$ *of* (i,j) *or* (j,i) *in* $flows > 0$ **then**
        set *capacity* of (i,j) in TSG to the maximum of $flow$ (i,j) and (j,i)
    else
        set *capacity* of (i,j) to 0
for *every edge e in graph TSG* **do**
    if *if capacity q of* $e > 0$ **then**
        add 1 to *occurrence* of e in graph XG
        add q to *average capacity* of e in XG
for *every edge e in graph XG* **do**
    if *occurrence of* $e > 1$ **then**
        divide *average capacity* of e by *occurrence* of e
if *the number of lines in timesteps* > 1 **then**
    $TSG = timesteps\_merged(XG)$ #see Algorithm 3.2
return TSG

instead of only optimising for one time step, the heuristic now creates an optimised network for each of the different time steps. The occurrence occ_e of all edges e over all the time steps, defined by

$$occ_e = number\ of\ timesteps\ where\ edge\ e\ occurs\ in\ optimised\ network \tag{3.9}$$

is saved. If there are four time steps, and an edge e is present in two of the four networks created, $occ_e = 2$. The average capacity $avgcap_e$ of all edges e over all time steps, defined by

$$avgcap_e = \frac{sum\ of\ q_e\ over\ all\ time\ steps}{occ_e} \tag{3.10}$$

is also saved. If edge e occurs twice over four time steps with capacities 10 and 20, $avgcap_e = \frac{10+20}{2} = 15$. The next step is to apply the second novel heuristic, the *timesteps_merged heuristic*, that will combine all the separate optimisations for each time step into one network. Pseudocode for the *timesteps_merged heuristic* can be viewed in Algorithm 3.2.

The heuristic starts by calculating the importance imp_e for all edges e over all the time steps, which is described as follows;

$$imp_e = RI\frac{occ_e}{\max(\{occ_e, e \in E\})} + (1 - RI)\frac{avgcap_e}{\max(\{avgcap_e, e \in E\})} \tag{3.11}$$

with parameter RI being the relative importance of edge occurrence over average edge capacity, which will be calibrated in Chapter 4. By dividing the occurrence of each edge by the maximum occurrence over all edges, and doing the same for all average capacities, they become fractions that are comparable to each other in the calculation of edge importance. After the importance of each edge is calculated, a list of all edges is created that ranks them from least important to most important. All edges are removed from the *complete graph* so that only nodes remain. Edges are then iteratively added to the node-only graph starting with the most important edge from the list. A *tree topology graph* is created by adding the most important edge that is not an existing edge and does not create a cycle until all nodes are connected. All nodes are connected with new edges as to ensure that all transmission capacity demands are met, as we have limited the capacity of existing edges to their existing capacity in this modelling step, which might not be sufficient to fulfil capacity demands. A tree topology graph is created, with no cycles, because cycles in the network that only consist of new edges will never be cost optimal. After the tree topology graph is created using the most important new edges, all existing edges that occurred during the separate time step optimisations are returned to the network, as these do have the ability to create cycles that are the most cost optimal layout.

The graph that has now been created is then prepared for optimisation by the *network simplex algorithm* in the same manner as in the *network_simplex_repurposing heuristic*. The *network_simplex_repurposing heuristic* assigns capacities to all the edges in the graphs for each time step and the maximum capacity assigned to each edge over all time steps is the capacity that is assigned to that edge in the graph that the *timesteps_merged heuristic* returns to the *network_simplex_repurposing heuristic*. Edge lengths of existing edges are restored, and the *base graph* is saved.

To summarise, when there is more than one time step present in the input files, the *network_simplex_repurposing heuristic* performs the following steps;

1. Create a copy of the complete graph to save edge occurrences and average capacities
2. Assign all nodes in the complete graph resulting from modelling step 4 with demands and supplies given in the input files.
3. Assign each edge in the complete graph with an upper capacity limit, depending on it being a new or existing edge.
4. Assign each edge in the complete graph with a cost function, depending on it being a new or existing edge.
5. Apply the *min_cost_flow algorithm* from the *networkX package*.
6. Repeat steps 2 to 5 for each time step, and save the occurrence and average capacity of each edge over the time steps.
7. Apply the *timesteps_merged* heuristic (see Algorithm 3.2).

Algorithm 3.2: timesteps_merged heuristic

Input: Complete graph XG with edge attributes *occurrence* and *average capacity* and repurposing cost coefficient rpc
Output: Base graph BG

create list L to save edge *importance*
let *timesteps* be the file in the input data that contains supply and demand profiles
for *every edge e in graph XG* **do**
    calculate *importance* of e following Equation 4.2
    append e and its *importance* to L
sort edges in L on *importance*
remove existing edges from L
remove all edges from XG, so that only nodes remain
while *XG is not connected* **do**
    add edge e, the edge in L with the highest *importance*, to XG
    remove e from L
    if *a cycle was created* **then**
        remove e from XG
add all existing edges to XG
Let YG be a copy of graph XG to save maximum capacities over timesteps
for *every edge e in graph YG* **do**
    set edge capacity to 0
for *every timestep in timesteps* **do**
    assign nodes in XG with supplies and demands from timestep
    for *every edge e in XG* **do**
        if *e is an existing edge* **then**
            set *upper capacity limit* of e to the existing capacity rq of e
            let cost of e be defined by $c_e = rpc \cdot l_e q_e$
        else
            set *upper capacity limit* of e to ∞
            let cost of e be defined by $c_e = l_e q_e$
    let TSG be a copy of graph XG
    let $flows$ be a dictionary of flows over edges
     $\#flows = min\_cost\_flow(XG)$
    for *every edge* (i,j) *in TSG* **do**
        if $flow$ *of* (i,j) *or* (j,i) *in* $flows > 0$ **then**
            set *capacity* of (i,j) in TSG to maximum of $flow$ (i,j) and (j,i)
        else
            set *capacity* of (i,j) to 0
    for *every edge e in graph TSG* **do**
        if *capacity of e in TSG* $>$ *capacity of e in YG* **then**
            replace capacity of e in YG by capacity of e in TSG
return YG

8. Save the *base graph*.

In Figure 3.11, the base network for the example case with four time steps is shown. We see that because we have excluded the scaling benefit of β, shortest paths are always the cheapest when considering new edges. This results in star shaped structures. In the next optimisation step, we will introduce the component of scaling benefits. We will also introduce the expansion of existing edges.

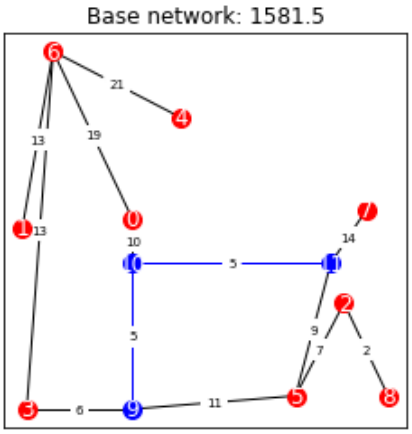

Figure 3.11: Base network graph with edge capacities

Step 6 - Creating the intermediate network

In step 5 we created a *base graph* that gives a cost minimised network layout that meets all needed transmission capacity but does not take into account expansion of existing connections and capacity-cost coefficient β. This optimisation step will include both those elements by applying the novel *joined_edges heuristic* to the *base graph* and thus creating the further optimised *intermediate graph*. The heuristic aims to iteratively combine edges to find and apply scaling benefits. Please refer to Algorithm 3.3 for pseudocode of the *joined_edges heuristic*.

The heuristic starts with the creation of a dictionary D of edge pairs EP in the *base graph*. Edge pairs are defined as pairs of edges that have one of their endpoints connected to the same node. For each edge pair, four pieces of data are stored in the dictionary, the angle EP_{angle} between the two edges at the common node, the shortest edge a of the pair, the longest edge b of the pair and the edge c between end points of a and b that are not located at the same node. Of the three edges e, their length l_e and capacity q_e is also stored in the dictionary. Edge c might not exist in the *base graph*, in which case its capacity in the dictionary equals $q_c = 0$. A visual example of an edge pair, and its data stored in the dictionary, is given in Figure 3.12.

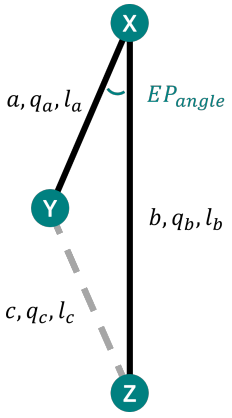

Figure 3.12: Example of an edge pair

The heuristic then takes the edge pair with the shortest angle, which is a good indicator of scaling benefit potential, which we will explain later, and checks whether adding the capacity of longer edge b to the capacities of edges a and c, and deleting edge b is cheaper than the original configuration of the edge pair. The formula for this is described by

$$l_a qn_a^\beta + l_c qn_c^\beta < l_a qo_a^\beta + l_b qo_b^\beta + l_c qo_c^\beta \tag{3.12}$$

where a is the shortest edge of the pair, b is the longest edge of the pair and c is the edge opposite to the angle. l is the edge length, qo its old capacity, qn its new capacity in the alternative layout and β the capacity-cost exponent. Equation 3.12 will return true if the alternative layout is cheaper. For a schematic example of the old and new layouts, refer to Figure 3.13.

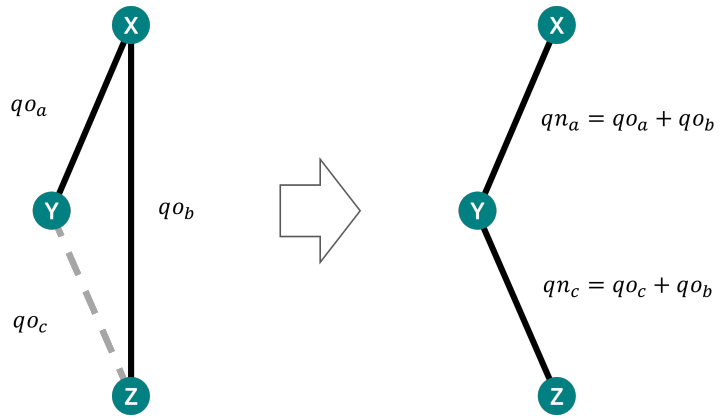

Figure 3.13: Example of local optimisation where q is the edge capacity

We stated before that small EP_{angle} is a strong indicator for scaling benefits. This is the case because capacities can be joined whilst keeping the increase in $l_e q_e$ low. When joining edges like in Figure 3.13, $l_e q_e$ will often increase because we are replacing a straight edge between two nodes by a longer pathway. Scaling coefficient β in edge cost function $c_e = l_e q_e^\beta$ and repurposing cost coefficient rpc in repurposing cost function $c_e = rpc \cdot l_e r q_e^\beta$ can make the new situation cheaper, however, whilst still allowing for the same capacities to reach the same nodes. If the new situation does indeed turn out to be cheaper than the original (Equation 3.12 returns true), the change is applied to the *base graph*. The dictionary will be updated according to the change in layout and the new edge pair with the shortest EP_{angle} is selected, and the iteration starts again.

If replacing the longest edge of the pair is not cheaper than the original situation, the heuristic will check whether replacing the shortest edge of the pair results in the cost reduction we are looking for. This calculation is described by

$$l_b qn_b^\beta + l_c qn_c^\beta < l_a qo_a^\beta + l_b qo_b^\beta + l_c qo_c^\beta \tag{3.13}$$

and will return true if the alternative layout is cheaper. For a visualisation of this situation, view Figure 3.14.

If neither of these alternative situations is cheaper, the edge pair is saved as 'unsuccessful' and skipped in further iterations. Figure 3.15 shows all iterations performed by the heuristic on the example case. The graph that results from the final improvement, in this case improvement 3, is saved as the *intermediate network*.

The calculations of new and old edge capacities qn and qo in Equation 3.12 and Equation 3.13 are dependent on a number of different factors, for a detailed account of these capacity calculations please refer to Appendix A.

In this modelling step, we are working with a graph that has to fulfil capacity demands for multiple time steps. This results in optimisations being performed on an undirected graph. Because of this, we can not take into account directions of flows through the edges and their magnitudes when performing the local optimisations described above. Adding edge capacities to each other ensures that the new layout

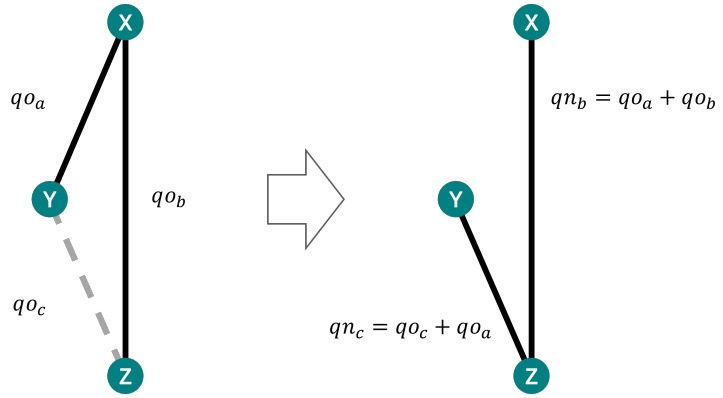

Figure 3.14: Example of local optimisation where q is the edge capacity

can satisfy all transport demands of the network, but edge capacities may be too large and could potentially be reduced, whilst still meeting capacity demands. This results in the possibility for optimisations in this step to be overlooked because of overcapacity as a result of joining edges. In the next modelling step this overcapacity is accounted for by applying the *min_cost_flow algorithm* which will account for overcapacities, but can not detect overlooked optimisations. This is a limitation to the model that should be looked into in later versions.

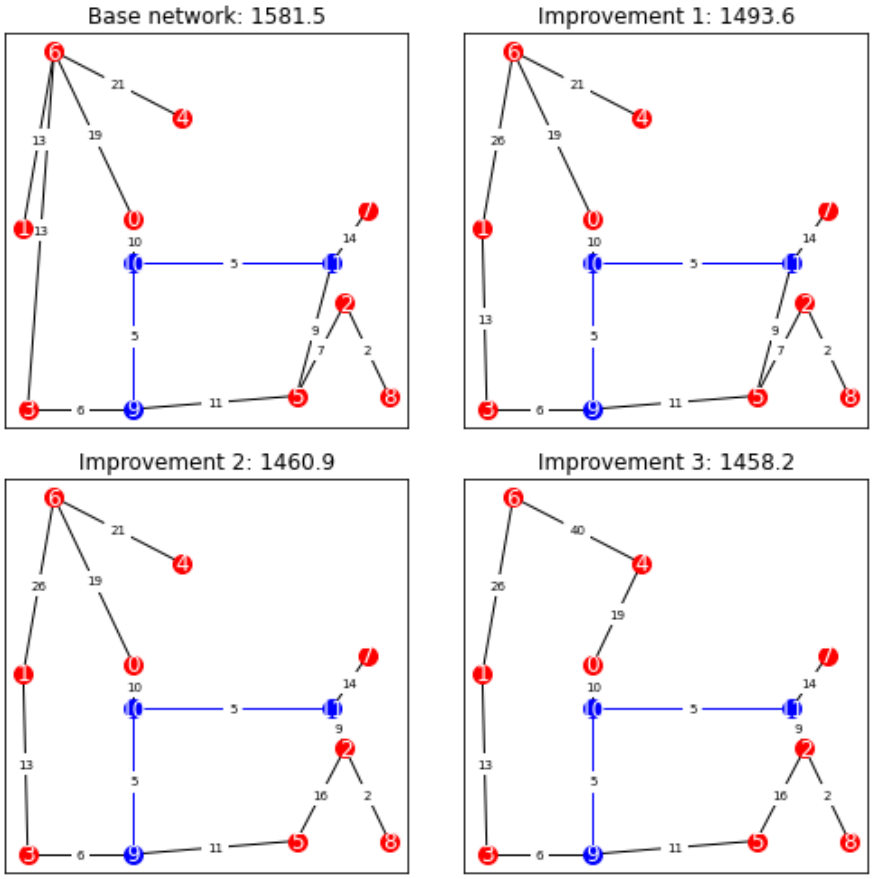

Figure 3.15: Iterations of modelling step *joined_edges heuristic*

Algorithm 3.3: joined_edges heuristic

Input: Base graph BG, capacity-cost coefficient β, repurposing cost coefficient rpc and input data from step 1
Output: Intermediate graph IG

```
1  let D be a dictionary to save all edgepairs in graph BG
2  create an empty list U to save all unsuccessful optimisation attempts
3  for every node n in graph BG do
4      if more than one edge is connected to n then
5          append each possible combination of two edges connected to n as
             edgepair to D
6  while there are still edgepairs in D do
7      if edgepair in U then
8          remove edgepair from D
9      for every edgepair in D do
10         determine the angle between the two edges in the edgepair
11         let a be the shortest edge in edgepair
12         let b be the longest edge in edgepair
13         let c be the edge opposite to angle      #has a capacity of 0 if it does
             not exist in BG)
14     sort all edgepairs in D on size of angle
15     for edgepair in D with the with smallest angle do
16         if adding capacity of b to capacity of a and c, and deleting b, is cheaper
             than the original situation, following Equation 3.12 then
17             add capacity of edge b to capacity of edge a in graph BG
18             add capacity of edge b to capacity of edge c in graph BG
19             remove edge b from graph BG
20         else if adding capacity of a to capacity of b and c, and deleting a, is
             cheaper than the original situation, following Equation 3.13 then
21             add capacity of edge a to capacity of edge b in graph BG
22             add capacity of edge a to capacity of edge c in graph BG
23             remove edge a from graph BG
24         else
25             append edgepair to U
26     update D if the layout of graph BG has changed
27 return BG
```

Step 7 - Creating the final network

The purpose of this final step is to take redundancies out of the *intermediate graph* created in step 6, thus creating the final cost minimised graph.

The *network_simplex_repurposing heuristic* is applied (Algorithm 3.1), but instead of applying it to the *complete graph* resulting from step 4 it is applied to the *intermediate graph* resulting from step 6. In case the capacity of an existing edge has been expanded in modelling step 6, the upper capacity limit for that edge is set to existing capacity rq_e plus the expanded capacity in step 10 of Algorithm 3.1 and step 21 of Algorithm 3.2. The edge cost calculations in step 11 of Algorithm 3.1 and step 22 of Algorithm 3.2 are changed to

$$c_e = \frac{rq_e}{q_e} \cdot l_e q_e \cdot rpc + \frac{q_e - rq_e}{q_e} \cdot l_e q_e \tag{3.14}$$

for that particular edge in order to properly take into account *rpc* during the application of the *network simplex* algorithm. Results of the application of this final step in the example experiment can be viewed in Figure 3.16.

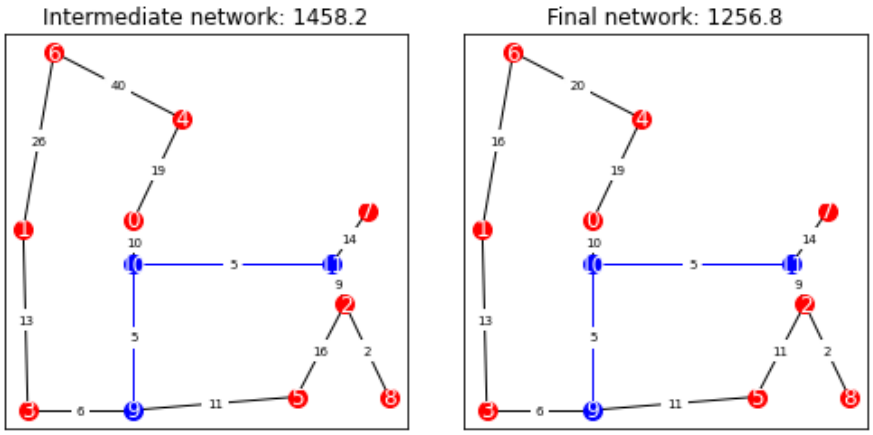

Figure 3.16: Final optimisation step

4 MODEL VERIFICATION AND CALIBRATION

In this chapter, we will first verify the inner working of the model by applying it to a number of simple test cases and mathematically assessing the modelling results. We will then calibrate the optimal value for the parameter RI that is used in the calculation of the importance of an edge.

4.1 VERIFICATION OF BASIC MODEL FUNCTIONALITY

In their guide to good modelling practice, Nikolic et al. (2019) suggest that a modeller should perform 'unit testing' as a means to demonstrate the basic functionalities of the model. In order to verify that basic functionalities of the created model work accordingly, a number of test cases have been created. These test cases serve the purpose of checking whether the model produces the expected results, and is therefore consistent with its intended purpose. Several test cases are described that put an increasing level of strain on the required complexity with which the model has to handle. In each of the tests, different values for β and rpc are used and model behaviour is analysed.

4.1.1 Test case 1 - The triangle

We start with a very simple test case that will allow us to verify whether repurposing costs are assigned correctly, and correctly included into the optimisation process. The optimal solution for this test case is easily checked by utilising the Pythagorean theorem of straight triangles.

The case consists of three nodes in total. A hydrogen production facility, represented by node 0, is at coordinates (0,100) with a hydrogen supply of magnitude 10. A factory that uses hydrogen as feedstock to produce polymer products is represented by node 1. Node 1 is located at coordinates (100,0) with a hydrogen demand of magnitude 10. An existing pipeline of capacity 10 is present between the production facility at coordinates (0,100) and a connection point, represented by node 2 at coordinates (100,100). The connection point at node 2 does not have a hydrogen supply or demand.

Test 1.1 - NOM benchmark

β: 1.00
rpc: 0.00

When setting repurposing to true, and rpc to zero, re-use of the existing pipeline should be free and the shortest path to connect demand to supply would be adding a pipeline with capacity 10 between node 2 and node 1. This would result in a total network costs of 1000, which is the cost of the single added pipeline. The model works as expected and produces the same optimal network as the NOM as shown in Figure 4.1.

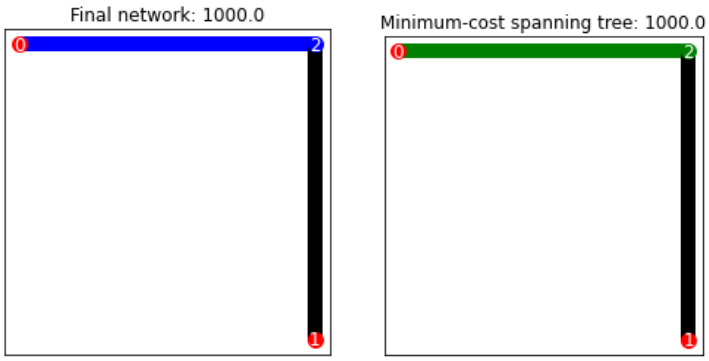

Figure 4.1: Triangle test $\beta = 1$, $rpc = 0$. Left: NROM. Right: NOM

Test 1.2 - Mathematical check of rpc in optimisation

β: 1.00
rpc: 0.40 & 0.42

Following Pythagoras theorem, the length of an edge between node 0 and node 1 is 141.42. Because of limitations to the *NetworkX* approach to the MCF problem, all edge lengths have to be rounded before optimisation. Therefore, in this case description we will also work with rounded edge lengths, and thus edge (0,1) has a length of 141. With a β value of one, the cost of this edge would be 1410. For the model to prefer creating a new edge between node 0 and node 1, as opposed to repurposing the edge between 0 and 2 and build a new one between 2 and 1, the cost of this new route should be cheaper. For the new route to be cheaper, the cost for repurposing the existing pipeline should exceed a cost of 410. To verify whether the model handles this situation correctly, two tests will be run where the rpc will be set to 0.40 in one run, and 0.42 in the other, resulting in repurposing costs of 400 and 420 respectively. If the model works as expected, the run with rpc at 0.40 will re-use the existing pipeline for a total network cost of 1400. In the case of rpc set to 0.42, re-use of the existing pipeline will result in a total network cost of 1420, exceeding the cost of creating an edge between nodes 0 and 2. Hence, the model should cost-optimise the network by not re-using the existing pipeline and replacing it by a pipeline between 0 and 2, for a total network cost of 1410. As can be viewed in Figure 4.2, the model worked as expected.

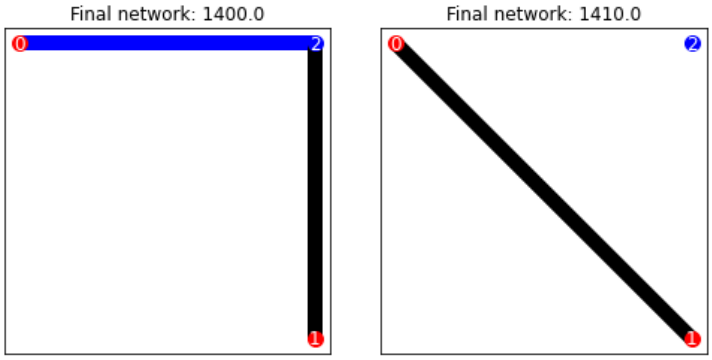

Figure 4.2: Triangle test $\beta = 1$. Left: $rpc = 0.40$. Right: $rpc = 0.42$

Test 1.3 - Mathematical check of rpc and β in optimisation

β: 0.50
rpc: 0.00 & 0.10

When introducing a β to the model that is a decimal number between zero and one, things start to get more complicated. First, we want to make sure that the capacity-cost exponent is properly applied to both existing, and new pipelines. For this purpose, we will first set the rpc to 0, so that the existing pipeline is free, and we can check whether the β is properly applied to new pipelines. With the β at 0.50 it is expected that the cost of the optimal network will be 316.2, which is the square root of the capacity of pipeline (1,2) times its length. Setting the rpc to 0.1 should add to that a cost of 31.6 for the repurposed pipeline (0,2), adding up to a total network cost of 347.8. As can be seen in Figure 4.3 the model functions as expected, with a minor deviation caused by rounding within the model.

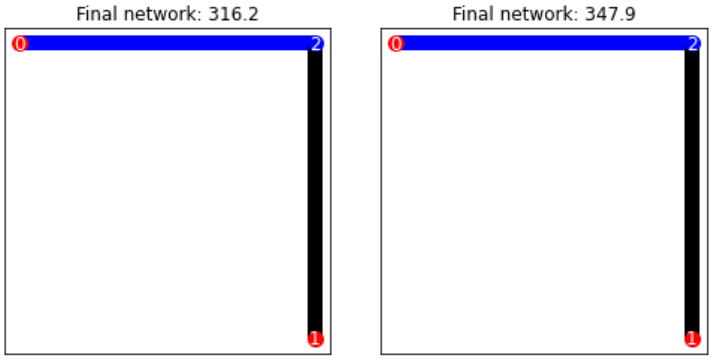

Figure 4.3: Triangle test β = 0.5. Left: rpc = 0.00. Right: rpc = 0.10

4.1.2 Test case 2 - The constrained triangle

Having verified the most basic workings of the model, it is now time to add to the complexity of the triangle test case. Instead of an existing pipeline (0,2) that has a capacity of 10 so that it can potentially fulfil all transport between nodes 0 and 1 we will now limit the existing capacity of pipeline (0,2) to 5.

Test 2.1 - NOM benchmark

β: 1.00
rpc: 0.00

Limiting the capacity of the existing pipeline (0,2) to 5 creates the possibility for a looped network to be the most cost-optimal network layout. Take, for example, a value of 0 for the rpc. The cheapest possible network layout would then be to use the existing pipeline, extend it with a pipeline (1,2) of capacity 5 but create a pipeline (0,2) with 5 capacity to transport the rest of the supply. The cost of this optimal network should account to 1205. Figure 4.4 shows that the model performs as expected, and that the solution is 14.8% cheaper than the solution of the NOM that is not able to create a looped network.

Test 2.2 - Mathematical check of rpc in optimisation

β: 1.00
rpc: 0.40 & 0.42

In a manner that is very similar to test case 1.2 we can derive that an rpc of 0.41 is the tipping point where both possible solutions yield the same result. Again, we will test this by running the model at both 0.40 and 0.42 rpc for the constrained triangle case. As expected, the model chooses the cost-optimal network layout in

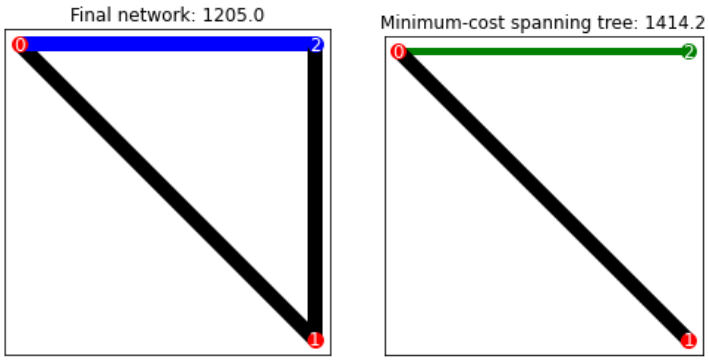

Figure 4.4: Constrained triangle test $\beta = 1$, $rpc = 0$. Left: NROM. Right: NOM

both cases which have a respective total network costs that amount to 1405 and 1410 as can be seen in Figure 4.5.

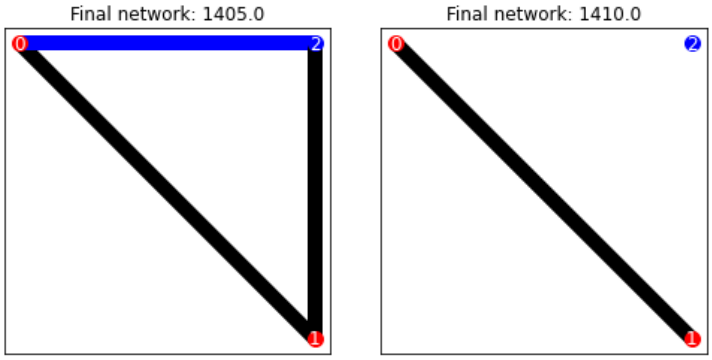

Figure 4.5: Constrained triangle test $\beta = 1$. Left: $rpc = 0.40$. Right: $rpc = 0.42$

4.1.3 Test case 3 - The double triangle

Our next step in complexing the test case is to mirror case 2 on both the X-axis and Y-axis. This will allow us to check whether the model also produces the expected results when it is presented with more degrees of freedom. Because test case 1 is mirrored, total network costs are expected to be twice that of the respective tests under test case 1.

The case consists of 5 nodes in total. A hydrogen production facility represented by node 0 is located at coordinates (0,200) with a supply of magnitude 10. A polymer production facility, represented by node 1, is located at coordinates (100,100) with a demand of magnitude 20. Another production facility, node 2, is located at coordinates (200,0) with a supply of 10. Two existing connections of capacity 10 are also present. The first is situated between the production facility at node 0 and coordinates (100,200), with node 3 automatically generated by the model at those coordinates with no supply or demand. The second existing connection is situated between the production facility at node 2 and coordinates (100,0), with node 4 automatically generated by the model at those coordinates with no supply or demand.

Test 3.1 - NOM benchmark

In this test, the same input variables were used as were used in test 1.1. The model operated as expected and produces the same result as the NOM. Results can be viewed in Figure 4.6.

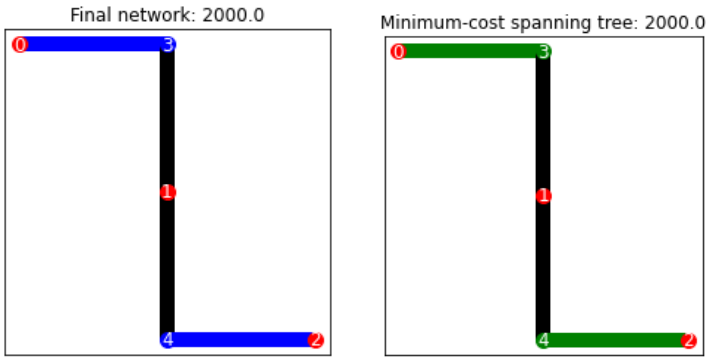

Figure 4.6: Double triangle test $\beta = 1$, $rpc = 0$. Left: NROM. Right: NOM

Test 3.2 - Mathematical check of rpc in optimisation

In this test, the same input variables were used as were used in test 1.2. The model operated as expected. Results can be viewed in Figure 4.7.

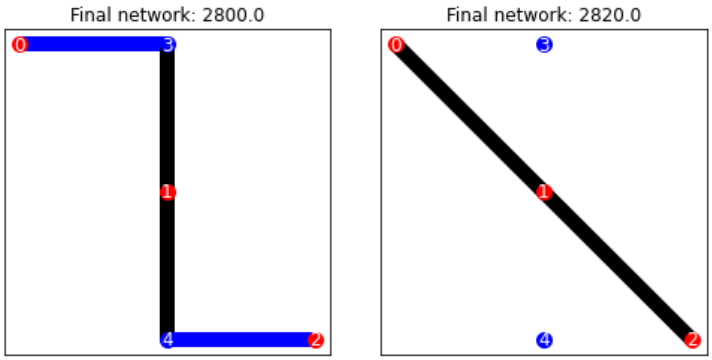

Figure 4.7: Double triangle test $\beta = 1$. Left: $rpc = 0.40$. Right: $rpc = 0.42$

Test 3.3 - Mathematical check of rpc and β in optimisation

In this test, the same input variables were used as were used in test 1.3. The model operated as expected. Results can be viewed in Figure 4.8.

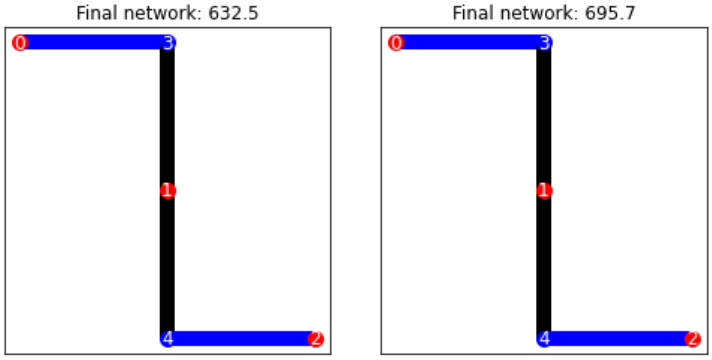

Figure 4.8: Double triangle test $\beta = 0.50$. Left: $rpc = 0.00$. Right: $rpc = 0.10$

4.1.4 Test case 4 - The constrained double triangle

Having verified the most basic workings of the model, it is now time to add to the complexity of the double triangle test case. This will be done in the same manner as in test case 2 by limiting the capacity of the existing edges to 5. Because test case 4 is exactly two times the size of test case 2, resulting optimal network costs are expected to be double that of the respective tests in case 2.

Test 4.1 - NOM benchmark

In this test, the same input variables were used as were used in test 2.1. The model operated as expected, and produces a 14.8% cheaper result than the NOM. Results can be viewed in Figure 4.9.

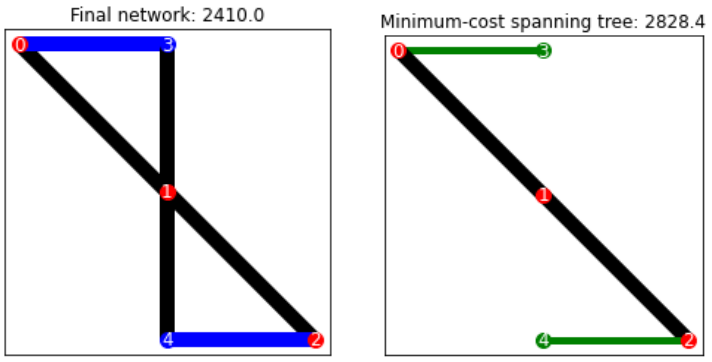

Figure 4.9: Constrained double triangle test $\beta = 1$, $rpc = 0$. Left: NROM. Right: NOM

Test 4.2 - Mathematical check of rpc in optimisation

In this test, the same input variables were used as were used in test 2.2. The model operated as expected. Results can be viewed in Figure 4.10.

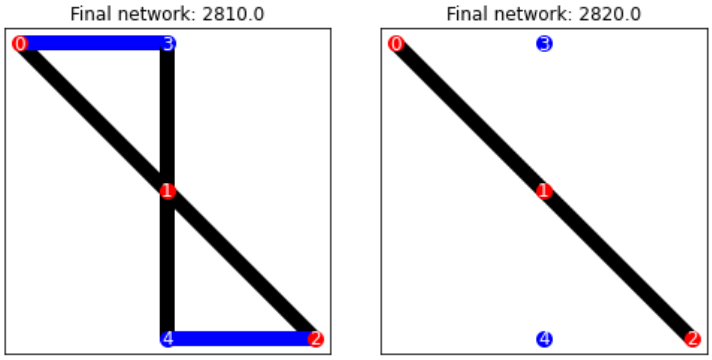

Figure 4.10: Constrained double Triangle test $\beta = 1$. Left: $rpc = 0.40$. Right: $rpc = 0.42$

4.1.5 Test case 5 - The diamond

In test cases 3 and 4 we have verified that the model works accordingly when faced with two separate loops that have to be created to find the cost-optimal network layout. For our next step, we want to find out whether this is also the case when faced with an optimal network layout that requires the creation of loops within loops.

The case consists of a total of 4 nodes. A production facility, represented by node 0, is located at coordinates (100,0) with a supply of 20. A polymer production facility at node 1 is located at coordinates (100,200) with a demand of 20. Two existing pipelines of capacity 10 are present, both stemming from the polymer production facility at node 1 and one reaching to connection points at coordinates (100,0) and the other to (100,200). At these coordinates two nodes are automatically generated by the model with no supply or demand. Node 2 is situated at (100,0), and node 3 at (100,200).

Test 5.1 - NOM benchmark

Because the existing edges (1,2) and (1,3) have sufficient capacity to transport all supply from node 1 to nodes 2 and 3, when setting rpc to zero, the optimal network layout should use the two existing edges and create two new edges (0,2) and (0,3) of capacity 10. Following the Pythagorean theorem, this should account for a total network cost of 2820. As shown in Figure 4.11, the model functions as expected and creates a 29.5% cheaper network than the original network.

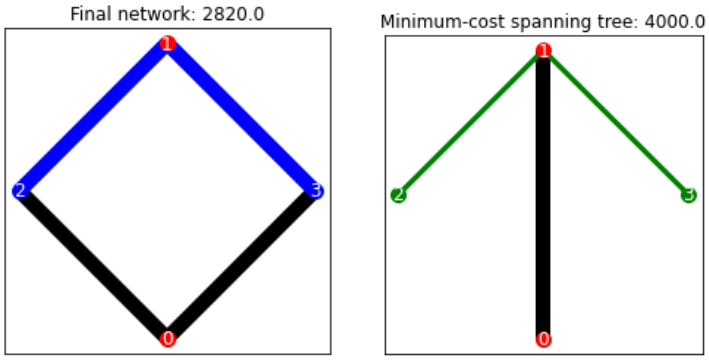

Figure 4.11: Diamond test $\beta = 1$, $rpc = 0$. Left: NROM. Right: NOM

Test 5.2 - Mathematical check of rpc in optimisation

β: 1.00
rpc: 0.40 & 0.42

As is the case in the previous tests, following the Pythagorean theorem it is required of the model that an rpc value below 0.41 will result in an optimal network layout that re-purposes the existing pipelines and creates new pipelines (0,2) and (0,3) of capacity 10. The total network cost is expected to be,

$$l_{(0,2)}q_{(0,2)} + l_{(0,3)}q_{(0,3)} + rpc \cdot l_{(1,2)}q_{(1,2)} + rpc \cdot l_{(1,3)}q_{(1,3)}, \tag{4.1}$$

which, when input with an rpc of 0.4 amounts to a total network cost of 3948. When the rpc value is above 0.41, one can mathematically deduce that the cost-optimal network no longer includes repurposed existing network, but rather a new pipeline (0,1) of capacity 20, which will cost 4000. As can be seen in Figure 4.12, the model handles the test as expected.

4.1.6 Test case 6 - The constrained diamond

In this test case, we will limit the capacity of the existing edges of the diamond to 5.

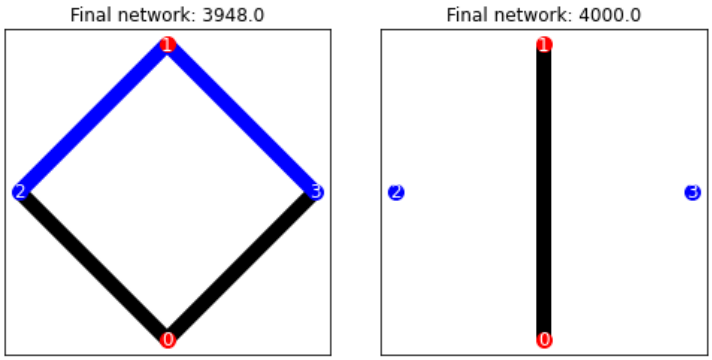

Figure 4.12: Diamond test $\beta = 1$. Left: $rpc = 0.40$. Right: $rpc = 0.42$

Test 6.1 - NOM benchmark

When limiting the existing capacity of pipelines (1,2) and (1,3) to 5, following Equation 4.1, the optimal network solution should be to transport a supply of 5 over each of the existing pipelines, creating two new pipelines (0,2) and (0,3) of capacity 5, and transporting the remaining supply over a new pipeline (1,0) of capacity 10. Figure 4.13 shows that the model performs according to our expectations, and that it creates a 14.8% cheaper network than the NOM.

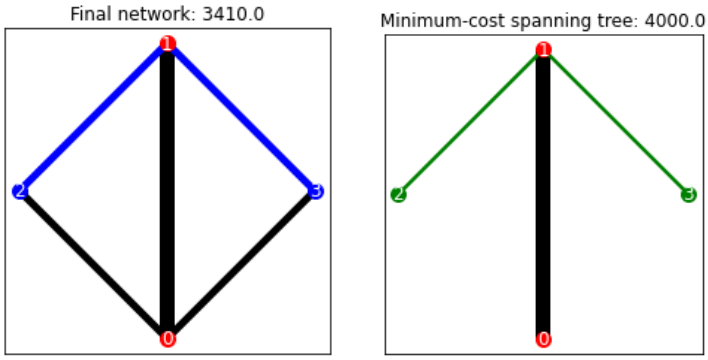

Figure 4.13: Constrained diamond test $\beta = 1$, $rpc = 0$. Left: NROM. Right: NOM

Test 6.2 - Mathematical check of rpc in optimisation

Just like the previous test cases, the point where both alternative network layouts cost the same is at an rpc value of 0.41. Values higher and lower than 0.41 should result in different cost-optimal network layouts. At 0.4 it can be mathematically deduced that the cost-optimal network layout involves two loops within a larger loop and costs 3974. When the rpc value is set at 0.42, the cost-optimal network will consist of one edge (0,1) with a capacity of 20 and a cost of 4000. Figure 4.14 shows that the model works as expected.

4.2 CALIBRATING THE MODEL

In this section we will calibrate the parameter RI that plays an important role in the calculation of edge importance, defined by

$$imp_e = RI \frac{occ_e}{\max(\{occ_e, e \in E\})} + (1 - RI) \frac{avgcap_e}{\max(\{avgcap_e, e \in E\})} \tag{4.2}$$

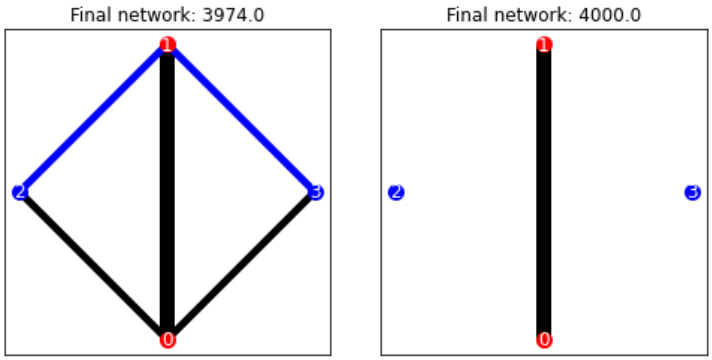

Figure 4.14: Constrained diamond test $\beta = 1$. Left: $rpc = 0.40$. Right: $rpc = 0.42$

which is used in Algorithm 3.2 to create the *base network* when multiple time steps are given. We are trying to find the value for RI for which the model produces the cheapest network layouts. RI represents the relative importance of occ_e over $avgcap_e$ in the calculation of imp_e. $RI = 0.00$ means that only $avgcap_e$ is used in the calculation of imp_e, $RI = 1.00$ means that only occ_e is used and $RI = 0.50$ means that both $avgcap_e$ and occ_e have an equal share in the calculation of imp_e. In order to calibrate the most optimal value for RI, the model is applied to 100 random experiments for different values of RI and rpc, and model results are analysed.

4.2.1 Randomised experiments for calibration

Creation of the 100 random experiments is done by using a heuristic by Heijnen (2019). The heuristic creates the input files for the model that consist of node coordinates, supply-demand sets and existing connections. Node coordinates and coordinates of the end points of existing connections are random. The number of nodes N in each experiment is a random integer between 5 and 15. The supply of each node is a random integer between -50 and 50, negative supply representing demand. The number of existing connections present in each experiment is a random integer between N and $2N$. This ensures a high level of existing infrastructure in the experiments, which is desired because the scope of application for the NROM is to networks with high levels of existing infrastructure. Each existing connection is assigned a random capacity between 0 and 100. Finally, the number of timesteps, i.e. supply-demand sets, is set to 6.

4.2.2 Calibration results

In order to determine the optimal value for RI, the NROM is applied to each of the 100 experiments at different values for RI and rpc. The reason for also changing rpc in the different runs is because the optimal value for RI might depend on the value of rpc. Running the experiments for different values of rpc might provide valuable insights regarding the relationship between rpc and the optimal value for RI, on which we can base calibration and recommendations for use of the model. The different combinations of RI and rpc result in 20 model runs for each of the 100 experiments (see Table 4.1). This in turn results in a total number of 2000 model runs. The additional benefit of performing a large amount of runs at this stage in the research, is that we can solve any bugs that occur during the running of the experiments, increasing model robustness as is recommended by Nikolic et al. (2019) in their guide to good modelling practice. For each of the 2000 runs, network costs and the values for input variables rpc and RI are saved to an Excel file. For each of the 100 experiments, four average costs are calculated (the average costs of experiments 1-5, 6-10, 11-15 and 16-20 of Table 4.1). This average cost is then used

as a benchmark to calculate the cost difference of each RI run to the average. In other words, how do the individual costs of experiments 1 to 5 relate to the average cost of experiments 1 to 5? This relationship is expressed as percentile deviation from the mean. This data allows us to eventually compare the performance of the model at different values for RI over 100 experiments and 4 values of rpc.

rpc \ RI	0.00	0.25	0.50	0.75	1.00
0.00	1	2	3	4	5
0.25	6	7	8	9	10
0.50	11	12	13	14	15
0.75	16	17	18	19	20

Table 4.1: 20 runs of one experiment

Table 4.2 shows the results for the 2000 model runs. Percentages shown are the average of percentile deviations from the mean over all runs. A score of 1% means that, on average, this value of RI produces networks that are 1% more expensive than the average cost of the networks created for all values of RI. We are looking for the value of RI that creates the cheapest network. Scores are colour coded per column, so that for each value of rpc, the value for RI that produces the cheapest network is green and the most expensive is red. On average, combining results from all values of rpc, $RI = 0.75$ performs best, creating networks that are 0.9% cheaper than the mean and 2.4% cheaper than the worst performing value $RI = 0.00$. These differences might seem small, but keep in mind that the envisioned European hydrogen transmission backbone is expected to cost up to 81 billion EUR before 2040 (Enagás et al., 2020). A cost reduction of 2.4% comes down to almost 200 million EUR that can be diverted to other causes. When separating the model runs by value for rpc, $RI = 0.75$ produces the cheapest networks at $rpc = 0.00$, $rpc = 0.50$ and $rpc = 0.75$. Only at $rpc = 0.25$ does $RI = 1.00$ produce the cheapest result by a small margin.

		rpc				
		0,00	0,25	0,50	0,75	Avg.
RI	0,00	1,2%	0,9%	1,3%	2,4%	1,5%
	0,25	0,1%	0,3%	0,2%	0,2%	0,2%
	0,50	-0,5%	-0,4%	0,0%	-1,4%	-0,6%
	0,75	-1,1%	-0,4%	-0,7%	-1,5%	-0,9%
	1,00	0,3%	-0,5%	-0,7%	0,3%	-0,2%

Table 4.2: Data for the calibration of RI

This analysis proves that occ_e is the more proficient indicator for creating cheap network layouts than $avgcap_e$. $avgcap_e$ does, however, contribute to creating cheaper network layouts in most cases. Including it in the optimisation produces better results than keeping it out of the equation all together by setting $RI = 1.00$. It can be concluded that $RI = 0.75$ is the best value to use in the model from now on.

5 CASE INTRODUCTION AND SCOPE

In Chapter 7 we will be applying the novel NROM to the case of repurposing NG pipelines for hydrogen transmission in the Netherlands. Chapter 6 is dedicated to describing the case in terms of model inputs. The purpose of this chapter is to describe the case at system level, and provide a technical and temporal scope for scenario building. First we will provide a societal context of our case followed by a description of the taxonomy of a national hydrogen grid, describing the system elements of hydrogen supply, demand, storage and transmission. We will describe what it means to repurpose existing infrastructure, and eventually provide the case with a technical and temporal scope.

Claims without reference in this section are based on reading material of the TU Delft course *Hydrogen Technology* by Mulder (2021).

5.1 SOCIETAL CONTEXT

Since the discovery of hydrogen as an element in 1776 by British scientist Henry Cavendish (1731-1810), its practical and industrial applications have been thoroughly investigated with varying success. In 1845 another British scientist by the name of Sir William Grove (1811-1896) demonstrated a hydrogen based invention he called the *gas battery*, a device that produces electricity and water by combining hydrogen and oxygen gases (The Editors of Encyclopaedia Britannica, 2020). His creation is currently widely know as the hydrogen fuel cell. Grove's invention sparked decades of research into hydrogen as a feed-stock, fuel, energy carrier and storage solution in a wide range of applications ranging from spacecraft to residential housing (Ogden, 2002). Its widespread possibilities for application, natural abundance and high sustainability potential make hydrogen a strong candidate energy carrier in a sustainable future.

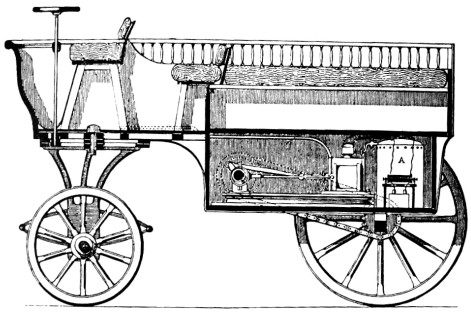

Figure 5.1: The Lenoir Hippomobile, first hydrogen powered vehicle. Source: Le Monde illustré (1860).

The European Commission (EC, 2019), striving to make Europe the first climate-neutral continent, has set out to reduce net emissions of greenhouse gases to zero by 2050. Because of its widespread possibilities for application in the industry, transport, power and buildings sectors across Europe and its lack of CO_2 emissions, hydrogen was identified by the EC (2020) as one of the key priorities for the European energy transition. Simultaneously, interest from venture capital and corporates is on the rise (Deloitte, 2020). In their European hydrogen roadmap, the Fuel Cells

and Hydrogen Joint Undertaking (2019) see several future roles for hydrogen in the European energy system.

- High heat processes in industry like the production of steel can be fuelled with hydrogen instead of coal, dramatically decreasing the carbon footprint. Electrification of these processes is difficult, and highly inefficient. Furthermore, the use of petrochemicals in industry for the production of chemical substances like polymers can be replaced with hydrogen. Reducing overall demand for fossil fuels, and subsequently reducing the carbon footprint of industry.
- Transport applications that involve movements of heavy loads over long distances are difficult to electrify, mainly because of a low energy density of chemical batteries. Examples of these applications are shipping, long-haul trucking and aviation. By using hydrogen, reducing the carbon footprint of these transport applications is made feasible. Transport of lighter loads like personal vehicles can also be powered by hydrogen, albeit under heavier competition from battery powered alternatives.
- An increase in the share of variable renewable energy sources like wind and solar coincidentally leads to an increase of demand for flexibility on the electricity market. Hydrogen, both as a storage medium and as a feedstock for dispatchable gas-fired power plants, has the ability to mitigate this variability in supply.

In order to get hydrogen from its supply to its demand source, it can be transported by means of truck, train, ship or pipeline (Li et al., 2019). With transport volumes expected to increase and transport expected to take place over longer distances, pipeline transmission appears to be the most future-proof way forward (Gasunie and TenneT, 2019, Tezel and Hensgens, 2021). Whilst investment costs are high, maintenance and operational costs are low for pipelines (Sievers and Krieg, 2016).

The Netherlands, thanks to its favourable location, large international port and existing NG infrastructure, has the potential to gain a leading position in the future hydrogen economy of the European Union (Government of the Netherlands, 2020). In order to ensure a leading position in this hydrogen economy, the Dutch government has set out to investigate the possibilities for re-purposing existing NG infrastructure and to have three to four GW of installed capacity of electrolysers by 2030 (Government of the Netherlands, 2019). Large industry players like Shell Netherlands, Gasunie, TenneT, and the ports of Groningen and Rotterdam have also shown interest in the development of green hydrogen infrastructure (Parnell, 2020, Port of Rotterdam, 2020). Repurposing NG infrastructure for hydrogen use has the potential to give a boost to the Dutch hydrogen economy, whilst at the same time giving new life to the, otherwise soon to be obsolete, Dutch gas grid.

According to a consortium of European gas grid operators including the Dutch operator Gasunie, a dedicated hydrogen infrastructure and economy will be emerging between now and 2030, evolving to maturity somewhere between 2040 and 2050 (Enagás et al., 2020). Dutch TSO Gasunie and TenneT (2019) expect that the Dutch case will allow for relatively easy construction of a dedicated hydrogen infrastructure, which in turn will reduce demand for synthetic hydrocarbon fuels. One of the main reasons is that existing NG infrastructure in the Netherlands can easily be repurposed for GH2 transport, with repurposed infrastructure expected to cost between 10 and 35% of building new infrastructure (Gasunie and TenneT, 2019, Tezel and Hensgens, 2021). An exploratory project into repurposing NG infrastructure for hydrogen transport in the Netherlands, called HyWay27, expect a nation-wide hydrogen network based on existing NG infrastructure (see Figure 5.2).

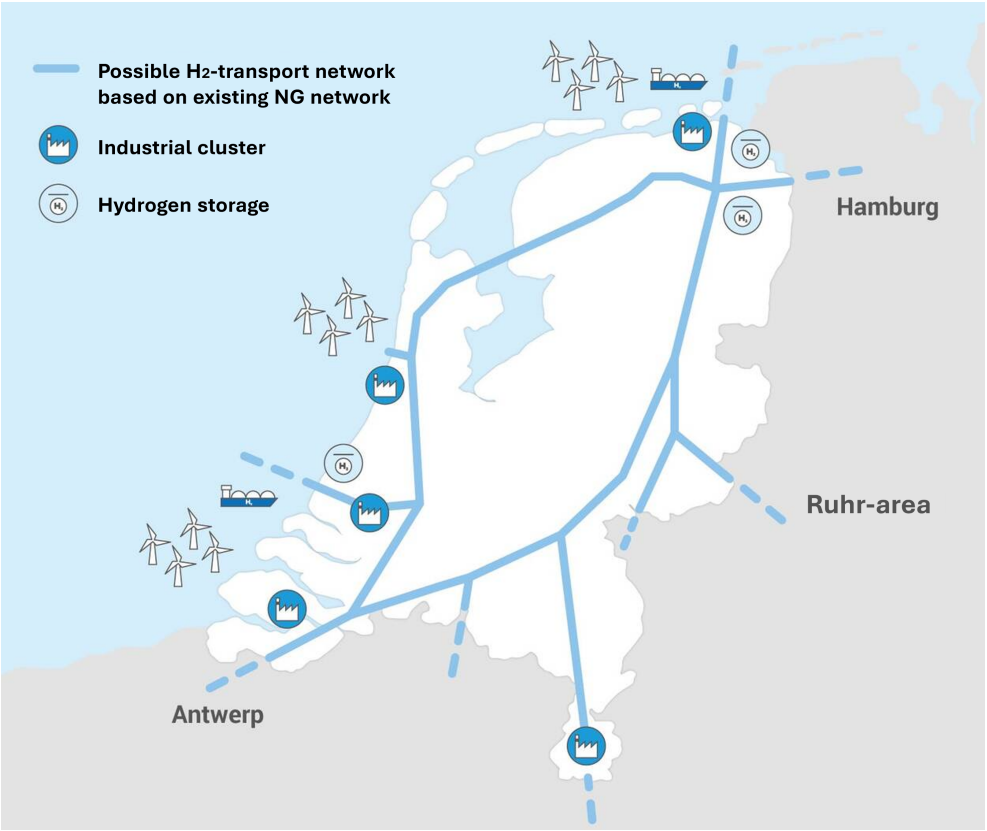

Figure 5.2: Dutch hydrogen grid envisioned in HyWay27. Source: Rijksoverheid.

5.2 TAXONOMY OF A DUTCH HYDROGEN GRID

National hydrogen networks are made of multiple system elements that work in unison. In this section we will describe the supply, demand, storage, and transmission aspects of national hydrogen networks.

5.2.1 Supply

Hydrogen supply exists in the forms of production, imports and storage unloading. Imports can take place via pipeline interconnections and shipping or trucking routes. Storage will be elaborated on later in the chapter. There are many ways for producing hydrogen (Shiva Kumar and Himabindu, 2019). Most literature uses colour coding to classify different types of hydrogen production. Below, we will briefly explain each of the types of hydrogen production using the colour coding used by National Grid Group (2021), which is the most complete collection of colour coded production types encountered.

Hydrogen can be produced in the form of Liquid Hydrogen (LH_2) or Gaseous Hydrogen (GH_2) from fossil fuels, biomass or renewable energy sources. Currently, about 96% of hydrogen is produced from fossil fuels (Shiva Kumar and Himabindu, 2019). Hydrogen produced by means of gasification of a coal feedstock is called *black hydrogen* when using black coal and *brown hydrogen* when using lignite (brown coal). Black and brown hydrogen are the types of hydrogen production that have the highest CO_2 emissions and are environmentally malicious. A more sustainable way to produce hydrogen is by transforming natural gas to hydrogen, hydrogen produced in this manner is called *grey hydrogen*, and currently forms the bulk of Dutch hydrogen production. It is possible for hydrogen production by means of natural gas to approach CO_2 neutrality by capturing the carbon and storing it by means of CCUS. This type of hydrogen production is called *blue hydrogen* produc-

tion and is often considered to be elemental in the transition towards fossil-free hydrogen production. Hydrogen produced by means of renewable assisted water splitting, also known as electrolysis, is called *green hydrogen*. In a carbon-neutral future, green hydrogen production is an essential contributor to the energy mix. Electricity from renewable energy sources like wind and solar can be used to produce hydrogen and mitigate fluctuations in electricity supply as a result of weather variations. When using electricity generated from nuclear power plants in electrolysis, the resulting hydrogen is called *pink hydrogen*. *Turquoise hydrogen* is the newest addition to the hydrogen production family, which is made using a process called methane pyrolysis. In methane pyrolysis, methane is transformed to hydrogen and pure carbon, which is subsequently stored. It is a sustainable means of producing hydrogen without using electricity, and has a high efficiency. Scaling possibilities of turquoise hydrogen have yet to be fully explored, and its place in the energy transition is yet unclear. The most basic type of hydrogen supply is *white hydrogen*, which is simply hydrogen that can be extracted from naturally occurring deposits. White hydrogen is currently not being extracted. Hydrogen can also be produced by biomass gasification, but Detz et al. (2019) expect no role for this type of hydrogen production in the Netherlands.

Currently, most Dutch hydrogen production is in the form of grey hydrogen (Detz et al., 2019). Enagás et al. (2020) expect a transition towards blue and green hydrogen supply that will start with transforming existing grey supply to blue, and later replacing most with green hydrogen production.

5.2.2 Demand

National demand of hydrogen can occur in the forms of hydrogen consumption, hydrogen exports and storage loading. Exports, like imports, can take place through pipeline interconnections and shipping or trucking routes. Storage loading will be addressed in the next section. Hydrogen consumption takes many forms. Detz et al. (2019) classified five hydrogen end-uses, (1) fuel for dispatchable electricity generation, (2) (seasonal) hydrogen storage, (3) fuel for (heavy duty) transport, (4) high-temperature heat and petrochemical processes in industry and (5) fuel for heating and cooking in buildings.

5.2.3 Storage

Hydrogen can be stored in various ways, usually in LH_2 or GH_2 forms. In materials-based hydrogen storage like chemical and physical sorption, hydrogen is integrated or combined with other materials ranging from ammonia to zeolites (Moradi and Groth, 2019). In physical-based hydrogen storage, hydrogen is contained in vessels in either liquid or gaseous form. When large storage volumes are required, like in a national hydrogen system, underground physical-based hydrogen storage is best practice (Zivar et al., 2021). In their recent study into the potential for underground gas storage in the Netherlands, van Gessel et al. (2018) found that hydrogen storage is technically feasible in salt caverns, empty gas caverns and above ground storage tanks. Most research suggests that storage in salt caverns is the best practice when storing large amounts of hydrogen (Moradi and Groth, 2019).

5.2.4 Transmission

Hydrogen can be transported by means of trucks, trains, ships, or pipelines. According to Sievers and Krieg (2016), pipeline transmission of hydrogen is the most efficient option when transporting large amounts of hydrogen over large distances, like in the case of a nationwide transmission network. Especially when taking repurposing of existing infrastructure in mind, pipelines are the most interesting form

of transmission to investigate in our case study. Transmission pipeline costs consists of cost of materials, right of way and labour costs (Reddi et al., 2016). This makes the costs related to pipeline construction dependent on case-specific conditions.

5.3 REPURPOSING EXISTING INFRASTRUCTURE

Gasunie and TenneT (2019) expect that repurposing existing NG infrastructure for gaseous hydrogen transport in the Netherlands will be relatively straightforward. Pipeline capacity in terms of MW transported changes when transforming NG infrastructure to hydrogen infrastructure. This is not something we have to account for in our modelling approach, as we will use pipeline diameter data from Gasunie Transport Services (2012), and translate that to hydrogen pipeline capacity using findings by Tezel and Hensgens (2021) and Gasunie. This calculation of capacity will be further elaborated on in Chapter 6. Costs related to repurposing are mainly the result of a process called hydrogen embrittlement, which is the deterioration of steel pipelines as a result of hydrogen absorption into the pipeline material (Feng et al., 2017). NG pipelines are not built to withstand embrittlement as a result of hydrogen transport, with hydrogen being a significantly smaller compound than NG. Existing imperfections in the steel can serve as regions that hydrogen diffuses towards, causing extra deterioration and eventually critical failures in the steel (Boot et al., 2021). Cerniauskas et al. (2020) summarised four ways of countering hydrogen embrittlement in repurposed NG pipelines for hydrogen transport:

- Pipelines can remain unmodified, and hydrogen embrittlement can be countered by intensifying maintenance and monitoring pipeline quality.
- A coating can be applied to all surfaces that are in direct contact with hydrogen, preventing the hydrogen molecules to cluster at imperfections in the steel.
- Gaseous inhibitors can be added to the hydrogen gas that will inhibit hydrogen embrittlement and reduce its effects.
- A pipeline can be inserted into existing NG infrastructure, in which case the inner pipeline is specifically designed for hydrogen transport and the outer pipeline provides the necessary safety and stability.

Dutch gas TSO Gasunie expects Dutch NG pipeline infrastructure to be repurposed by means of coating (Gasunie and TenneT, 2019) and expect pipeline repurposing costs to range from 10 to 35% of the cost of building a new pipeline (Tezel and Hensgens, 2021).

Not all NG infrastructure will be repurposed for hydrogen transport. Gasunie and TenneT (2019) expect that large parts of the High Calorific Natural Gas (H-gas) network will be repurposed for hydrogen transport, whereas the Low Calorific Natural Gas (L-gas) network will remain in use for NG transport and eventually be repurposed for transport of other gases like methane and CO_2. For this reason, our case will be focusing on repurposing existing H-gas pipeline infrastructure and L-gas infrastructure is not included. Because regional NG demand for heating and cooking in the buildings sector is currently supplied by the distribution network, which is in turn supplied by the L-gas transmission network (Gasunie Transport Services, 2012), and future hydrogen demand in this sector is expected to remain relatively small (Detz et al., 2019), hydrogen demand for heating and cooking is not included in the case study.

5.4 SCOPING THE CASE

A consortium of European gas grid operators published a report in which they envision a dedicated hydrogen backbone emerging in the coming decades (Enagás et al., 2020). In 2030, they envision mostly industrial demand (198-432 PJ/yr) in the Netherlands that will be fulfilled by local blue and centralised green and blue hydrogen production, with a focus on blue hydrogen production. In 2040 the infrastructure is expected to approach maturity with demand rising in all sectors, resulting in a national demand of 432-684 PJ/yr. This demand will be met by blue and green hydrogen production, each accounting for around 50% of total production. The share of green hydrogen production is expected to increase towards 2050, with the EC (2019) aiming for full carbon neutrality. Based on these expectations by Enagás et al. (2020), the case study will focus on blue and green hydrogen production sources.

To summarise, the focus of this thesis will be on pipeline transmission of gaseous hydrogen from blue and green hydrogen production sources to four end-uses: (1) fuel for dispatchable electricity generation, (2) (seasonal) hydrogen storage, (3) fuel for (heavy duty) transport in the transport sector and (4) high-temperature heat and non-energy use of hydrogen in industry. We assume that all hydrogen produced will be of sufficient quality to be used in all end-use sectors. Regarding imports and exports, we will be focusing on international pipeline connections and shipping routes. A visualisation of the scoped down hydrogen supply chain is shown in Figure 5.3.

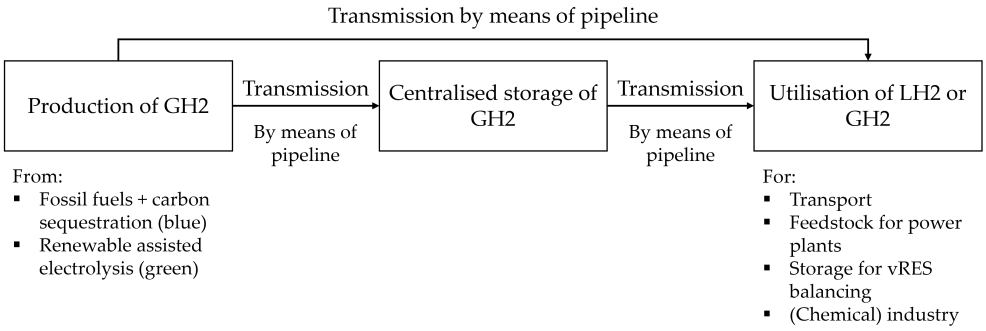

Figure 5.3: Scoped hydrogen supply chain

Current Dutch H-gas infrastructure is expected to be repurposed as hydrogen transmission pipelines, whereas L-gas will remain in use for alternative transport purposes like methane and CO_2 (Gasunie and TenneT, 2019).

6 CASE STUDY

In Chapter 7 we will be applying the NROM to seven scenarios. The purpose of this chapter is to build those scenarios and express them in terms of model inputs. As input, the NROM requires three input files for each scenario; (1) node coordinates, (2) coordinates and capacities of existing connections and (3) demand and supply sets for each node, divided into time steps. It also requires values for two input variables; repurposing cost coefficient rpc and capacity-cost exponent β.

We will start the chapter by determining values for the input variables, after which we will elaborate on the temporal scope and resolution of the scenarios. Next we will determine node coordinates as locations of supply and demand, and we will determine what existing infrastructure is available for repurposing in each scenario. Finally, national hourly supply and demand is regionalised and supply-demand sets are created.

6.1 PREPARING THE INPUT VARIABLES

In Chapter 5 we have established that the relationship between pipeline diameter and cost is linear, but the relationship between pipeline capacity and cost is not. Increasing pipeline capacity by a factor of 1 will increase pipeline cost by a factor lower than 1. The relationship between pipeline capacity and cost is determined by the capacity-cost exponent β, which is also one of the three input variables of the NROM. For hydrogen pipelines, β corresponds to a value of approximately 0.6 (André et al., 2013, Heijnen et al., 2020), which is the value we will use for our scenarios.

The final input variable is the novel variable rpc, that represents the relative cost of repurposing existing infrastructure as opposed to creating new infrastructure. $rpc = 1$ indicates that repurposing existing infrastructure is just as expensive as building it new, and $rpc = 0$ means that existing pipelines can be used without cost. In our case study, rpc will not be fixed to a certain amount, but will be alternated between $0.1, 0.25$ and 0.35, which represents the repurposing cost range expected by Gasunie and TenneT (2019).

6.2 TEMPORAL RESOLUTION

6.2.1 Introducing the scenarios

The seven scenarios we will be building in this chapter are divided over three moments in time, 2030, 2040 and 2050. Scenario *2030* is created to represent the situation in 2030. Because no usable information was found on existing infrastructure available in 2040, two scenarios were created for that year. Scenario *2040(30)* represents the supply and demand situation in 2040, with existing infrastructure present that is expected to be available in 2030. Scenario *2040(50)* also represents the supply and demand situation in 2040, but with the expected infrastructure available in 2050. For the year 2050 we created four scenarios that are based on an energy infrastructure exploration by Netbeheer Nederland (2021). Scenario *2050(RG)* represents the situation in 2050 when policy is dominated by regional governance of the

energy transition, with local authorities taking the initiative. In scenario *2050(NG)*, policy is steered by governance on a national level, with nationwide energy projects being the status quo. Scenario *2050(EG)* assumes a strong role for the European Union, with national initiatives being heavily influenced by EU policy. In scenario *2050(IG)*, the energy transition is globally embraced, and energy policy is mostly influenced by free global energy markets. Quintel Intelligence (2014) integrated the 2050 scenarios into the Energy Transition Model (ETM), which will provide us with hourly supply and demand data for these scenarios. Data on existing infrastructure is mostly taken from Tezel and Hensgens (2021), with supporting data taken from various sources including Gasunie Transport Services (2012), Gasunie and TenneT (2019).

6.2.2 Maximum demand capacity snapshots

The ETM provides us with hourly supply and demand data for our 2050 scenarios. This data is used to create maximum capacity demand envelopes for each 2050 scenario, following a method adopted from Detz et al. (2019). Maximum capacity demand envelopes for the 2030 and 2040 scenarios are later extrapolated from the 2050 scenarios.

A maximum capacity demand envelope is a method for determining the maximum transport requirements of a networked system. The total operating envelope of the network that contains all possible transmission capacity demands is defined by four snapshots; (1) high supply and high demand, (2) high supply and low demand, (3) low supply and high demand and (4) low supply and low demand. When investigating maximum transmission capacity requirements of the network, we can leave out the low supply and low demand snapshot, as this does not require a large available transmission capacity in the system (Detz et al., 2019). We are left with an operating envelope defined by three points, of which we can assume that all maximum transmission capacity demands of the system lie within that envelope. Figure 6.1 shows the operating envelope with the maximum capacity demand envelope highlighted.

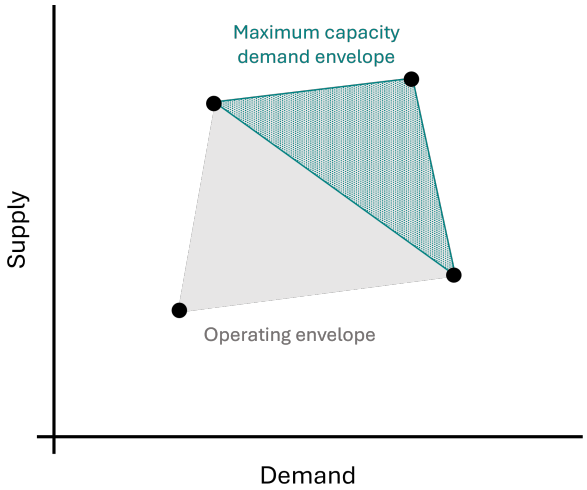

Figure 6.1: Schematic of the operating envelope

Because we are working with hourly data from the ETM, the snapshots we use are defined as an hour in the year. For each 2050 scenario, we will create two maximum transmission capacity envelopes. One for *'average weather year 2015'* and one for *'extreme weather year 1987'* to ensure that the capacity demands for both extreme situations and business as usual are taken into account. For the high supply and low demand snapshots, we take the hour in the year when most hydrogen is loaded

into storage. For the low supply and high-demand snapshots, we take the hour in the year when most hydrogen is unloaded from storage. The high supply and high demand is extrapolated from the other two snapshots by taking supply numbers from the high supply and low demand snapshot, and taking demand numbers from the low supply and high-demand snapshot. This will be further elaborated later in the chapter.

Two maximum transmission capacity demand envelopes with two hourly snapshots each result in four snapshots per scenario that will be taken from the ETM data. To view the timestamps for all snapshots taken from the ETM for each scenario, please refer to Appendix B.

6.3 NODE COORDINATES

The model demands a geographical input in the form of coordinates of nodes that represent locations of supply and/or demand. Following our scope determined in Chapter 5 we will be focusing on blue hydrogen production, green hydrogen production, industrial demand, power demand, storage, transport demand, imports and exports.

6.3.1 Industrial clusters

Industrial hydrogen demand and supply are currently mainly situated in five industrial clusters; *Rotterdam-Moerdijk*, *Noordzeekanaalgebied*, *Chemelot (Limburg)*, *Smart Delta (Zeeland)* and *Noord-Nederland*, and will remain so in the coming decades (Enagás et al., 2020, Netbeheer Nederland, 2021, Tezel and Hensgens, 2021). Centralised blue hydrogen production is also expected to take place in the industrial clusters. Transport demand will be fulfilled in the industrial clusters as well, as is it expected that hydrogen for use in transport will be trucked to pump-stations from industrial clusters (Detz et al., 2019).

6.3.2 Centralised hydrogen storage

In 2030, hydrogen is stored locally at places of production or demand Detz et al. (2019). Storage will therefore not be included in the *2030* scenario. According to Netbeheer Nederland (2021), maximum hydrogen storage capacity demands in 2050 range between 10 and 47 Terawatt hours. It is expected that future hydrogen storage will mainly be situated in salt cavern storage facilities, as this is the safest option and is expected to face the least societal backlash (Gasunie and TenneT, 2019). Over 70% of Dutch salt cavern storage capacity is located in Groningen, with its salt caverns accounting for roughly 31 Terawatt hours of effective storage capacity (van Gessel et al., 2018). In Figure 6.2, a map of salt cavern locations, provided by van Gessel et al. (2018), in and around Groningen is shown. For the purpose of this thesis we will assume that all hydrogen stored, will be stored in salt cavern storage facilities in Hoogezand, Zuidwending and Winschoten. For the *2040(30)* and *2040(50)* scenarios, we assume that the salt caverns in Groningen are already in use.

6.3.3 Imports and exports

The import and export points of the H-gas network are located in Zeeland, Limburg, Noord-Holland and Groningen (CBS, 2019a). The two international trade points located in Zeeland, Zelzate and Zandvliet, are combined into one node in our modelling scenarios. The same is done for the three points located in Limburg, Bocholtz, Vetschau and 's-Gravenvoeren, and the four points located in Groningen. The international connection in Noord-Holland is the sub-sea BBL pipeline that connects

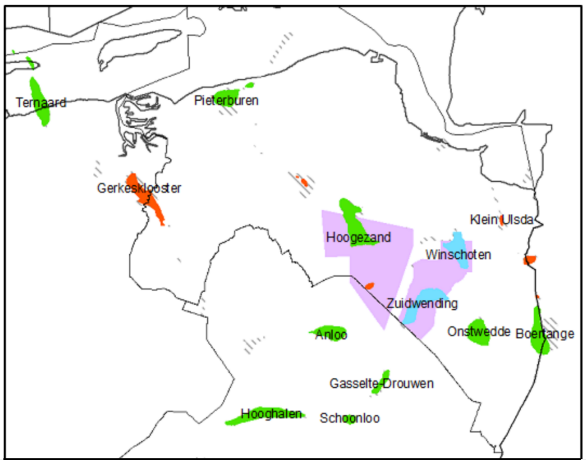

Figure 6.2: Locations of salt caverns in and around Groningen (salt domes in green and salt pillows in purple)

Julianadorp to the UK. For all scenarios, we assume that pipeline imports and exports are evenly distributed among these four connections.

It is also possible to import and export hydrogen through Dutch harbours. Imports and exports through these channels will be assigned to the Noord-Nederland, Noordzeekanaalgebied, Smart Delta and Rotterdam-Moerdijk industrial clusters that respectively are home to the Groningen Seaports, Port of Amsterdam, Zeeland Seaports and the Port of Rotterdam.

6.3.4 Overview of node locations

When combining all the information above, we can create a map of locations of future hydrogen demand and supply (see Figure 6.3).

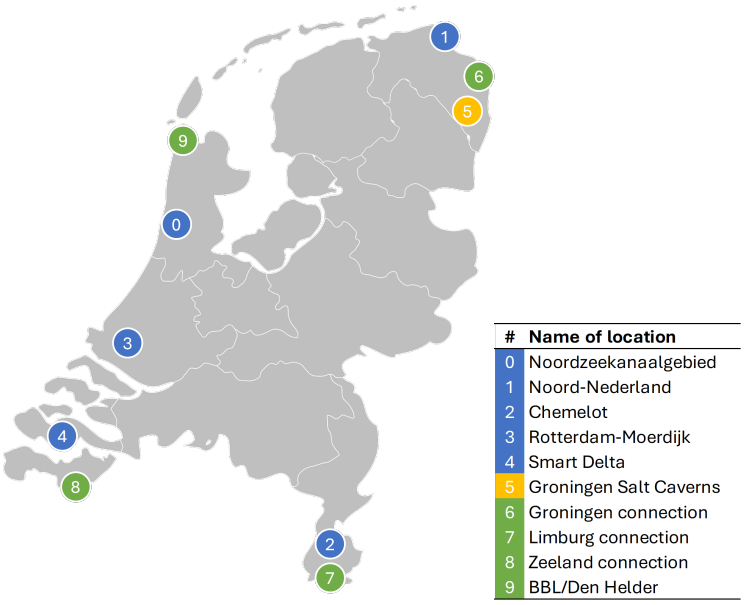

Figure 6.3: Map of locations of hydrogen supply and demand (industrial clusters in blue, storage in yellow and import/export locations in green)

6.4 EXISTING INFRASTRUCTURE

Together with Gasunie, Tezel and Hensgens (2021) identified pipeline infrastructure that could be made ready for repurposing by 2030. We will assume that the entry points of these pipelines that are not in the vicinity of an industrial cluster will allow for connection of new pipelines, so-called entry points. Available existing infrastructure and its expected maximum capacities can be seen in Figure 6.4a.

For the 2050 scenarios, we assume that all H-gas infrastructure will be available for repurposing. In order to identify available infrastructure, we use the gas infrastructure maps by made public by Gasunie Transport Services (2012). The schematic map can be seen in Appendix D, the detailed map was also used for building the scenarios. As no information is shared on capacities of these connections, several assumptions have to be made. Firstly, we will assume that all existing H-gas pipelines have a diameter of 36 inches. By 2050, Gasunie expects to be able to increase system pressure to 66 bar, which allows 36-inch pipelines to transport a theoretical maximum capacity of 10.6 GW (Tezel and Hensgens, 2021). Because this maximum capacity is theoretical, in our scenarios we will use a practical maximum capacity of 8 GW, which is roughly 75% of the theoretical maximum capacity. Entry points where new pipelines can be connected to the existing infrastructure are also included in the input file, and taken from Gasunie Transport Services (2012). In terms of GGT, these entry nodes are transshipment nodes with no supply or demand. In order to not overcomplicate the network layout, entry points close to industrial clusters are not included and assumed to be included into the industrial cluster. Available existing infrastructure and its maximum capacities can be seen in Figure 6.4, with entry points indicated by red hexagons. In the input files the GW data is translated to MW as that is the metric used in the hourly snapshots of the ETM.

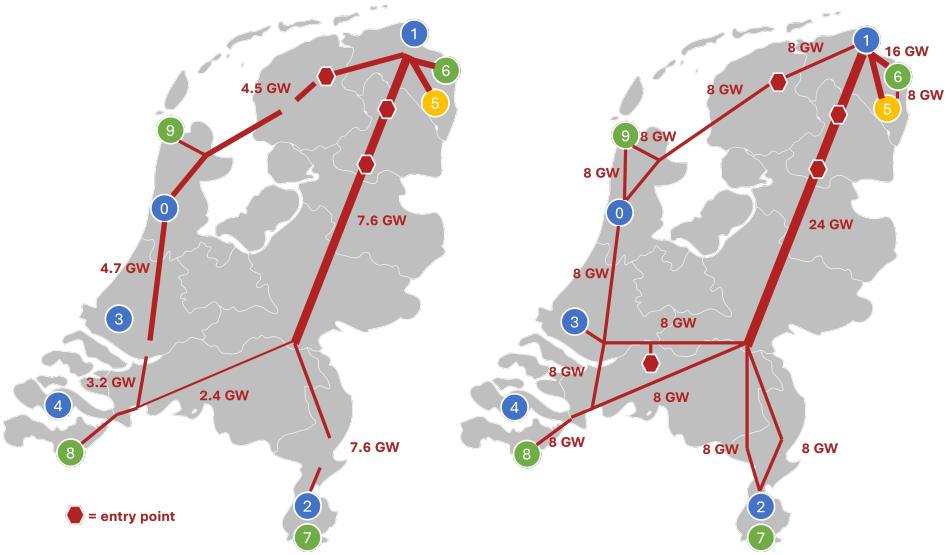

(a) 2030 **(b)** 2050

Figure 6.4: Available capacity of existing infrastructure in 2030 and 2050

According to Tezel and Hensgens (2021), existing infrastructure will gradually become available between 2030 and 2050. They have not shared further information or predictions, nor has other information been found on available NG infrastructure available in 2040. The *2040(30)* and *2040(50)* scenarios will provide insight into infrastructure requirements for the year 2040 by applying the infrastructures available in 2030 and 2050 to the supply and demand situation of 2040. These insights will be discussed in Chapter 7.

6.5 REGIONALISATION OF DEMAND AND SUPPLY DATA

Hourly supply and demand data extracted from the ETM is of a nationwide resolution. When building the scenarios, we should therefore regionalise the data by allocating national demand to all nodes in Figure 6.3. This is done by creating allocation keys, which are described below.

6.5.1 Industrial demands and supplies

In their roadmap to climate neutrality by 2050, the industrial cluster of *Rotterdam-Moerdijk* is expecting to import considerate amounts of hydrogen through the port of Rotterdam (Klimaattafel Haven en Industrie Rotterdam-Moerdijk, 2020). They also expect to install a significant amount of electrolyser capacity that will be fed electricity from offshore wind to produce hydrogen. In the distant future, they also expect that hydrogen will be produced at offshore locations and transported to the industrial cluster through sub-sea pipelines.

The *Noord-Nederland* industrial cluster, in their roadmap to climate neutrality in 2050, also expects to install a considerable amount of electrolyser capacity that will be able to convert electricity from offshore wind and imports to hydrogen expecting to scale up to a maximum of 1.5 GW of installed capacity (Industrietafel Noord-Nederland, 2020). It also expects to have hydrogen powered plants produce electricity. Despite being home to the Eemshaven, a considerably sized transshipment port, the cluster does not expect any imports or exports of hydrogen through international shipping according to their roadmap.

In their roadmap to climate neutrality in 2050, the industrial cluster *Noordzeekanaalgebied* expects to perform large-scale overseas hydrogen import by 2040 (Noordzeekanaalgebied, 2020). It also plans to have a large installed capacity of electrolysers fed by offshore wind electricity, expecting to be able to deploy a capacity of around the order of 1 GW. A large amount of hydrogen is expected to be used by industry in the region, but they see value in a hydrogen backbone connection to the other industrial clusters to provide flexibility.

The industrial cluster *Chemelot* expects to produce 24 PJ of hydrogen each year by 2050, according to their roadmap to climate neutrality in 2050 (Chemelot-tafel, 2020). They expect most of their production to be blue hydrogen production, but are open to importing green hydrogen through the hydrogen backbone if financially competitive.

The *Smart Delta* industrial cluster, in their roadmap to climate neutrality in 2050, currently being the largest source of both supply and demand of hydrogen, expect to be a key player in the future hydrogen economy (Smart Delta Resources, 2020). With only the industrial cluster of *Rotterdam-Moerdijk* coming close to their scale of hydrogen infrastructure, they expect an installed electrolyser capacity ranging from 3 to 4 GW. They expect to be able to produce up to 95 PJ of hydrogen yearly by 2050. With the North-Sea port as an important hydrogen hub, they also expect large-scale imports by ship.

Allocation keys industry

Using data compiled by Weeda and Segers (2020), we have created the allocation key for Dutch hydrogen demand and supply in the industrial clusters in 2020, which can be seen in Table 6.1. The demand and supply allocation keys are the same because currently all supply is locally used by industry (Netbeheer Nederland, 2021).

Between 2020 and 2050, a gradual increase in hydrogen transmission between the industrial clusters is expected, as local supplies no longer meet local demands (Netbeheer Nederland, 2021). Using the roadmaps from each industrial cluster, we have created three industry allocation keys for 2030, 2040 and 2050. These keys are

Table 6.1: Allocation key industrial clusters 2020

	Ro-Mo	NZKG	Chem.	SmDe	No-Ne
Ind. H_2 supply	43%	3%	14%	33%	7%
Ind. H_2 demand	43%	3%	14%	33%	7%

respectively shown in Table 6.2, Table 6.3 and Table 6.4. For 2050, this allocation key serves as a source key that will be adapted to each of the scenarios accordingly.

Table 6.2: Allocation key industrial clusters 2030

	Ro-Mo	NZKG	Chem.	SmDe	No-Ne
Ind. H_2 supply	42%	4%	11%	34%	9%
Ind. H_2 demand	43%	3%	14%	33%	7%

Table 6.3: Allocation key industrial clusters 2040

	Ro-Mo	NZKG	Chem.	SmDe	No-Ne
Ind. H_2 supply	41%	6%	8%	34%	11%
Ind. H_2 demand	43%	3%	14%	33%	7%

Table 6.4: Allocation key industrial clusters 2050

	Ro-Mo	NZKG	Chem.	SmDe	No-Ne
Ind. H_2 supply	39%	8%	5%	35%	13%
Ind. H_2 demand	43%	3%	14%	33%	7%

Allocation key international shipping

Four of the five industrial clusters are home to international ports. Refer to Table 6.5 for the allocation key of national shipping imports to these four harbours. The allocation key is based on CBS (2021) data on wet bulk transport numbers for these harbours in 2020.

Table 6.5: Allocation key international imports and exports through harbours

	Ro-Mo	NZKG	Chem.	SmDe	No-Ne
International shipping	77%	18%	0%	4%	1%

Offshore wind

Green hydrogen production will take place close to wind farm locations, moving offshore in more distant scenarios (Enagás et al., 2020). Of all electricity produced in offshore wind-farms, 35% is expected to be fed into mainland infrastructure at the Rotterdam industrial cluster, 30% at Den Helder, 15% at the Noord-Nederland industrial cluster, 10% at the Noordzeekanaalgebied industrial cluster, 5% and Borssele and 5% at Terneuzen (Netbeheer Nederland, 2021). The combined 10% that land in Terneuzen and Borssele will both be assigned to the Zeeland industrial cluster. The 30% that land in Den Helder are assumed to be used in electrolysis in the Noordzeekanaalgebied industrial cluster.

6.5.2 Transport demands

Earlier, we established that hydrogen for end uses in transport will be transported from industrial clusters to pump-stations by means of truck. This means that an allocation key for transport hydrogen demand will have to be created that allocates transport demand to the five industrial clusters in the scenario.

We will first allocate each industrial cluster with a service area for its hydrogen trucks. These service areas were specified by first computing a Voronoi diagram of the industrial clusters, a Voronoi diagram being the partition of a plane into regions close to each of a given set of objects. For an image of the Voronoi diagram, refer toAppendix C. To generate the diagram, Alex Beutel's Interactive Voronoi Diagram Generator was used. The Voronoi diagram, being a mathematical approach, is not very practical to use directly for scenario building. To create more realistic service areas, as shown in Figure 6.5, the Voronoi diagram was used as a basis and adapted according to province borders and road access. The allocation key shown in Table 6.6 was then created by combining the service areas with data from the CBS (2019b).

Figure 6.5: Service areas for transport demands of hydrogen, diagonal lines in provinces, indicate a 50/50 split between two clusters.

Table 6.6: Transport allocation key

	Ro-Mo	NZKG	Chem	SmDe	No-Ne
Transport H_2 demand	30%	38%	13%	2%	17%

6.6 SUPPLY AND DEMAND SETS

Because of a lack of hourly data available for the years of 2030 and 2040, we will extrapolate national hydrogen demands for these years from the hourly data set of 2050. Because of this, we will first explain how the supply-demand sets for 2050 are created and follow with the supply-demand sets of 2030 and 2040. The full supply-demand sets that serve as input for the model can be viewed in Appendix E.

6.6.1 Supply and demand sets 2050

These scenarios are based on the energy infrastructure exploration by Netbeheer Nederland (2021). Hourly supply and demand data is extracted from the ETM, where the scenarios are already integrated under the name *II3050*. Demands from the household and buildings sectors are removed from the hourly demand and supply sets, as these are outside the scope of this research. Imbalances are met by subtracting household and buildings demands evenly from storage, industrial and import supplies. Transmission losses are ignored as they are very low and don't have an impact on the final optimisation outcomes. Snapshots of high supply and low demand are taken from the hour in the year when there is most expected storage loading. Snapshots of low supply and high demand are taken from the hour with the most expected storage unloading. Moments of high supply and high demand are extrapolated from the other two snapshots by copying the supply from the snapshot with high supply and the demand from the snapshot with high demand. Supply and demand are subsequently balanced by taking any shortages from storage, or storing oversupplies in storage.

The national hourly data taken from the ETM is then allocated to the different industrial clusters in the network using allocation keys for industrial demand and supply. Storage can be directly taken from the national data, as we only have one storage node. Import and export through pipelines is evenly allocated to the four different nodes, with exports and imports through ship being allocated to the industrial clusters.

2050(RG)

In this climate neutral scenario, there is a strong emphasis on governance through local communities with a high level of autonomy. The Netherlands is almost completely self-sufficient in terms of energy, with limited imports and exports of hydrogen. Imports and exports that do take place, take place through each of the international connections equally. Hydrogen is produced from a combination of solar PV and offshore and onshore wind, causing a more equal spread of hydrogen production. Green hydrogen is used mainly in the industry and power sectors. The full allocation key for this scenario can be seen in Table 6.7.

Table 6.7: Allocation key industrial clusters in 2050(RG) scenario.

	Ro-Mo	NZKG	Chem.	SmDe	No-Ne
Ind. H_2 supply	36%	9%	9%	30%	16%
Ind. H_2 demand	43%	3%	14%	33%	7%
Transport H_2 demand	30%	38%	13%	2%	17%

2050(NG)

In this scenario, the Dutch national government implements national legislation that incentivises the completion of large-scale renewable infrastructure projects, with an emphasis on offshore wind. This results in a higher hydrogen production in industrial clusters close to where electricity produced offshore comes to land. The Netherlands is largely self-sufficient, with only limited imports and exports through each of the international pipeline connections equally. The energy sector is subject to strong electrification and green hydrogen is widely used in the industry and power sectors. The full allocation key for this scenario can be seen in Table 6.8.

Table 6.8: Allocation key industrial clusters in 2050(NG) scenario

	Ro-Mo	NZKG	Chem.	SmDe	No-Ne
Ind. H_2 supply	39%	15%	2%	30%	14%
Ind. H_2 demand	43%	3%	14%	33%	7%
Transport H_2 demand	30%	38%	13%	2%	17%

2050(EG)

In this scenario, the European Union influences national policy by implementing a CO_2 tax. Green hydrogen produced from solar and wind energy is used in industry as both a fuel and raw material. CCUS is widely applied to produce blue hydrogen, resulting in a smaller hydrogen economy than in the other scenarios. Imports occur through international shipping and pipeline equally. The full allocation key for this scenario can be seen in Table 6.9.

Table 6.9: Allocation key industrial clusters in 2050(EG) scenario

	Ro-Mo	NZKG	Chem.	SmDe	No-Ne
Ind. H_2 supply	39%	8%	5%	35%	13%
Ind. H_2 demand	43%	3%	14%	33%	7%
Transport H_2 demand	30%	38%	13%	2%	17%
International H_2 shipping	77%	18%	0%	4%	1%

2050(IG)

In this international scenario, energy demands and supplies are governed by the international markets. Hydrogen produced in other regions is cheap, and is therefore largely imported. Imports occur mostly by ship, with an estimated 90% of imports coming from international shipping and the remaining imports coming from international pipeline connections. CCUS is more widely used than in the *2050(NG)* and *2050(RG)* scenarios. The Port of Rotterdam plays an important role in this scenario as a European hydrogen hub. The full allocation key for this scenario can be seen in Table 6.10.

Table 6.10: Allocation key industrial clusters in 2050(IG) scenario

	Ro-Mo	NZKG	Chem.	SmDe	No-Ne
Ind. H_2 supply	39%	8%	5%	35%	13%
Ind. H_2 demand	43%	3%	14%	33%	7%
Transport H_2 demand	30%	38%	13%	2%	17%
International H_2 shipping	77%	18%	0%	4%	1%

6.6.2 Supply and demand sets 2030 and 2040

For both the 2030 and 2040 scenarios, we use hourly data from the *2050(NG) scenario* as a base for extrapolation, as this is the scenario that results in the highest transmission capacity demands. This way we can investigate capacity demands for those scenarios under high levels of hydrogen transmission.

Scenario 2030

By 2030, Detz et al. (2019) expect only industrial demand of hydrogen. Detz et al. (2019) also expect total industrial hydrogen demand in 2030 to be around 70% of the

industrial demand expected in 2050 and that all hydrogen supply in 2030 will be in the form of blue or grey hydrogen production. Because of the constant nature of blue and grey hydrogen supply and industrial hydrogen demand, we can assume a constant hydrogen supply and demand for 2030. The average hourly industrial hydrogen demands and supplies are thus calculated from the average hourly ETM data of 2050, and multiplied by 70%. Imbalance is assumed to be imported or exported through all interconnection pipelines equally, as no centralised hydrogen storage is expected at this point in time (van Gessel et al., 2018). These national supplies and demands are then allocated using the allocation key in Table 6.2.

Scenarios 2040

By 2040, Detz et al. (2019) expect hydrogen demand to have grown in every sector, with total hydrogen demand in 2040 to be around 70% of the total demand expected in 2050. In 2040, hydrogen demand is met by an equal share of green and blue hydrogen production. We can therefore not assume a constant hydrogen demand and supply like we did in the *2030* scenario. An increase of hydrogen demand in every sector means that transport demands also have to be included, resulting in the allocation key shown in Table 6.11. Because of the expected 50/50 share of blue and green hydrogen production, we assume that 50% of hydrogen supply and demand is constant (blue hydrogen) and calculate it by taking the average of all hourly demand data from *2050(NG)* multiplied by 70%. The other 50% is not constant (green hydrogen) and is calculated by multiplying the six snapshots from the *2050(NG)* scenario by 70%. The resulting supply-demand set can be viewed in Appendix E.

Table 6.11: Allocation key total hydrogen demand and supply 2040

	Ro-Mo	NZKG	Chem.	SmDe	No-Ne
Ind. H_2 supply	41%	6%	8%	34%	11%
Ind. H_2 demand	43%	3%	14%	33%	7%
Transport H_2 demand	30%	38%	13%	2%	17%

6.7 TRANSLATING RELATIVE COSTS TO REAL COSTS

Network costs, as calculated by the model, are not expressed in any currency. The costs are expressed in monetary units (MU), where the cost of a new pipeline is expressed by the multiplication of $lq^{0.6}$ with pipeline length l, capacity q and capacity-cost exponent β at a value of 0.6. If we want to express network and pipeline costs in EUR, we have to find out how much EUR equate 1 MU. Capacities q in the scenario are expressed in MW. Lengths l are arbitrary, and should be scaled to kilometres. In our scenarios, the distance between the Eemshaven and Ravenstein is 443 length units. In the real world, the distance between those two points is 200 km. This means that each length unit in the scenarios equates roughly 450 meters. We can then deduct that 1 km of 36-inch pipeline, having a capacity of 8000 MW, costs $\frac{1}{0.45} \cdot 8000^{0.6} = 488.2MU$.

Sievers and Krieg (2016) found that in 2011, 36-inch and 40-inch pipelines in the United States cost respectively 2.18 and 2.46 million EUR per kilometre. More recent research by Sönnichsen (2021) found that hydrogen transmission pipeline costs range from 1.92 to 3.93 million EUR per kilometre globally, without disclosing pipeline capacities or diameters. Enagás et al. (2020) used an estimated transmission pipeline cost of 2.5 to 3.36 million EUR per kilometre for 48-inch hydrogen pipelines in their exploratory research into a European hydrogen backbone. Judging from these more recent researches and comparing them with findings from Sievers and

Krieg (2016) from 2011, we can safely assume that prices of hydrogen transmission pipelines have not changed significantly. We will therefore be using the price found by Sievers and Krieg (2016) for 36-inch pipelines in this research, equating 1 MU to 4465 EUR, and using this to translate model results to EUR.

7 RESULTS AND DISCUSSION

In this chapter, we will discuss the results of applying the NROM to the cases created in Chapter 6. We will first share and discuss the case-specific results of each scenario separately, followed by a general discussion. We will then assess NROM performance by comparing results for each scenario to results created by the NOM for the same scenarios. We will end the chapter with some notes on model application. Costs in this chapter are not expressed in currency, but are relative costs only for comparing different scenarios with each other. All pipeline capacities are expressed in MW.

7.1 CASE RESULTS

In this section, we will present the case specific results. Results for each scenario will first be shown and individually discussed, after which we will discuss our overall findings. New pipelines are shown in black, and existing pipelines are either (1) blue, (2) brown or (3) purple depending on whether they are (1) not used at full capacity, (2) used at full capacity or (3) used at full capacity and complemented with a new parallel pipeline.

7.1.1 Results 2030

Optimal network layouts for the *2030* scenario are shown in Figure 7.1 and their respective costs can be seen in Table 7.1.

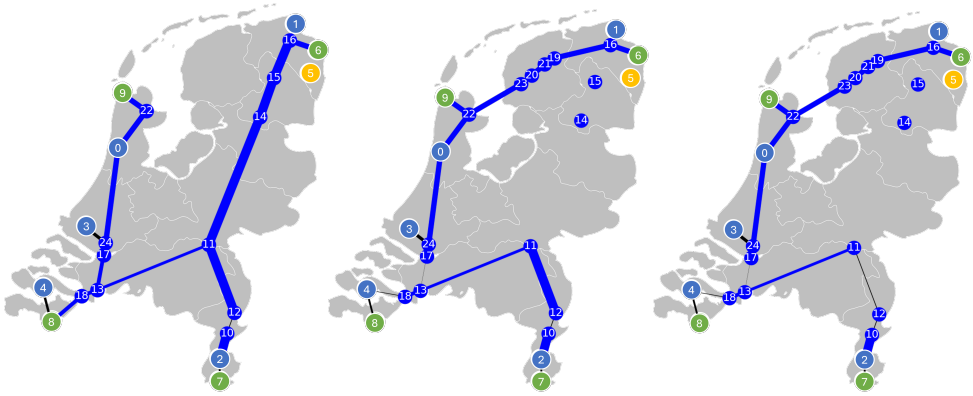

(a) $rpc = 0.10$ **(b)** $rpc = 0.25$ **(c)** $rpc = 0.35$

Figure 7.1: Optimal network layouts for 2030 scenario

Table 7.1: Optimal network layout costs for 2030 scenario (billion EUR)

rpc	Total cost	Repurposing cost	New pipeline cost
0.1	0.192	0.104	0.088
0.25	0.300	0.187	0.113
0.35	0.358	0.216	0.141

We find that the existing NG pipelines made available by Gasunie are sufficient to transport all hydrogen that needs to be transported in 2030. Investment costs for the network range from 192 to 358 million EUR, depending on the repurposing cost coefficient. Even though existing capacity is abundant in this scenario, there are still costs related to building new pipelines. This has two main reasons. The first reason is that some locations of supply and demand are not connected to the network of existing infrastructure. Examples of this are the industrial clusters *Rotterdam-Moerdijk* (node 3) and *Smart Delta* (node 4). The second reason is that at higher values for rpc, it can become cheaper to build a new pipeline with sufficient capacity, than repurposing a pipeline with a large overcapacity. Examples of this are stretches (11,12) and (13,17), where at lower values for rpc, existing infrastructure is repurposed, whereas at higher values a new pipeline is built.

Another interesting observation is that the two network layouts at $rpc = 0.25$ and $rpc = 0.35$ differ significantly from the layout at $rpc = 0.10$. In the latter, flows from and to the Groningen area are directed through repurposed pipelines in the east of the country, whereas in the other scenarios, flows are directed through a combination of new and repurposed pipelines in the west. The new pipelines created are (19,20) and (20,23). A plausible explanation for this is that at $rpc = 0.10$, repurposing the stretch of pipelines in the east of the country is cheaper than the combination of repurposing and building new pipelines on the shorter western stretch of the country. As repurposing costs rise, however, the combination of repurposing and supplementing the western stretch of pipelines becomes the more economical choice.

When investigating the connection of the *Smart Delta* industrial cluster to the backbone, we find that in the $rpc = 0.10$ scenario, repurposing stretch (8,18) and building a new stretch (4,8) is the cheapest option, whereas in the other scenarios it is cheaper to build a new connection (4,18) instead of repurposing the stretch (8,18). This can also be explained by the fact that at higher values for rpc, repurposing pipelines at overcapacity becomes less beneficial.

7.1.2 Results 2040

The results for the 2040 scenario are split up into two parts. First, we will assess the 2040 scenario with existing capacity made available by Gasunie in 2030 (see Figure 6.4a) in the *2040(30)* scenario. We will then look at the 2040 scenario with the existing capacity available in 2050 (see Figure 6.4b) in the *2040(50)* scenario.

2040(30) scenario

Optimal network layouts for the *2040(30)* scenario are shown in Figure 7.2 and their respective costs can be seen in Table 7.2.

Table 7.2: Optimal network layout costs for *2040(30)* scenario (billion EUR)

rpc	Total cost	Repurposing cost	New pipeline cost
0.1	1.329	0.127	1.202
0.25	1.495	0.318	1.178
0.35	1.622	0.419	1.203

Capacities made available by Gasunie in 2030 are no longer sufficient in 2040, as both the scale and the variability of supply and demand have increased, resulting in exponentially greater transport demands. This results in high network investment costs ranging from 1.329 to 1.622 billion EUR, consisting mostly of new pipeline costs. We see that almost all existing infrastructure is fully utilised, indicated by the brown pipelines. Stretches (0,22) and (13,17) are supplemented with parallel pipelines, indicated by purple. New, high-capacity pipelines are installed between

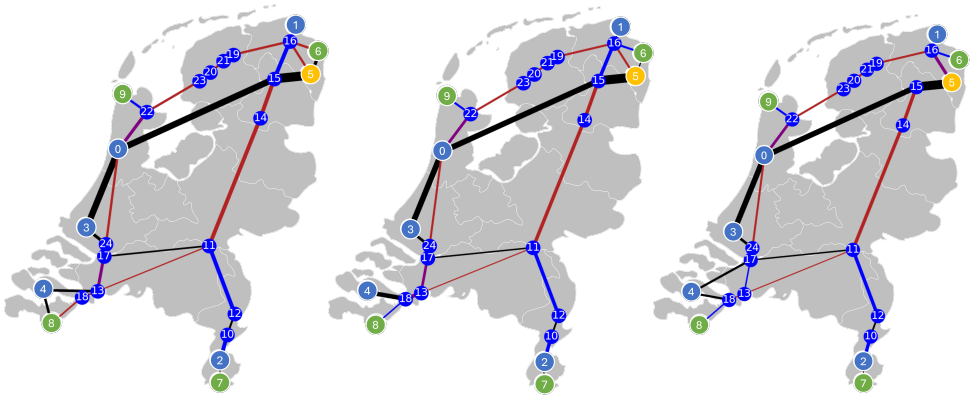

(a) $rpc = 0.10$ **(b)** $rpc = 0.25$ **(c)** $rpc = 0.35$

Figure 7.2: Optimal network layouts for *2040(30)* scenario

the *Groningen Salt Caverns* and the industrial clusters of *Rotterdam-Moerdijk* and *Noordzeekanaalgebied*. New pipelines (0,3), (0,15) and (5,15) were created with respective capacities 12369, 12226 and 17627-19969 MW.

Investigating the situation in Groningen more closely, we see that, depending on rpc, the pipeline layout between nodes 5, 6, 15 and 16 differs. The main difference is that in the $rpc = 0.35$ scenario, the existing pipeline (15,16) is not repurposed, but in stead a new, parallel pipeline (5,16) is installed. This pipeline also seems to replace the new pipeline (5,6) that is present in the other two scenarios. This can be explained by the fact that at a higher value for rpc, repurposing pipeline (15,16) becomes less beneficial and alternative routes become cheaper.

2040(50) scenario

Optimal network layouts for the *2040(50)* scenario are shown in Figure 7.3 and their respective costs can be seen in Table 7.3.

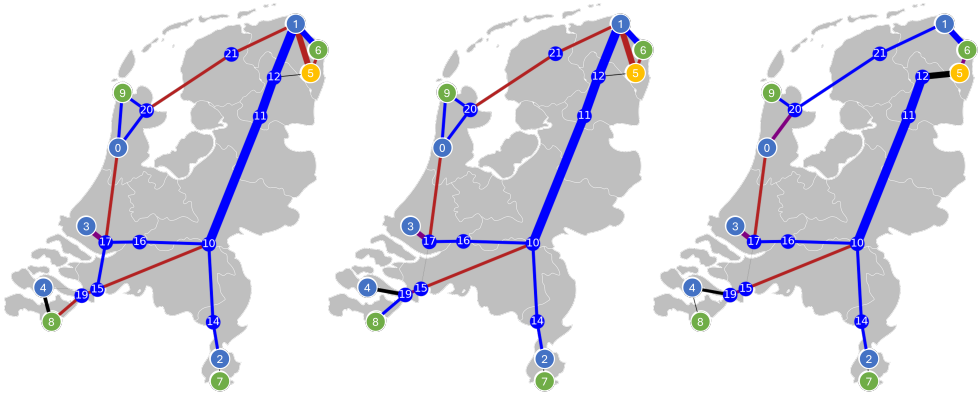

(a) $rpc = 0.10$ **(b)** $rpc = 0.25$ **(c)** $rpc = 0.35$

Figure 7.3: Optimal network layouts for *2040(50)* scenario

Table 7.3: Optimal network layout costs for *2040(50)* scenario (billion EUR)

rpc	Total cost	Repurposing cost	New pipeline cost
0.1	0.434	0.273	0.161
0.25	0.835	0.660	0.175
0.35	1.056	0.740	0.315

Available infrastructure made available in 2050, i.e. all pipelines in the H-gas network, will be largely sufficient to meet all capacity demands in 2040. As a result, investment costs are significantly lower than the *2040(30)* scenario, with investment costs ranging from 0.434 to 1.056 billion EUR. Costs are mainly caused by repurposing of existing infrastructure. Capacity demands in 2040 do however push the existing H-gas network to its limits, as can be seen by the existing pipelines being used at maximum capacity, indicated by their brown colour. This results in several network expansions. The 8000 MW pipeline (3,17), connecting industrial cluster *Rotterdam-Moerdijk* to the backbone needs to be complemented with an additional pipeline of 5182 MW and the industrial cluster *Smart Delta* needs a new pipeline connection, as no existing pipeline is present. At rpc values of 0.10 and 0.25, an extra capacity of 1807 MW is needed to connect the *Groningen Salt Caverns* (node 5) to the backbone in the form of pipeline (5,12), as capacity demand slightly exceeds existing capacity present. In the $rpc = 0.35$ scenario, building a higher capacity pipeline (5,12) becomes more economical than repurposing the existing pipelines (1,5) and (1,12).

In Noord-Holland, higher values for rpc cause a significant change in the optimal network layout. At $rpc = 0.35$, instead of repurposing pipeline (0,9) between the industrial cluster *Noordzeekanaalgebied* and the international pipeline connection towards the UK, it becomes cheaper to build a new pipeline (0,20) parallel to the existing pipeline on that stretch.

When comparing the *2040(30)* and *2040(50)* scenarios, it is clear that increasing the amount of NG available for repurposing by 2040 is of paramount importance to keeping hydrogen transmission network costs low. If Gasunie does not manage to free a significant level of capacity by 2040, network costs could increase fivefold. Freeing up the entire H-gas network by 2040 will pose an enormous challenge, as this requires natural gas transmission through the H-gas network to be reduced to zero. There is a high probability that this will not be possible, and trade-offs have to be made.

7.1.3 Results 2050

We have investigated four 2050 scenarios with different levels of governance. Results for each of these scenarios are assessed in this section. For these scenarios, we will also use supply and demand profiles to assess and compare the results. Time steps in the supply and demand plots are as follows: step 0, 1 and 2 are respectively the (1) high supply, low demand, (2) the low supply, high demand and (3) the high supply, high demand snapshots of weather year 2015. Steps 3, 4 and 5 are represented by the same snapshots in the same order for weather year 1987.

2050(RG)

As we can see in Figure 7.4, this scenario has very large spikes of storage unloading from the Groningen Salt Cavern Storage-facility (GSCS) in times of high industrial demand. In times of high industrial supply, a lot of hydrogen is stored in the GSCS, especially in extreme weather year 1987. This can mainly be explained by the limited amount of imports and exports in this scenario. From this data, we expect that a lot of capacity demands are put on the pipelines connecting the GSCS to the industrial clusters, with an emphasis on the large clusters of *Rotterdam-Moerdijk* and *Smart Delta*.

Optimal network layouts for the *2050(RG)* scenario are shown in Figure 7.5 and their respective costs can be seen in Table 7.4.

When policy aims at national governance of the energy transition, we find that available existing capacity is not enough to fully connect supply to demand. All existing capacity is utilised, and new capacity is installed, especially between the *Groningen Salt Caverns* and the industrial cluster of *Rotterdam-Moerdijk*. Because of

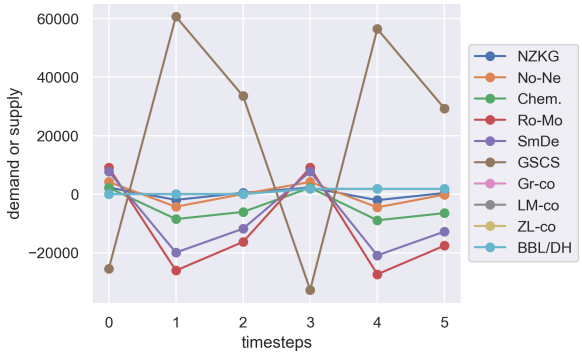

Figure 7.4: Supplies and demands over time steps in *2050(RG)* scenario

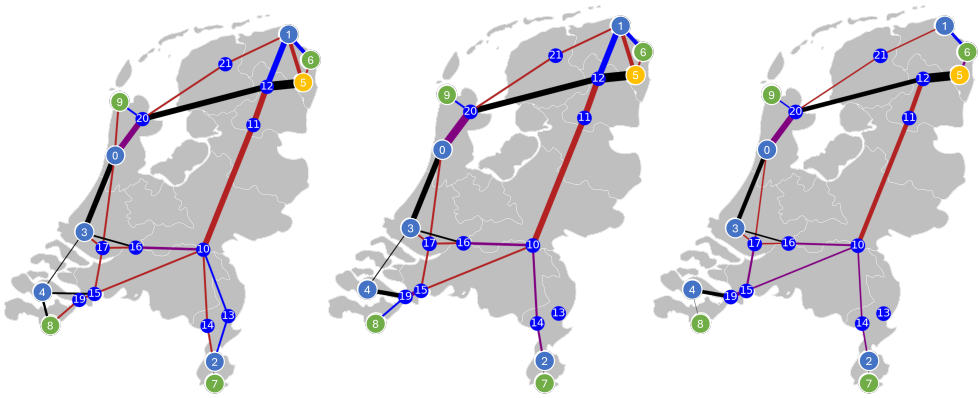

(a) $rpc = 0.10$ **(b)** $rpc = 0.25$ **(c)** $rpc = 0.35$

Figure 7.5: Optimal network layouts for *2050(RG)* scenario

Table 7.4: Optimal network layout costs for *2050(RG)* scenario (billion EUR)

rpc	Total cost	Repurposing cost	New pipeline cost
0.1	1.798	0.295	1.503
0.25	2.212	0.656	1.555
0.35	2.456	0.771	1.685

the large installed capacity of new pipelines, investment costs are high, ranging from 1.798 to 2.456 billion EUR. Repurposing costs make up a relatively small share of this cost because of the higher levels of new pipelines.

Infrastructure to the industrial cluster *Chemelot* in Limburg starts to get saturated in this scenario, and additional existing pipelines are used in the area when $rpc = 0.10$. For the other two values for *rpc*, building new, parallel pipelines is the more economical choice to meet transmission demands in the area.

Similar to the 2030 and 2040 scenarios, pipelines in the Groningen area are differently organised in the $rpc = 0.35$ run than in the $rpc = 0.10$ and 0.25 runs for this scenario, resulting from alternative routing becoming cheaper.

2050(NG)

This scenario has a very similar supply and demand set as the *2050(RG)* scenario, as can be seen when comparing Figure 7.6 to Figure 7.4. Peaks in both supply and demand are larger in this scenario, so it is expected that the networks in this scenario are similar, but more expensive and require more new infrastructure.

Optimal network layouts for the *2050(NG)* scenario are shown in Figure 7.7 and their respective costs can be seen in Table 7.5.

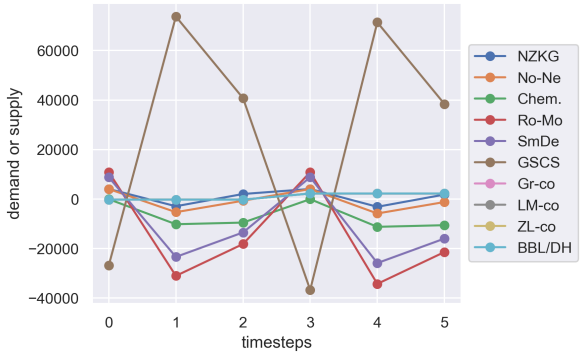

Figure 7.6: Supplies and demands over time steps in *2050(NG)* scenario

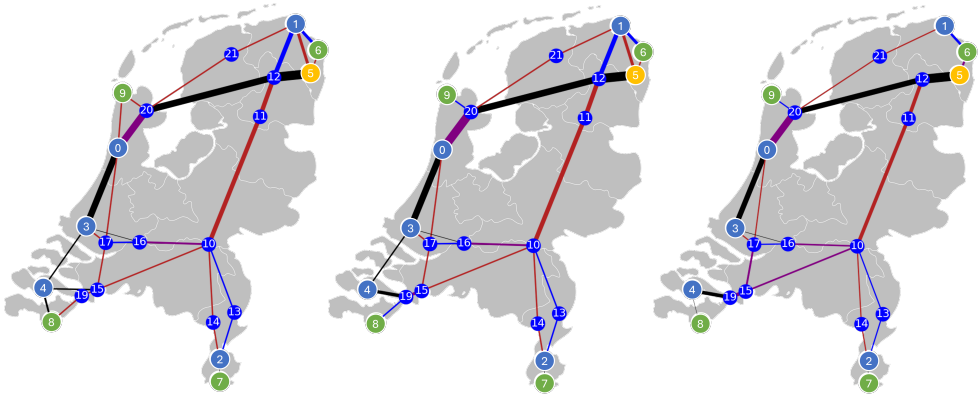

(a) $rpc = 0.10$ **(b)** $rpc = 0.25$ **(c)** $rpc = 0.35$

Figure 7.7: Optimal network layouts for *2050(NG)* scenario

Table 7.5: Optimal network layout costs for *2050(NG)* scenario (billion EUR)

rpc	Total cost	Repurposing cost	New pipeline cost
0.1	2.189	0.295	1.894
0.25	2.613	0.713	1.900
0.35	2.850	0.850	2.000

The model produces the expected results. With network layouts being very similar to those in the *2050(RG)* scenario, but more extra capacity installed. Especially between the *Groningen Salt Caverns* and the industrial clusters *Rotterdam-Moerdijk* and *Smart Delta*, a significant amount of extra capacity is added. This results in high investment costs ranging from 2.189 to 2.850 billion EUR for this scenario, with costs mainly resulting from the building of new pipelines. When comparing the *2050(RG)* and *2050(NG)* scenarios, we find that repurposing costs are similar, and the higher cost in this scenario is mainly caused by instalment of new pipelines of higher capacity.

Extra capacity is installed across the board, with larger capacity demands resulting in repurposing of all existing capacity in Limburg being the most economical option across no matter the value for *rpc*, as opposed to in the *2050(RG)* scenario, where the building of new pipelines was cheaper than repurposing existing infrastructure in the runs at higher *rpc*. Apart from the Limburg area, at all values for *rpc*, this scenario has the same network layout as the *2050(RG)* scenario.

2050(EG)

From the demand and supply sets in Figure 7.8 we can see that in this scenario, the maximum capacity demands on the transmission infrastructure are not as high as in the other scenarios. This is a result of a high level of local production and use in this scenario, reducing the demand for transmission infrastructure.

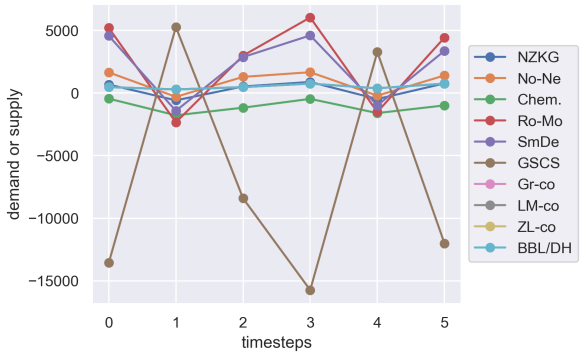

Figure 7.8: Supplies and demands over time steps in *2050(EG)* scenario

Optimal network layouts for the *2050(EG)* scenario are shown in Figure 7.9 and their respective costs can be seen in Table 7.6.

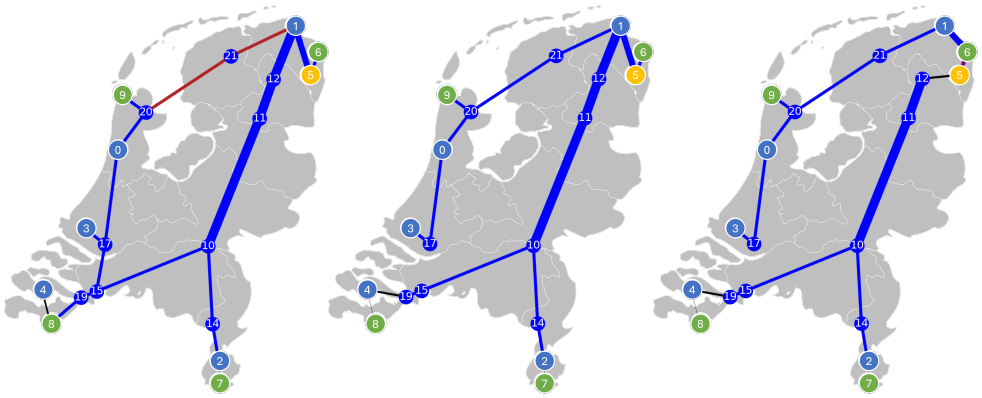

(a) $rpc = 0.10$ **(b)** $rpc = 0.25$ **(c)** $rpc = 0.35$

Figure 7.9: Optimal network layouts for *2050(EG)* scenario

Table 7.6: Optimal network layout costs for *2050(EG)* scenario (billion EUR)

rpc	Total cost	Repurposing cost	New pipeline cost
0.1	0.289	0.234	0.055
0.25	0.626	0.544	0.082
0.35	0.832	0.674	0.158

When policy is steered by European governance, we find that the existing NG infrastructure available is mostly sufficient to satisfy transmission demands. Because of large levels of CCUS throughout the EU, the hydrogen economy is relatively small in this scenario. Investment costs range from 289 to 832 million EUR, with little investments in new pipelines. The only infrastructure built, when $rpc = 0.10$ and 0.25, is to connect the industrial cluster *Smart Delta* to the backbone. When $rpc = 0.35$, building new pipelines along the stretches (5,12) and (5,6) becomes cheaper than repurposing existing pipelines (1,5) and (1,12). This is a trend that we are seeing across all scenarios.

An interesting observation is that when $rpc = 0.10$, stretch (15,17) is repurposed, something that does not happen when $rpc = 0.25$ and 0.35. This results in a network that is more expensive than it needs to be. An explanation could be that the limitation to the model that causes it to miss certain optimisations, discussed in Chapter 3, happens in this case. This behaviour should be more closely investigated in further research.

2050(IG)

In the demand and supply plots in Figure 7.10 we see that large amounts of imports and exports through the Dutch ports create supply and demand peaks in industrial clusters with large ports, especially in the port of Rotterdam. Looking at the high supply, low demand scenario of extreme weather year 1987. We see that a large import of 18060 MW in one hour, is expected by the ETM to be mostly stored in the *Groningen Salt Caverns*. It is therefore expected that the model fully utilises existing infrastructure around the *Rotterdam-Moerdijk* industrial cluster and creates extra capacity where necessary.

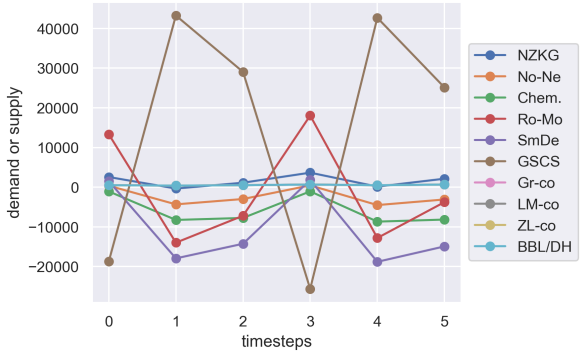

Figure 7.10: Supplies and demands over time steps in *2050(IG)* scenario

Optimal network layouts for the *2050(IG)* scenario are shown in Figure 7.11 and their respective costs can be seen in Table 7.7.

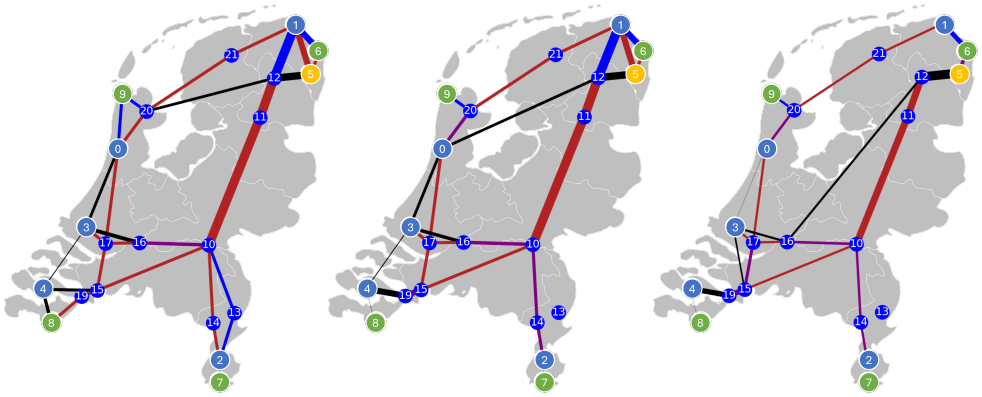

(a) $rpc = 0.10$ **(b)** $rpc = 0.25$ **(c)** $rpc = 0.35$

Figure 7.11: Optimal network layouts for *2050(IG)* scenario

In this scenario, global markets dominate supplies and demands. As expected, extra capacity is installed between the industrial clusters in the west of the country and the *Groningen Salt Cavern Storage*. This is the result of large shipping imports to and exports from the industrial clusters of *Rotterdam-Moerdijk* and *Noordzeekanaalgebied*. These imports and exports are mostly met by storage in Groningen. The network layout is very similar to the *2050(RG)* and *2050(NG)* scenarios, albeit with

Table 7.7: Optimal network layout costs for *2050(IG)* scenario (billion EUR)

rpc	Total cost	Repurposing cost	New pipeline cost
0.1	1.180	0.295	0.885
0.25	1.611	0.638	0.973
0.35	1.843	0.771	1.072

a lower installed capacity of new pipelines. This results in significantly lower investment costs, ranging from 1.180 to 1.843 billion EUR. Repurposing costs in this scenario are similar to those in the *2050(RG)* and *2050(NG)* scenarios, but costs for new pipelines are reduced significantly as a result of lower supply and demand peaks.

As in the previous scenarios, the optimal network layout in Groningen differs when *rpc* is high. For each value of *rpc*, the pipeline connecting the *Groningen Salt Caverns* to the industrial clusters in the west is oriented differently.

7.1.4 An investigation into regret for 2050 network layouts

Because we are working with high levels of uncertainty when forecasting scenarios for 2050, now be investigating possible 2050 network layouts and their expected levels of regret. For each of the four 2050 optimal network layouts at $rpc = 0.25$, we will calculate the level of over- or underinvestment when one of the other scenarios turns out to be true. Because we have no information on returns on investments, we will use three different indicators for regret to analyse the different network layouts. We will calculate the maximum underinvestment, the maximum overinvestment and the minimal maximum over- or underinvestment, also called the minimax regret. Please note that in this investigation into regret, we do not investigate whether the transmission capacities of the networks are sufficient to meet transmission demands in other scenarios, as we are solely looking at investment costs. The only network of which we know for certain that it suffices the capacity demands of all scenarios is the *2050(ALL)* network.

Besides analysing the optimal network layouts for each of the four 2050 scenarios, we will also create novel networks that are optimal when supply and demand data of different scenarios are combined, to try and find a network layout with the least regret. Scenarios are combined by combining supply and demand data of different scenarios into one input file. All investigated network layouts and their respective data can be viewed in Appendix F

No underinvestment

When the aim of building a hydrogen network for 2050 is spending the least amount of money, whilst keeping the chances of underinvestment at zero, the optimal network layout for scenario *2050(ALL)* should be built. We know that this scenario meets all transmission capacity demands, regardless of what scenario turns out to be true. The maximum overinvestment when building this network is 2.049 billion EUR.

The minimal maximum over- or underinvestment

When aiming at building infrastructure that has the lowest possible maximum or minimum underinvestment, also known as the minimax regret, we advise investing in the optimal network layout for scenario *2050(IG)*. When building this network, the maximum overinvestment that will be made is 985 million EUR, and the maximum underinvestment is 1.002 billion EUR.

7.1.5 A note on existing pipeline size

In Chapter 6, based on assumptions made by Tezel and Hensgens (2021) in the *HyWay27* project and resulting from a lack of information from Gasunie Transport Services (2012), we assumed that all existing NG pipelines in the Dutch H-gas network are 36 inches in diameter. Due to time constraints related to this research, we were not able to investigate the implications of this assumption being wrong. We found this possibility too interesting to completely ignore, so we re-ran the model for the *2050(NG)* scenario, assuming that all existing pipelines are 48 inches in diameter. Tezel and Hensgens (2021), together with Gasunie, state that 48-inch hydrogen pipelines have roughly double the capacity of 36-inch pipelines. Integrating this information into the model input files, and running the model at $rpc = 0.25$ we find the optimal network layout seen in Figure 7.12b. Figure 7.12a shows the optimal network for the same scenario and input variables when existing pipelines are of 36-inch diameter.

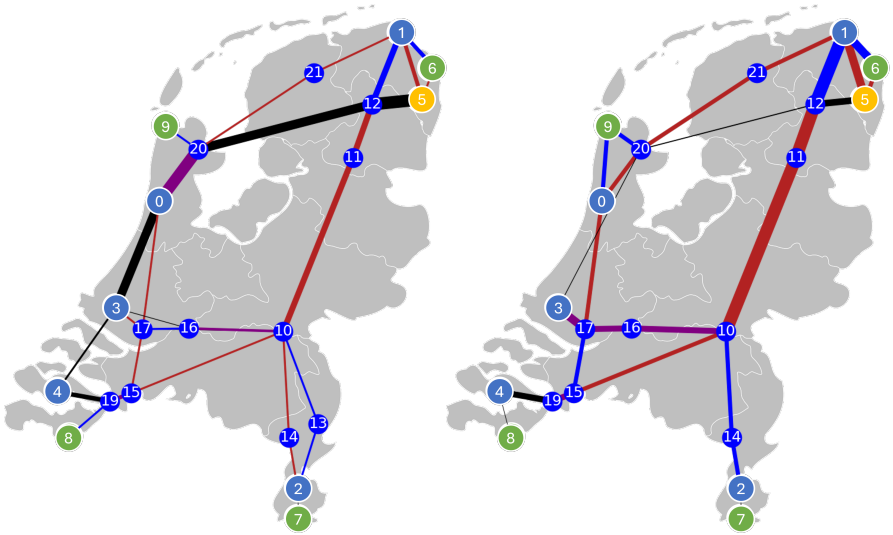

(a) 36-inch pipelines **(b)** 48-inch pipelines

Figure 7.12: Comparison of 36-inch and 48-inch existing pipelines for *2050(NG)* scenario

The total cost of the network layout when existing pipelines are of 48-inch diameter are 1.897 billion EUR, with 1.005 billion EUR directed to repurposing costs and 0.892 billion EUR to the building of new pipelines. Even when all available pipelines are 48-inch, the NG infrastructure available is still not sufficient to meet all demands in the scenario with the largest transmission capacity demands. The network is, however, 27.4% cheaper because more infrastructure is available for repurposing. Repurposing costs naturally also take up a larger share of the total network cost when more capacity is available. Besides fully utilising existing transport capacity, an extra capacity of 4200 MW is needed to connect the *Groningen Salt Caverns* to the industrial clusters in the west of the country.

7.1.6 Case discussion

In Table 7.8, an overview is shown of the network costs for all scenarios, paired with information about the levels of new and repurposed infrastructure.

Timeline

The existing NG infrastructure that Gasunie expects to make available by 2030 is sufficient to meet all transmission demands by that time. Except for connecting the industrial clusters *Rotterdam-Moerdijk* and *Smart Delta* to the hydrogen backbone,

Table 7.8: Network costs for all experiments (billion EUR) and share of new and repurposed pipelines

Scenario	*rpc*	Total cost	Repurposing		New pipelines	
2030	0.1	0.192	0.104	54%	0.088	46%
	0.25	0.300	0.187	62%	0.113	38%
	0.35	0.358	0.216	60%	0.141	40%
	∞	0.381				
2040(30)	0.1	1.329	0.127	10%	1.202	90%
	0.25	1.495	0.318	21%	1.178	79%
	0.35	1.622	0.419	26%	1.203	74%
	∞	1.599				
2040(50)	0.1	0.434	0.273	63%	0.161	37%
	0.25	0.835	0.660	79%	0.175	21%
	0.35	1.056	0.740	70%	0.315	30%
	∞	1.720				
2050(RG)	0.1	1.798	0.295	16%	1.503	84%
	0.25	2.212	0.656	30%	1.555	70%
	0.35	2.456	0.771	31%	1.685	69%
	∞	2.701				
2050(NG)	0.1	2.189	0.295	13%	1.894	87%
	0.25	2.613	0.713	27%	1.900	73%
	0.35	2.850	0.850	30%	2.000	70%
	∞	3.088				
2050(EG)	0.1	0.289	0.234	81%	0.055	19%
	0.25	0.626	0.544	87%	0.082	13%
	0.35	0.832	0.674	81%	0.158	19%
	∞	1.180				
2050(IG)	0.1	1.180	0.295	25%	0.885	75%
	0.25	1.611	0.638	40%	0.973	60%
	0.35	1.843	0.771	42%	1.072	58%
	∞	2.438				
2050(ALL)	0.1	2.251	0.295	13%	1.956	87%
	0.25	2.675	0.713	27%	1.962	73%
	0.35	2.984	0.850	28%	2.134	72%
	∞	3.088				

and a few minor connections in Limburg, no additional transmission capacity is needed. This is in line with findings by Tezel and Hensgens (2021).

By 2040, that same infrastructure is no longer sufficient to meet all transmission demands. An extra capacity of approximately 12200 MW is required connecting industrial clusters *Rotterdam-Moerdijk* and *Noordzeekanaalgebied* to storage in the *Groningen Salt Caverns*, with the final stretch requiring a capacity that exceeds 17000 MW. The complete H-gas network, however, would provide just enough capacity to meet transmission demands in 2040. The H-gas network, however, can only be fully repurposed for hydrogen transport when no more NG has to be transported through it. This will probably only be feasible by 2050, when complete carbon neutrality is expected. In all 2050 scenarios, except the *2050(EG)* scenario, it is expected that extra transmission capacity will be required connecting industrial clusters *Rotterdam-Moerdijk* and *Noordzeekanaalgebied* to storage in the *Groningen Salt Caverns*. This capacity requirement exceeds the requirements in the *2040(30)* scenario by roughly a factor of 2, capacity in 2050 on those stretches occasionally exceeding 40,000 MW.

By investing in those stretches towards 2040, it is possible to simultaneously make sure that transmission capacity requirements for 2040 are met, and to prepare for an increase of transmission demand by 2050.

Percentages of existing pipelines

An interesting observation is that increasing the repurposing cost from 0.1 to 0.25 results in roughly a doubling of total repurposing costs in most scenarios. This indicates that within that range, repurposing existing pipelines remains the most profitable solution in most cases. Increasing the repurposing cost from 0.25 to 0.35 however, does not result in a significant cost increase in any of the scenarios. In some scenarios, it even results in a cost decrease of total repurposing costs. This means that in the range between $rpc = 0.25$ and $rpc = 0.35$, building new pipelines is often cheaper than repurposing existing stretches. These findings indicate that the relationship between final network cost and rpc are not linear, and keeping rpc below a certain threshold can result in large cost savings. This effect should be further investigated.

7.2 MODELLING RESULTS

In this section, we will assess the modelling performance of the NROM. We will first share results of a comparison with results from the NOM. We will then re-evaluate the scenario studies earlier in this chapter through the lens of model performance.

7.2.1 A comparison of model performance

To validate the workings of the NROM, and identify the types of cases it is applicable to, we will compare its results at $rpc = 0$ and $rpc = \infty$ with results for the same experiments ran by the NOM. The runs at $rpc = 0$ represent use of existing infrastructure at no cost, and $rpc = \infty$ indicates that it is not possible to repurpose existing infrastructure. These are the only two values for rpc that the NOM is capable of simulating, by simply turning repurposing on or off in its interface. Results for these runs for all scenarios shown in Table 7.9.

We find that in the case of $rpc = 0$, the NROM outperforms the NOM in every scenario. Ranging from a low-cost reduction of 0.25% in the 2030 scenario, to a cost reduction of over 785% in the *2050(EG)* scenario. Taking a closer look at the *2050(EG)* scenario, we find that the reason for the NOM performing so poorly, is its inability to create cycles in the network layout results in an unnecessary pipeline (3,12) being created (see Figure 7.13). The NROM simply uses the existing infrastructure present with cycles included, and does not create any unnecessary new infrastructure. It appears to be the case that the higher the share of existing pipelines in the final network layout, the larger the difference between NOM and NROM performance. But further research should be done to investigate the relationship.

When setting $rpc = \infty$, the NOM outperforms the NROM by around 10%. As the model was created with repurposing existing infrastructure in mind, we are not unhappy with this result. It gives a first indication that the NROM does a good job at approaching cost-minimal solutions in case there is no existing infrastructure present, but the model should be applied to more example cases to further study its performance. Taking a closer look at the *2050(IG)* scenario, which has the highest difference between NOM and NROM performance at $rpc = \infty$, we find that the NROM is not as proficient as the NOM at making tree topology network layouts (see Figure 7.14).

Table 7.9: NROM performance compared to the NOM (percentile difference in network cost)

Scenario	Model	*rpc*	Total cost	NROM performance
2030	NOM	0	0.089	
		∞	0.381	
	NROM	0	0.088	-0.25%
		∞	0.381	+0.07%
2040(30)	NOM	0	1.391	
		∞	1.531	
	NROM	0	1.202	-15.70%
		∞	1.599	+4.25%
2040(50)	NOM	0	1.395	
		∞	1.531	
	NROM	0	0.161	-764.96%
		∞	1.720	+11.01%
2050(RG)	NOM	0	2.059	
		∞	2.485	
	NROM	0	1.479	-39.18%
		∞	2.701	+8.02%
2050(NG)	NOM	0	2.960	
		∞	2.790	
	NROM	0	1.862	-58.95%
		∞	3.088	+9.65%
2050(EG)	NOM	0	0.488	
		∞	1.041	
	NROM	0	0.055	-785.86%
		∞	1.180	+11.75%
2050(IG)	NOM	0	1.896	
		∞	2.094	
	NROM	0	0.885	-114.21%
		∞	2.438	+14.13%

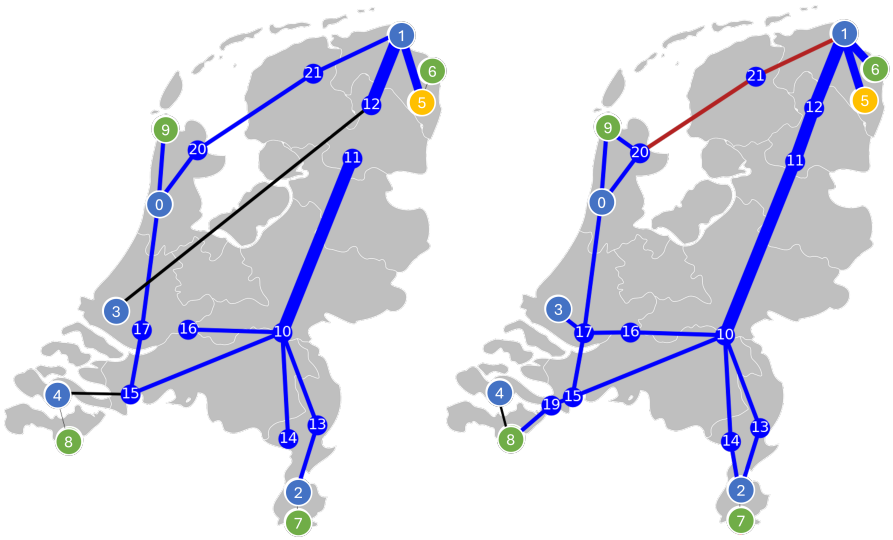

(a) NOM **(b)** NROM

Figure 7.13: NOM and NROM network layouts for *2050(EG)* scenario at $rpc = 0$

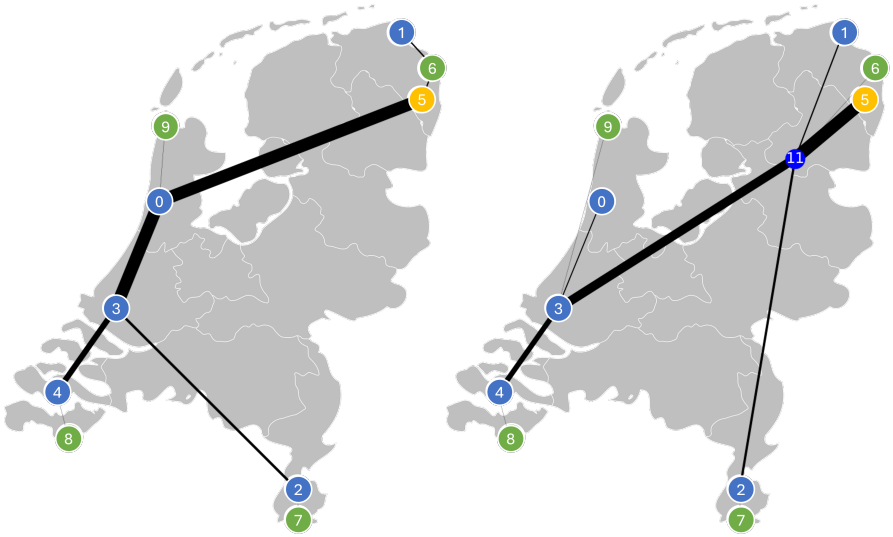

(a) NOM (b) NROM

Figure 7.14: NOM and NROM network layouts for *2050(IG)* scenario at $rpc = \infty$

7.2.2 General findings on model performance

Assessing the different future hydrogen scenarios earlier in this chapter gave us an up close look into the behaviour of the model. We find that the model only creates new pipelines when existing capacity connecting the same nodes is fully utilised. The exception being, of course, when repurposing existing infrastructure becomes more expensive than building it new. It should also be noted that the NROM always produces cheaper network layouts at $rpc = 0.35$, than the NOM creates for the same networks without repurposing infrastructure. No particular quirks in the different network layouts were found that require a deeper investigation, but applying the model to more cases in the future is important in being able to give a more generalised judgement on model performance. These first results, however, look promising.

7.2.3 Validity of results

In the recently published *HyWay27* project, Tezel and Hensgens (2021) and Gasunie estimated the Dutch hydrogen backbone to require an investment of 1.5 billion EUR, with 0.85 billion EUR required for the repurposing of existing NG infrastructure, and 0.65 billion EUR necessary to build new transmission pipelines. Taking the average cost over the four 2050 scenarios based on the scenario builds by Netbeheer Nederland (2021), we find that our model calculates an average total network cost of 1.708 billion EUR, with 0.546 billion EUR directed to repurposing existing infrastructure and 1.162 reserved for the construction of new pipelines. No information was shared by Tezel and Hensgens (2021) on how they built their scenario, so it is difficult to pinpoint how the difference in costs come about, but they are close enough to validate that our model produces results that can be generalised to the real world.

7.2.4 Limitations and notes on model use

In our modelling approach, we used the network simplex package as a basis for the *combined-simplex heuristic* used in steps 3 and 5. A limitation of the network simplex package is that it can encounter problems when working with edge lengths that have decimal numbers (NetworkX Developers, 2004b). Therefore, all edge lengths

have to be rounded before each optimisation with the heuristic. This results in small inaccuracies in outcomes and optimisations. These inaccuracies become significantly smaller when working with larger numbers in the model. When using the model, it is therefore suggested to use large numbers when possible. For example, if distances between nodes are described in tens of kilometres, define the input coordinates in meters. The same principle goes for capacities and demands and supplies.

When the network is fully connected by existing pipelines, meaning that all nodes are connected to all other nodes, and these existing pipelines do not fully meet the capacity demands, the combined simplex heuristic will not be able to find a solution. It is not expected that these types of situations will occur when studying gas infrastructures, unless one would be interested in a small subnetwork of the larger system. We have only encountered these problems when validating the inner workings of the model in the first part of Chapter 4.

When building the scenario, several assumptions and decisions were made that limit the generalisability of our modelling results. This was done in order to simplify the case so that we could properly test the workings of the NROM, and make the analysis more clear. One of the simplifications made is the assumption that all hydrogen demands and supplies take place in the five large industrial clusters. This excludes a large portion of industry that is more spread throughout the country and is also known as the sixth industrial cluster (FNLI and VNP, 2020). This sixth cluster is expected to also have a significant demand of hydrogen by 2050.

8 CONCLUSION AND RECOMMENDATIONS

This research was aimed at finding an answer to the following main research question:

> What is a suitable network optimisation approach that aids in the design of cost-effective future network layouts, taking into account repurposing of existing infrastructure?

In this chapter we will answer the sub-questions formulated in Chapter 1, discuss the scientific and practical contributions of this research and reflect on the research process.

8.1 MODEL FORMULATION

The first two sub-questions of this research were aimed at identifying a suitable methodology for networked system cost minimisation, taking into account repurposing of existing infrastructure and the exploration of different system configurations.

1. How can networked infrastructure be modelled, minimising investment costs?

2. How can the repurposing of existing infrastructure and the exploration of different system configurations be taken into account in the modelling approach?

In Chapter 2, we identified GGT as the most promising approach to modelling such problems, and selected the NOM by Heijnen et al. (2020) for adaption. In order to integrate the repurposing of existing infrastructure, two main changes to the model had to be made. A cost related to the repurposing of existing infrastructure had to be included into the objective function of the NOM. A review of the literature in Chapter 2 provided enough inspiration on how to integrate this element, and the repurposing of existing infrastructure was included in the form of a variable repurposing coefficient rpc. As far as we know, a network optimisation model that allows users to manually change conditions for repurposing existing infrastructure has never been built.

In Chapter 1 we established that in order to properly include the repurposing of existing infrastructure into the optimisation, cycles in existing infrastructure had to be taken into account, as well as the possibility for creation of new cycles using existing infrastructure. The NOM is not capable of either of those things, as it uses heuristics based on tree-topology networks. A deep dive into GGT in Chapter 3 found that the *network simplex approach* to the *min cost flow problem* was a suitable approach to this problem, and that *Python's NetworkX module* contains this algorithm. The novel *network_simplex_repurposing heuristic* was able to prepare the input files for optimisation by the algorithm (see black lines in Algorithm 3.1) and subsequently run the optimisation.

However, the objective of this research, as defined in Chapter 1, included the integration of temporal resolution into the approach. The *network simplex approach* to

the *min cost flow problem* is not able to include multiple timesteps into its optimisation, so the *network_simplex_repurposing heuristic* had to be expanded (see teal lines in Algorithm 3.1). Another novel heuristic called the *timesteps_merged heuristic* was created to be able to combine all timesteps into one optimised network (see Algorithm 3.2). Redundancies are then removed from the network by the *joined_edges heuristic* (see Algorithm 3.3). This combination of novel heuristics allows for the cost minimisation of a networked system layout, whilst taking into account the repurposing of existing infrastructure and keeping model operation simple and quick and application flexible. To the best of our understanding, no such model has ever been built.

8.2 MODEL APPLICATION

After completion of the model, it was applied to the case of repurposing NG infrastructure for hydrogen transmission in the Netherlands in sub-questions three and four.

> 3. How can the model be applied to the case of repurposing NG pipelines for hydrogen transport?

Because the flexibility of the model lies in its input files, application of the model to our case did not require any further modelling. First, we decided on values for the scaling cost exponent β and repurposing cost coefficient rpc, and assigning them those values in the model interface. The input files were subsequently created for the different scenarios following extensive case study into demand and supply profiles, locations of supply and demand and existing infrastructure. Besides the NOM, on which the NROM is based, no other models have been encountered in our review of relevant literature that allow for similar levels of flexibility in use.

> 4. What insights are created by the model when applied to the case of repurposing NG pipelines for hydrogen transport?

Application of the NROM provided valuable insights regarding the implications of repurposing NG pipeline infrastructure for hydrogen transmission. The available infrastructure made available by Gasunie by 2030 is sufficient to meet most transport capacity demands. Except for the connection of the industrial clusters to the repurposed NG infrastructure, no extra capacity is necessary. Repurposing existing infrastructure significantly reduces total network investment costs, and also provides a durable alternative to reuse otherwise obsolete infrastructure.

By 2040, the existing NG pipeline infrastructure made available for repurposing to hydrogen pipelines is no longer sufficient to meet all capacity demands. Especially between the *Groningen Salt Caverns* and the industrial clusters of *Noordzeekanaalgebied* and *Rotterdam-Moerdijk*, additional transmission capacity is required. If Gasunie would gradually make extra stretches of NG pipelines available for repurposing between 2030 and 2040, transmission investment costs could be reduced by 600 to 900 million EUR, depending on the costs related to repurposing.

Assuming a 36-inch diameter of NG pipelines available for repurposing, existing infrastructure is no longer sufficient in 2050 to meet transmission capacity demands. Only in the *European governance* scenario, where hydrogen production and demand is low, is the existing infrastructure sufficient. In the *regional, national and international governance* scenarios, several new stretches of high-capacity pipelines are necessary to meet all transmission demands. Extra capacity is especially needed connecting the *Groningen Salt Caverns* to the industrial clusters of *Rotterdam-Moerdijk* and *Noordzeekanaalgebied*. These stretches coincide with the extra transmission capacity demands in 2040. A synergy is possible when Gasunie starts investing in an overcapacity for 2040 on those stretches, preparing the network for the increased

2050 capacity demands. In this way, the extra infrastructure has only got to be built once and scaling benefits can most optimally be utilised. A short investigation into a 2050 network layout with existing pipelines of 48-inch indicated that even in that extreme case, the instalment of new pipelines is necessary to meet all transmission capacity demands. This can be explained by a large variability in supply and demand in sustainable energy systems with high levels of wind and solar power.

8.3 POSSIBILITIES FOR FURTHER RESEARCH

As is typical of scientific inquiry, for every question answered in this research, a multitude of new questions is uncovered. This creates interesting possible directions for further research. Further research can be divided into three general directions; further research into the model, a broadening and deepening of the case study, and application of the model to different cases.

8.3.1 Further research into the model

Several shortcomings of the modelling approach have been discussed in previous chapters. These shortcomings each incentivise further research. In Algorithm 3.3, the model attempts to remove redundancies from the model by combining edges. Because we work with multiple timesteps, between which directions of flow for certain edges might differ, edge flow directions can not be taken into account when joining edges. This results in the possibility of optimisations to be missed because of an overcapacity in the calculation. Further research into this behaviour of the model could result in an increased efficiency of the model's outcomes. In that same algorithm, edge pairs are defined as pairs of edges connected to three nodes, with one edge opposite to the angle between the two edges (see Figure 3.12). There could also be instances where pairs of edges have multiple edges instead of the one edge c. As a result of time constraints with relation to this research, this was not further explored. Further research into these possible optimisations could further increase NROM efficiency. The NOM included several functionalities that were left out in the NROM due to time constraints. One of those functionalities is the possibility to include obstacles through which no pipelines can be built and routing restrictions that force certain routes to be used as modelling constraints. Another NOM functionality not present in the NROM is the capacity expansion coefficient cpc, that allows for the cost of capacity expansion to be different from the building of a new pipeline. Implementing these functionalities into the NROM increases model functionality and should be further researched. The addition of repurposing costs in the NROM can also be expanded on by, for example, allowing for different values of rpc for different existing pipelines. We consider the previously mentioned areas of exploration as most valuable and interesting, but that does not mean that the possibilities for exploration are limited to these areas only.

8.3.2 Expanding the case study

In this research, we applied the NROM to the case of repurposing NG pipeline infrastructure for hydrogen transmission. This created interesting insights, but also uncovered promising directions for further research. Inclusion of capacity cost coefficient cpc, as discussed in the previous paragraph, would create the possibility for differentiating the cost of building new pipelines besides existing infrastructure and elsewhere. This increases the generalisability of the outcomes, as pipelines installed besides existing infrastructure tend to be cheaper because of the circumvention of licensing costs. Another interesting direction for further research is cost differentiation of pipelines. This will allow model users to use different costs for

pipelines when, for example, sub-sea and land pipelines are both possible or when different types of soil have to be crossed. Existing NG infrastructure is not the only infrastructure that might be used in a future hydrogen transmission grid. There are already short stretches of hydrogen pipelines installed, for example between the ports of Rotterdam and Antwerp. This existing hydrogen infrastructure was not included in our case study, as the possibility for differentiating repurposing costs between different pipelines is not present in the NROM. In Chapter 7 we have already touched on the subjects of regret, and larger capacity existing pipelines. It would be interesting for these topics to be further explored.

8.4 REFLECTIONS ON THE RESEARCH

After the application of the model to our case, we can discuss the general applicability of the model and answer the final sub-question.

5. What can be learned about the general applicability of the model?

8.4.1 How well does the model work?

Comparing NROM to NOM performance in Chapter 7, we found that the NROM performs especially well in cases where there is a combination of large transport capacity demands and high levels of existing infrastructure present. For certain scenarios, the NROM was found to outperform the NOM by more than 750% in terms of optimal network cost. The NOM outperforms the NROM when repurposing is not possible, but the least efficient network the NROM created was only 14.13% more expensive than the network created by the NOM for the same case. An acceptable inefficiency, considering the NROM was created to analyse the implications of the repurposing of existing infrastructure.

During the research, we have attempted to create randomised experiments to test model generalisability to a range of different cases. We found that when using automated random experiment creation, utilising a heuristic by Heijnen (2019), it is difficult to create realistic cases. Real-world cases

8.4.2 How can the model be used?

By applying the NROM to the case of repurposing existing NG pipeline infrastructure for hydrogen transmission, we have gained valuable insights regarding the general applicability of the model. For a case to deem fit for investigation by the NROM, locations of supply and demand must be able to be expressed in terms of coordinates in a two-dimensional plane. Supply and demand data should be provided in the form of timesteps. These timesteps do not necessarily have to be in the form of a maximum capacity demand snapshot but can also represent chronological timesteps like hours, days or seconds. Existing infrastructure should be present in fixed locations, and should be expressed in terms of capacities of the new form of flow, in our case hydrogen. It has to be possible to express repurposing costs as a fixed fraction of new infrastructure cost.

Examples of cases the NROM include, CCUS, methane, ammonia, water irrigation or fibre-optics pipeline layout when repurposing existing pipeline infrastructure. Another possible application of the model is to transport infrastructure like the repurposing of existing provincial roads to highways and potential possibility for application to waterway layout.

We have demonstrated how the model can be used to gain insights into design implications for repurposing NG pipelines for hydrogen transmission. These insights can provide valuable input for policy decisions in local, national or international

governments. Utility companies like Gasunie can use the model to gain insight into their future investments, which in turn can provide input for negotiations with governments about possible funding.

BIBLIOGRAPHY

Abdin, Z., Zafaranloo, A., Rafiee, A., Mérida, W., Lipiński, W., and Khalilpour, K. R. (2020). Hydrogen as an energy vector.

Accenture (2020). The Future Dutch District Heating System.

Ackerman, E., Fox, J., Pach, J., and Suk, A. (2009). On grids in topological graphs. *Proceedings of the Annual Symposium on Computational Geometry*, pages 403–412.

ACT Acorn (2019). Factsheet 3: Pipeline Re-use, Can Oil & Gas Pipelines be Re-used for CO 2 Transportation? Technical report.

Afman, M. and Rooijers, F. (2017). Net voor de Toekomst. Technical report, CE Delft.

Al-Breiki, M. and Bicer, Y. (2021). Comparative life cycle assessment of sustainable energy carriers including production, storage, overseas transport and utilization. *Journal of Cleaner Production*, 279.

André, J., Auray, S., Brac, J., De Wolf, D., Maisonnier, G., Ould-Sidi, M. M., and Simonnet, A. (2013). Design and dimensioning of hydrogen transmission pipeline networks. *European Journal of Operational Research*, 229(1):239–251.

André, J., Auray, S., De Wolf, D., Memmah, M. M., and Simonnet, A. (2014). Time development of new hydrogen transmission pipeline networks for France. *International Journal of Hydrogen Energy*, 39(20):10323–10337.

Arabzadeh, V., Mikkola, J., Jasiūnas, J., and Lund, P. D. (2020). Deep decarbonization of urban energy systems through renewable energy and sector-coupling flexibility strategies. *Journal of Environmental Management*, 260:110090.

Bandilla, K. W. (2020). Carbon Capture and Storage. *Future Energy: Improved, Sustainable and Clean Options for Our Planet*, pages 669–692.

Baufumé, S., Grüger, F., Grube, T., Krieg, D., Linssen, J., Weber, M., Hake, J. F., and Stolten, D. (2013). GIS-based scenario calculations for a nationwide German hydrogen pipeline infrastructure. *International Journal of Hydrogen Energy*, 38(10):3813–3829.

Beals, S. (2003). A Practical Method for Installation of Optical Fiber Cable in Metropolitan Area Gas Distribution and Service Pipelines.

Boot, T., Riemslag, T., Reinton, E., Liu, P., Walters, C. L., and Popovich, V. (2021). Assessing the Susceptibility of Existing Pipelines to Hydrogen Embrittlement. *Minerals, Metals and Materials Series*, 5:722–729.

CBS (2019a). International trade in gas in the Netherlands. Technical report.

CBS (2019b). Regionale prognose 2020-2050; bevolkingsontwikkeling, regioindeling 2018.

CBS (2021). Hoeveel vracht gaat er via Nederlandse zeehavens?

Cerniauskas, S., Jose Chavez Junco, A., Grube, T., Robinius, M., and Stolten, D. (2020). Options of natural gas pipeline reassignment for hydrogen: Cost assessment for a Germany case study. *International Journal of Hydrogen Energy*, 45(21):12095–12107.

Chandra Mohan, B. and Baskaran, R. (2012). A survey: Ant Colony Optimization based recent research and implementation on several engineering domain. *Expert Systems with Applications*, 39(4):4618–4627.

Chemelot-tafel (2020). Regioplan cluster Chemelot.

Chen, Y. and Zhu, J. (2019). A graph theory-based method for regional integrated energy network planning: A case study of a China–U.S. low-carbon demonstration city. *Energies*, 12(23).

Dagdougui, H. (2012). Models, methods and approaches for the planning and design of the future hydrogen supply chain. *International Journal of Hydrogen Energy*, 37(6):5318–5327.

d'Amore, F., Romano, M. C., and Bezzo, F. (2021). Carbon capture and storage from energy and industrial emission sources: A Europe-wide supply chain optimisation. *Journal of Cleaner Production*, 290:125202.

De Villiers, N., Van Rooyen, G. C., and Middendorf, M. (2018). Sewer network design layout optimisation using ant colony algorithms. *Journal of the South African Institution of Civil Engineering*, 60(3):2–15.

Deloitte (2020). Will hydrogen be the surprise of this decade?

Detz, R. J., Lenzmann, F. O., and Weeda, M. (2019). Future Role of Hydrogen in the Netherlands. Technical report, TNO, Petten.

Dijkstra, E. (1959). A note on two problems in connexion with graphs. *Numerische Mathematik*, 1(1):269–271.

Dorigo, M. (1992). Optimization, Learning and Natural Algorithms. *Ph.D. Thesis, Politecnico di Milano*.

EC (2019). A European Green Deal.

EC (2020). Powering a climate-neutral economy.

Elahi, N., Shah, N., Korre, A., and Durucan, S. (2017). Multi-stage Stochastic Optimisation of a CO2 Transport and Geological Storage in the UK. *Energy Procedia*, 114:6514–6525.

Enagás, Energinet, Fluxys Belgium, Gasunie, GRTgaz, NET4GAS, OGE, ONTRAS, Snam, Swedegas, and Teréga (2020). European Hydrogen Backbone: How a Dedicated Hydrogen Infrastructure can be Created. Technical report.

Feng, H., Chi, Q., Ji, L., Li, H., and Yang, K. (2017). Research and development of hydrogen embrittlement of pipeline steel. *Corrosion Science and Protection Technology*, 29(3):318–322.

FNLI and VNP (2020). Klimaattransitie door de Nederlandse Industrie.

Frey, D. D., Herder, P. M., Wijnia, Y., Subrahmanian, E., Katsikopoulos, K., and Clausing, D. P. (2009). The Pugh Controlled Convergence method: Model-based evaluation and implications for design theory. *Research in Engineering Design*, 20(1):41–58.

Frey, D. D., Herder, P. M., Wijnia, Y., Subrahmanian, E., Katsikopoulos, K., De Neufville, R., Oye, K., and Clausing, D. P. (2010). Research in engineering design: The role of mathematical theory and empirical evidence. *Research in Engineering Design*, 21(3):145–151.

Fuel Cells and Hydrogen Joint Undertaking (2019). Hydrogen Roadmap Europe: A Sustainable Pathway for the European Energy Transition. Technical report, European Union.

Garber, M., Sarkani, S., and Mazzuchi, T. (2017). A Framework for Multiobjective Decision Management with Diverse Stakeholders. *Systems Engineering*, 20(4):335–356.

Gasunie and TenneT (2019). Infrastructure Outlook 2050: A joint study by Gasunie and TenneT on integrated energy infrastructure in the Netherlands and Germany. Technical report.

Gasunie Transport Services (2012). Het Transportnetwerk .

Gim, B., Boo, K. J., and Cho, S. M. (2012). A transportation model approach for constructing the cost effective central hydrogen supply system in Korea. *International Journal of Hydrogen Energy*, 37(2):1162–1172.

Givoni, M. and Perl, A. (2017). Rethinking Transport Infrastructure Planning to Extend Its Value over Time:. *https://doi.org/10.1177/0739456X17741196*, 40(1):82–91.

Government of the Netherlands (2019). Klimaatakkoord hoofdstuk Waterstof. chapter 5.7.

Government of the Netherlands (2020). HyWay 27 kick-off: The Dutch Ministry of Economic Affairs and Climate Policy, Gasunie and TenneT look into using national gas grid to develop hydrogen infrastructure.

Guo, M. and Shah, N. (2015). Bringing Non-energy Systems into a Bioenergy Value Chain Optimization Framework. *Computer Aided Chemical Engineering*, 37:2351–2356.

Heijnen, P., Chappin, E., and Nikolic, I. (2014). Infrastructure network design with a multi-model approach: Comparing geometric graph theory with an agent-based implementation of an ant colony optimization. *JASSS*, 17(4).

Heijnen, P. W. (2019). Generate random examples for NOM.

Heijnen, P. W. (2020). Tutorial Optimal Network Layout Version 2.0.

Heijnen, P. W., Chappin, E. J., and Herder, P. M. (2020). A method for designing minimum-cost multisource multisink network layouts. *Systems Engineering*, 23(1):14–35.

Herder, P. M., De Joode, J., Ligtvoet, A., Schenk, S., and Taneja, P. (2011). Buying real options – Valuing uncertainty in infrastructure planning. *Futures*, 43(9):961–969.

Hwangbo, S., Lee, I. B., and Han, J. (2017). Mathematical model to optimize design of integrated utility supply network and future global hydrogen supply network under demand uncertainty. *Applied Energy*, 195:257–267.

Industrietafel Noord-Nederland (2020). Voortgang regioplannen Noord-Nederland.

International Energy Agency (2021). A new era for CCUS.

Invernizzi, D. C., Locatelli, G., Velenturf, A., Love, P. E., Purnell, P., and Brookes, N. J. (2020). Developing policies for the end-of-life of energy infrastructure: Coming to terms with the challenges of decommissioning. *Energy Policy*, 144:111677.

IRENA and Methanol Institute (2021). Innovation Outlook: Renewable Methanol. Technical report, Abu Dhabi.

Jagannath, A., Madhuranthakam, C. M. R., Elkamel, A., Karimi, I. A., and Almansoori, A. (2018). Retrofit Design of Hydrogen Network in Refineries: Mathematical Model and Global Optimization. *Industrial and Engineering Chemistry Research*, 57(14):4996–5023.

Johnson, N. and Ogden, J. (2012). A spatially-explicit optimization model for long-term hydrogen pipeline planning. *International Journal of Hydrogen Energy*, 37(6):5421–5433.

Kalitventzeff, B. (1991). Mixed Integer Non-linear Programming and Its Application to the Management of Utility Networks. 18:183–207.

Kelly, D. J. and O'neill, G. M. (1991). *The Minimum Cost Flow Problem and The Network Simplex Solution Method*. PhD thesis, National University of Ireland, Dublin.

Kennedy, J. and Eberhart, R. (1995). Particle Swarm Optimization. *Purdue School of Engineering and Technology*.

Kim, M. and Kim, J. (2016). Optimization model for the design and analysis of an integrated renewable hydrogen supply (IRHS) system: Application to Korea's hydrogen economy. *International Journal of Hydrogen Energy*, 41(38):16613–16626.

Klimaattafel Haven en Industrie Rotterdam-Moerdijk (2020). Clusterplan industriecluster Rotterdam-Moerdijk.

Koutrouli, M., Karatzas, E., Paez-Espino, D., and Pavlopoulos, G. A. (2020). A Guide to Conquer the Biological Network Era Using Graph Theory. *Frontiers in Bioengineering and Biotechnology*, 0:34.

Kruskal, J. B. (1956). On the shortest spanning subtree of a graph and the traveling salesman problem. *Proceedings of the American Mathematical Society*, 7(1):48–48.

Lenz, R. and Schwarz, R. (2016). Optimal Looping of Pipelines in Gas Networks. *undefined*.

Li, L., Manier, H., and Manier, M. A. (2019). Hydrogen supply chain network design: An optimization-oriented review.

Liu, R., Li, J., and Chen, Q. (2017). A route optimization method for urban power pipeline network layout. *Proceedings of 2016 5th International Conference on Computer Science and Network Technology, ICCSNT 2016*, pages 381–385.

Luo, S. T., Cui, W., and Yang, J. W. (2011). Distribution network optimization reconfiguration based on hybrid algorithm. *2011 International Conference on Electrical and Control Engineering, ICECE 2011 - Proceedings*, pages 2194–2197.

Marocco Stuardi, F., MacPherson, F., and Leclaire, J. (2019). Integrated CO2 capture and utilization: A priority research direction. *Current Opinion in Green and Sustainable Chemistry*, 16:71–76.

Middleton, R. S., Kuby, M. J., and Bielicki, J. M. (2012). Generating candidate networks for optimization: The CO 2 capture and storage optimization problem. *Computers, Environment and Urban Systems*, 36(1):18–29.

Moradi, R. and Groth, K. M. (2019). Hydrogen storage and delivery: Review of the state of the art technologies and risk and reliability analysis.

Moreno-Benito, M., Agnolucci, P., and Papageorgiou, L. G. (2017). Towards a sustainable hydrogen economy: Optimisation-based framework for hydrogen infrastructure development. *Computers and Chemical Engineering*, 102:110–127.

Mtolera, I., Haibin, L., Ye, L., Bao-Feng, S., Xue, D., and Ma, X. Y. (2014). Optimization of tree pipe networks layout and size, using particle swarm optimization. *WSEAS Transactions on Computers*, 13:219–230.

Mulder, F. (2021). SET3085: Hydrogen Technology (Q4 2020/21).

Murthy Konda, N., Shah, N., and Brandon, N. P. (2012). Dutch hydrogen economy: evolution of optimal supply infrastructure and evaluation of key influencing elements. *Asia-Pacific Journal of Chemical Engineering*, 7(4):534–546.

National Grid Group (2021). The hydrogen colour spectrum.

Netbeheer Nederland (2021). Het Energiesysteem van de Toekomst. Technical report, Netbeheer Nederland.

NetworkX Developers (2004a). networkx.algorithms.flow.min_cost_flow - NetworkX 2.6.2 documentation.

NetworkX Developers (2004b). networkx.algorithms.flow.network_simplex - NetworkX 2.6.2 documentation.

Nicholas Salmon and René Bañares-Alcántara (2021). Green ammonia as a spatial energy vector: a review. *Sustainable Energy & Fuels*, 5(11):2814–2839.

Nikolic, I. ., Lukszo, Z. ., Chappin, E. ., Warnier, M. ., Kwakkel, J. ., Bots, P. ., and Brazier, F. (2019). Guide for Good Modelling Practice in policy support. *Citation*.

Noordzeekanaalgebied (2020). Regioplan Noordzeekanaalgebied.

Ogden, J., Jaffe, A. M., Scheitrum, D., McDonald, Z., and Miller, M. (2018). Natural gas as a bridge to hydrogen transportation fuel: Insights from the literature. *Energy Policy*, 115:317–329.

Ogden, J. M. (2002). Hydrogen: The fuel of the future? *Physics Today*, 55(4):69–75.

Papanikolaou, P., Christodoulopoulos, K., and Varvarigos, E. (2018). Optimization techniques for incremental planning of multilayer elastic optical networks. *Journal of Optical Communications and Networking*, 10(3):183–194.

Parnell, J. (2020). Shell Exploring World's Largest Green Hydrogen Project.

Pettie, S. and Ramachandran, V. (2002). An Optimal Minimum Spanning Tree Algorithm. *Journal of the ACM*, 49(1):16–34.

Poli, R. (2007). An Analysis of Publications on Particle Swarm Optimisation Applications.

Port of Rotterdam (2020). Rotterdam boosts hydrogen economy with new infrastructure.

Prim, R. C. (1957). Shortest connection networks and some generalizations. *The Bell System Technical Journal*, 36(6):1389–1401.

Quintel Intelligence (2014). Energy Transition Model.

Reddi, K., Mintz, M., Elgowainy, A., and Sutherland, E. (2016). Challenges and Opportunities of Hydrogen Delivery via Pipeline, Tube-Trailer, Liquid Tanker and Methanation-Natural Gas Grid. In Stolten, P. D. D. and Emonts, D. B., editors, *Hydrogen Science and Engineering: Materials, Processes, Systems and Technology*, volume 1-2, chapter 35, pages 1–1138. Wiley-VCH Verlag GmbH & Co. KGaA, Weinheim, Germany.

Regufe, M. J., Pereira, A., Ferreira, A. F., Ribeiro, A. M., and Rodrigues, A. E. (2021). Current developments of carbon capture storage and/or utilization–looking for net-zero emissions defined in the paris agreement. *Energies*, 14(9).

Schiebahn, S., Grube, T., Robinius, M., Tietze, V., Kumar, B., and Stolten, D. (2015). Power to gas: Technological overview, systems analysis and economic assessment for a case study in Germany. *International Journal of Hydrogen Energy*, 40(12):4285–4294.

Seo, S. K., Yun, D. Y., and Lee, C. J. (2020). Design and optimization of a hydrogen supply chain using a centralized storage model. *Applied Energy*, 262:114452.

Shi, L. H. (2009). A mixed integer linear programming for medical waste reverse logistics network design. *2009 International Conference on Management Science and Engineering - 16th Annual Conference Proceedings, ICMSE 2009*, pages 1971–1975.

Shiva Kumar, S. and Himabindu, V. (2019). Hydrogen production by PEM water electrolysis – A review. *Materials Science for Energy Technologies*, 2(3):442–454.

Sievers, S. and Krieg, D. (2016). Pipelines for Hydrogen Distribution. In Stolten, P. D. D. and Emonts, D. B., editors, *Hydrogen Science and Engineering: Materials, Processes, Systems and Technology*, volume 1-2, chapter 36, pages 1–1138. Wiley-VCH Verlag GmbH & Co. KGaA, Weinheim, Germany.

Silva, A. P., Ravagnani, M. A., and Biscaia, E. C. (2009). Particle swarm optimisation applied in retrofit of heat exchanger networks. *Computer Aided Chemical Engineering*, 27(C):1035–1040.

Simpson, T. W., Miller, S., Tibor, E. B., Yukish, M. A., Stump, G., Kannan, H., Mesmer, B., Winer, E. H., and Bloebaum, C. L. (2017). Adding Value to Trade Space Exploration When Designing Complex Engineered Systems. *Systems Engineering*, 20(2):131–146.

Sivanandam, S. and Deepa, S. (2008). Introduction
}to Particle Swarm Optimization and Ant Colony Optimization. In *Introduction to Genetic Algorithms*, chapter 11, pages 403–424. Springer, Berlin, Heidelberg.

Smart Delta Resources (2020). Regioplan 2030-2050.

Sönnichsen, N. (2021). Global hydrogen pipelines' costs by type.

Sun, P., Qian, Y., Duan, D., Niu, J., Zheng, H., Zhou, R., Yang, Z., and Yang, X. (2014). Research on Laying Optic-Fiber Cable with Oil (Gas) Pipelines in Large Slope Areas. *ICPTT 2014 - Proceedings of the 2014 International Conference on Pipelines and Trenchless Technology*, pages 401–413.

Svensson, R., Odenberger, M., Johnsson, F., and Strömberg, L. (2004). Transportation systems for CO2—application to carbon capture and storage. *Energy Conversion and Management*, 45(15-16):2343–2353.

Tezel, G. and Hensgens, R. (2021). HyWay 27: waterstoftransport via het bestaande gasnetwerk?

The Editors of Encyclopaedia Britannica (2020). Sir William Robert Grove, British physicist.

Thulasiraman, K. (2016). Basic Graph Algorithms. In Thulasiraman, K., Arumugam, S., Brandstadt, A., and Nishizeki, T. T., editors, *Handbook of Graph Theory, Combinatorial Optimization, and Algorithms*, chapter 2, pages 21–58. 1 edition.

Thulasiraman, K. and Arumugam, S. (2016). Basic Concepts in Graph Theory and Algorithms. In Thulasiraman, K., Arumugam, S., Brandstadt, A., and Nishizeki, T. T., editors, *Handbook of Graph Theory, Combinatorial Optimization, and Algorithms*, chapter 1, pages 3–20. 1 edition.

Torkomany, M. R., Yusuf, M. M., Elkholy, M., Abdelrazek, A. M., and Fath, H. E. (2020). Optimum reliable design of water distribution systems using particle swarm optimization considering pumping power and tank siting. *2020 Advances in Science and Engineering Technology International Conferences, ASET 2020*.

Urbanucci, L. (2018). Limits and potentials of Mixed Integer Linear Programming methods for optimization of polygeneration energy systems. *Energy Procedia*, 148:1199–1205.

Vaidyanathan, B., Ahuja, R. K., Orlin, J. B., and Magnanti, T. L. (2016). Minimum Cost Flow Problem. In Thulasiraman, K., Arumugam, S., Brandstadt, A., and Nishizeki, T. T., editors, *Handbook of Graph Theory, Combinatorial Optimization, and Algorithms*, chapter 5, pages 114–176. 1 edition.

van Gessel, S., Breunese, J., Juez Jarre, J., Huijskes, T., and Remmelts, G. (2018). Ondergrondse Opslag in Nederland. Technical report, TNO.

Weeda, M. and Segers, R. (2020). The Dutch hydrogen balance, and the current and future representation of hydrogen in the energy statistics. Technical report, TNO, Petten.

Weimann, L., Gabrielli, P., Boldrini, A., Kramer, G. J., and Gazzani, M. (2019). On the role of H2 storage and conversion for wind power production in the Netherlands. *Computer Aided Chemical Engineering*, 46:1627–1632.

Weisz, P. B. (2004). Basic choices and constraints on long-term energy supplies.

Werner, S. (2013). District Heating and Cooling. *Reference Module in Earth Systems and Environmental Sciences*.

Werner, S. (2017). International review of district heating and cooling. *Energy*, 137:617–631.

Wickham, D., Hawkes, A., and Jalil-Vega, F. (2022). Hydrogen supply chain optimisation for the transport sector – Focus on hydrogen purity and purification requirements. *Applied Energy*, 305.

Wirfs-Brock, J. (2014). Half Century Old Pipelines Carry Oil And Gas Load — Inside Energy.

Yamchi, H. B., Safari, A., and Guerrero, J. M. (2021). A multi-objective mixed integer linear programming model for integrated electricity-gas network expansion planning considering the impact of photovoltaic generation. *Energy*, 222:119933.

Yang, X.-S. and Karamanoglu, M. (2020). Nature-inspired computation and swarm intelligence: a state-of-the-art overview. In *Nature-Inspired Computation and Swarm Intelligence*, chapter 1, pages 3–18. Academic Press.

Yoon, E. S. and Han, C. (2009). A Review of Sustainable Energy – Recent Development and Future Prospects of Dimethyl Ether (DME). *Computer Aided Chemical Engineering*, 27(C):169–175.

Zachary, W. (1986). A Cognitively Based Functional Taxonomy of Decision Support Techniques. *Human-Computer Interaction*, 2(1):25–63.

Zarghami, A., Gunawan, I., and Schultmann, F. (2019). The application of graph theory to public infrastructure asset management.

Zhou, Y., Ma, Y., Wang, J., and Lu, S. (2021). Collaborative planning of spatial layouts of distributed energy stations and networks: A case study. *Energy*, 234:121205.

Zhu, Z., Sun, C., Zeng, J., and Chen, G. (2018). Optimization of natural gas transport pipeline network layout: A new methodology based on dominance degree model. *Transport*, 33(1):143–150.

Zivar, D., Kumar, S., and Foroozesh, J. (2021). Underground hydrogen storage: A comprehensive review. *International Journal of Hydrogen Energy*, 46(45):23436–23462.

A CALCULATIONS JOINED EDGES

The *joined-edges heuristic* uses old and new edge capacities to locally calculate whether alternative network layouts are cheaper. The old and new edge capacities are calculated differently, depending on the types of edge included. Below are the calculations for all combinations of edges.

Table A.1: Capacity calculations for pipeline a in optimisation step 3 when replacing pipeline b.

Pipeline type	Capacity condition	qn_a	qo_a
Existing	$q_a > rq_a$	$rpc \cdot rq_a^\beta + (q_a + q_b - rq_a)^\beta$	$rpc \cdot rq_a^\beta + (q_a - rq_a)^\beta$
	$q_a + q_b > rq_a$	$rpc \cdot rq_a^\beta + (q_a + q_b - rq_a)^\beta$	$rpc \cdot rq_a^\beta$
	$q_a + q_b < rq_a$	$rpc \cdot rq_a^\beta$	$rpc \cdot rq_a^\beta$
New		$(q_a + q_b)^\beta$	q_a^β

Table A.2: Capacity calculations for pipeline b in optimisation step 3 when replacing pipeline a.

Pipeline type	Capacity condition	qn_b	qo_b
Existing	$q_b > rq_b$	$rpc \cdot rq_b^\beta + (q_a + q_b - rq_b)^\beta$	$rpc \cdot rq_b^\beta + (q_b - rq_b)^\beta$
	$q_a + q_b > rq_b$	$rpc \cdot rq_b^\beta + (q_a + q_b - rq_b)^\beta$	$rpc \cdot rq_b^\beta$
	$q_a + q_b < rq_b$	$rpc \cdot rq_b^\beta$	$rpc \cdot rq_b^\beta$
New		$(q_a + q_b)^\beta$	q_b^β

Table A.3: Capacity calculations for pipeline c in optimisation step 3 when replacing pipeline b.

Pipeline type	Capacity condition	qn_c	qo_c
Existing	$q_c > rq_c$	$rpc \cdot rq_c^\beta + (q_c + q_b - rq_c)^\beta$	$rpc \cdot rq_c^\beta + (q_c - rq_c)^\beta$
	$q_c + q_b > rq_c$	$rpc \cdot rq_c^\beta + (q_c + q_b - rq_c)^\beta$	$rpc \cdot rq_c^\beta$
	$q_c + q_b < rq_c$	$rpc \cdot rq_c^\beta$	$rpc \cdot rq_c^\beta$
New		$(q_c + q_b)^\beta$	q_c^β

Table A.4: Capacity calculations for pipeline c in optimisation step 3 when replacing pipeline a.

Pipeline type	Capacity condition	qn_c	qo_c
Existing	$q_c > rq_c$	$rpc \cdot rq_c^\beta + (q_c + q_a - rq_c)^\beta$	$rpc \cdot rq_c^\beta + (q_c - rq_c)^\beta$
	$q_c + q_a > rq_c$	$rpc \cdot rq_c^\beta + (q_c + q_a - rq_c)^\beta$	$rpc \cdot rq_c^\beta$
	$q_c + q_a < rq_c$	$rpc \cdot rq_c^\beta$	$rpc \cdot rq_c^\beta$
New		$(q_c + q_a)^\beta$	q_c^β

B TIMESTAMPS FOR SNAPSHOTS

In the building of our scenarios, maximum capacity demands are represented by hourly snapshots of different combinations of high and low supply and demand. Below is an overview of the timestamps of each of these snapshots for each scenario and weather year.

Table B.1: Timestamps of snapshots used from the ETM

Scenario	Year	Snapshot	Timestamp
Regional Governance	2015	High supply / low demand	6-9-2050 07:00
		Low supply / high demand	19-1-2050 18:00
		High supply / high demand	n/a
	1987	High supply / low demand	26-7-2050 13:00
		Low supply / high demand	19-1-2050 18:00
		High supply / high demand	n/a
National Governance	2015	High supply / low demand	6-9-2050 07:00
		Low supply / high demand	10-2-2050 18:00
		High supply / high demand	n/a
	1987	High supply / low demand	26-7-2050 13:00
		Low supply / high demand	19-1-2050 18:00
		High supply / high demand	n/a
European Governance	2015	High supply / low demand	23-8-2050 15:00
		Low supply / high demand	23-1-2050 18:00
		High supply / high demand	n/a
	1987	High supply / low demand	7-6-2050 04:00
		Low supply / high demand	14-1-2050 07:00
		High supply / high demand	n/a
International Governance	2015	High supply / low demand	28-7-2050 16:00
		Low supply / high demand	19-1-2050 18:00
		High supply / high demand	n/a
	1987	High supply / low demand	7-6-2050 04:00
		Low supply / high demand	19-1-2050 18:00
		High supply / high demand	n/a

C VORONOI DIAGRAM OF INDUSTRIAL CLUSTERS

In building our scenarios, a Voronoi diagram was created as the basis for the creation of a service area for the trucks of each industrial cluster that supply local pump stations with hydrogen for transport demand. This diagram is depicted below.

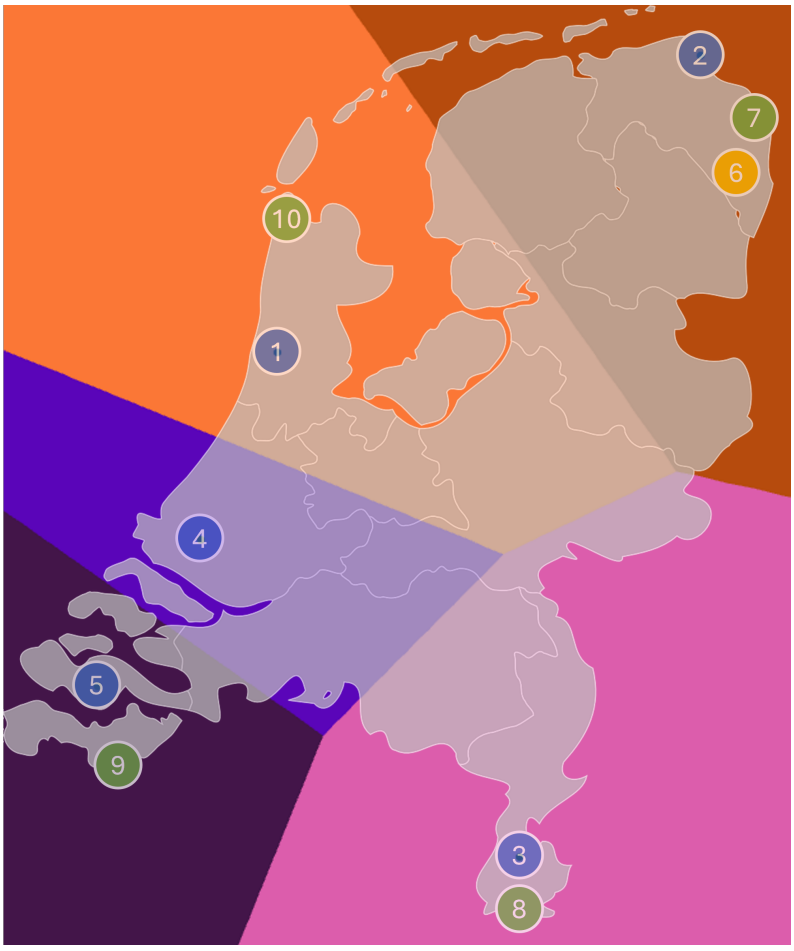

Figure C.1: Voronoi diagram of industrial clusters

D SCHEMATIC GAS INFRASTRUCTURE MAP

As a basis for identifying existing NG capacity available for repurposing in our different scenarios, we used transport infrastructure maps from Gasunie Transport Services (2012). The schematic map is shown below, the detailed map can be found here.

Figure D.1: Schematic gas infrastructure map by GTS

E | DEMAND AND SUPPLY SETS

In this appendix, you will find the supply-demand sets that were used as input for the different scenarios. Data is represented as the supply for each node in each time step in MW, negative supply indicating a demand. In the 2030 scenario, there are two time steps, one for each weather year. The 2040 and 2050 scenarios each have six time steps that represent high supply, low demand (H/L), low supply, high demand (L/H) and high supply, high demand (H/H) snapshots for each weather year.

E.1 2030

#	Name	**2015**	**1987**
0	Noordzeekanaalgebied	82	-160
1	Noord-Nederland	171	-383
2	Chemelot	-97	-960
3	Rotterdam-Moerdijk	218	-2719
4	Smart Delta	278	-2038
5	Salt Cavern Storage	-	-
6	GR import/export	-163	1565
7	LI import/export	-163	1565
8	ZL import/export	-163	1565
9	BBL/Den Helder	-163	1565

E.2 2040

		2015			**1987**		
#	Name	H/L	L/H	H/H	H/L	L/H	H/H
0	Noordzeekanaalgebied	138	-1265	-572	-19	-1500	-807
1	Noord-Nederland	1121	-1805	-535	809	-2301	-1031
2	Chemelot	456	-3779	-2856	76	-4527	-3604
3	Rotterdam-Moerdijk	4103	-10798	-6064	2650	-13382	-8648
4	Smart Delta	3911	-7820	-3894	2752	-9846	-5920
5	Salt Cavern Storage	-9389	25807	14261	-12840	24984	13438
6	GR import/export	85	85	85	1643	1643	1643
7	LI import/export	85	85	85	1643	1643	1643
8	ZL import/export	85	85	85	1643	1643	1643
9	BBL/Den Helder	85	85	85	1643	1643	1643

E.3 2050

Regional Governance		2015			1987		
#	Name	H/L	L/H	H/H	H/L	L/H	H/H
0	Noordzeekanaalgebied	2255	-1961	484	2255	-2050	395
1	Noord-Nederland	4184	-4296	50	4183	-4503	-156
2	Chemelot	2201	-8511	-6066	2200	-8923	-6479
3	Rotterdam-Moerdijk	9070	-26101	-16321	9067	-27369	-17589
4	Smart Delta	7687	-19949	-11799	7685	-20922	-12772
5	Salt Cavern Storage	-25513	60702	33536	-32698	56459	29293
6	GR import/export	29	29	29	1827	1827	1827
7	LI import/export	29	29	29	1827	1827	1827
8	ZL import/export	29	29	29	1827	1827	1827
9	BBL/Den Helder	29	29	29	1827	1827	1827

National Governance		2015			1987		
#	Name	H/L	L/H	H/H	H/L	L/H	H/H
0	Noordzeekanaalgebied	4066	-2909	2039	4065	-3135	1813
1	Noord-Nederland	4045	-5303	-685	4044	-5830	-1212
2	Chemelot	-52	-10172	-9512	-54	-11225	-10565
3	Rotterdam-Moerdijk	10885	-31036	-18171	10879	-34270	-21405
4	Smart Delta	8812	-23383	-13486	8808	-25864	-15968
5	Salt Cavern Storage	-26824	73735	40747	-36686	71380	38393
6	GR import/export	-233	-233	-233	2236	2236	2236
7	LI import/export	-233	-233	-233	2236	2236	2236
8	ZL import/export	-233	-233	-233	2236	2236	2236
9	BBL/Den Helder	-233	-233	-233	2236	2236	2236

European Governance		2015			1987		
#	Name	H/L	L/H	H/H	H/L	L/H	H/H
0	Noordzeekanaalgebied	680	-584	525	884	-480	772
1	Noord-Nederland	1651	-300	1290	1665	-208	1404
2	Chemelot	-448	-1779	-1170	-466	-1602	-988
3	Rotterdam-Moerdijk	5206	-2338	2990	6037	-1513	4434
4	Smart Delta	4574	-1419	2873	4603	-988	3373
5	Salt Cavern Storage	-13563	5268	-8408	-15739	3275	-12011
6	GR import/export	475	288	475	754	379	754
7	LI import/export	475	288	475	754	379	754
8	ZL import/export	475	288	475	754	379	754
9	BBL/Den Helder	475	288	475	754	379	754

International Governance		**2015**			**1987**		
#	Name	H/L	L/H	H/H	H/L	L/H	H/H
1	Noordzeekanaalgebied	2561	-346	1127	3661	142	2139
2	Noord-Nederland	366	-4330	-2979	455	-4508	-3098
3	Chemelot	-1060	-8255	-7750	-1053	-8676	-8159
4	Rotterdam-Moerdijk	13352	-13981	-7195	18060	-12801	-3763
5	Smart Delta	1513	-17941	-14256	1825	-18805	-14923
6	Salt Cavern Storage	-18736	43261	29049	-25620	42696	25132
7	GR import/export	501	398	501	668	488	668
8	LI import/export	501	398	501	668	488	668
9	ZL import/export	501	398	501	668	488	668
10	BBL/Den Helder	501	398	501	668	488	668

F CALCULATIONS OF REGRET

We have calculated maximum over and underinvestments, and minimax regret for 9 different network layouts. The four optimal network layouts for scenarios *2050(RG)*, *2050(NG)*, *2050(EG)* and *2050(IG)* are among the network layouts analysed. Optimal network layouts are also analysed when demand and supply data is combined in the input files indicated by *2050(RG+IG)*, *2050(NG+IG)*, *2050(RG+NG)*, *2050(RG+IG+NG)* and *2050(ALL)*. Table F.1 shows the data for all network layouts investigated. On the left-hand side, we see the different optimal network layouts. In the top of the table, we see the four scenarios that can become reality. For each of the combinations of network layout and scenario outcome, we have calculated the over- or underinvestment.

Scenario	2050(RG)	2050(NG)	2050(EG)	2050(IG)
2050(RG)	0	-0,401	1,586	0,601
2050(NG)	0,401	0	1,987	1,002
2050(EG)	-1,586	-1,987	0	-0,985
2050(IG)	-0,601	-1,002	0,985	0
2050(RG+IG)	0,02	-0,381	1,606	0,621
2050(NG+IG)	0,463	0,062	2,049	1,064
2050(RG+NG)	0,443	0,042	2,029	1,044
2050(RG+IG+NG)	0,463	0,062	2,049	1,064
2050(ALL)	0,463	0,062	2,049	1,064

Table F.1: Calculations of over- and underinvestments

COLOPHON

This document was typeset using LaTeX. The document layout was generated using the arsclassica package by Lorenzo Pantieri, which is an adaption of the original classicthesis package from André Miede.


TU Delft